

MeteorNews

ISSN 2570-4745

VOL 5 / ISSUE 5 / SEPTEMBER 2020



*Comet Neowise with -9mag bolide by Tioga Gulon
26 July 2020 at 23:12 UTC village Cérilly, Allier, France*

- Oleg Igorevich Belkovich
- chi Cygnids
- Lyrids
- Spectral observations
- Radio observations
- Fireballs

Contents

Obituary Oleg Igorevich Belkovich (1934 – 2020) <i>Galina Ryabova</i>	285
Possible upcoming return of the chi Cygnids in September 2020 <i>Peter Jenniskens</i>	287
Meteors and 2018 LF ₅ <i>John Greaves</i>	290
Some Near Earth Objects and meteor associations <i>John Greaves</i>	295
Results of spectral observations of meteor showers and sporadic meteors from October 2018 until May 2020 <i>Takashi Sekiguchi</i>	300
The Lyrids and a minor antihelion outburst in 2020 <i>Thomas Weiland</i>	314
Lyrids 2020: successful campaign! <i>Koen Miskotte</i>	317
Meteor observations from Midden-Eierland on the Dutch island of Texel <i>Koen Miskotte</i>	321
Observations January 3-4, 2020 <i>Pierre Martin</i>	324
June 2020 report CAMS BeNeLux <i>Paul Roggemans</i>	328
RMS cameras as alternative for Watec in CAMS <i>Paul Roggemans</i>	330
Delta Aquariids and Perseids 2020. Radio meteor observation report in the world <i>Hiroshi Ogawa</i>	336
Radio meteors June 2020 <i>Felix Verbelen</i>	338
Radio meteors July 2020 <i>Felix Verbelen</i>	345
Once upon a time, we had a comet and a fireball <i>Tioga Gulon</i>	352
Fireball events over Spain in July 2020 <i>José María Madiedo</i>	357

Obituary

Oleg Igorevich Belkovich

(1934 – 2020)

Galina Ryabova

Tomsk State University, Kievskaya str. 109/6-62, 634034 Tomsk, Russia
rgo@rambler.ru

On July 11, 2020, at 5 am, Professor Oleg Belkovich passed away after a long illness.



Figure 1 – Oleg Belkovich in June 1989 during the Asteroids, Comets and Meteors conference at Uppsala University Sweden (photo by Paul Roggemans).

Oleg Belkovich was born in Kazan, into a family of an astronomer. His father, Igor Vladimirovich Belkovich, world-renowned researcher of the Moon, worked in Engelgardt Astronomical Observatory (EAO), situated in a forest, 20 km from Kazan, from 1928 until his death in 1949. Oleg graduated from Kazan State University (KSU) in 1957, as a radio physicist. His first work was as an engineer in a radio astronomical laboratory in KSU. In 1964, he got his first scientific degree (candidate of science — an equivalent of PhD). From 1965 to 1970, Oleg worked as an assistant and assistant professor in the radio astronomy department at KSU. In the years 1966 – 1967, he completed a scientific internship in England, at the University of Sheffield, working with the famous meteor researcher Professor T. R. Kaiser.

In 1970, Oleg transferred to work in the EAO as a deputy director for scientific work; at the same time, he served as the head of the meteor department. In 1977 – 1991, he served as director of the EAO. As director of an observatory he had to deal not only with scientific, but also with organizational and economic work. The astronomical observatory is an autonomous institution in which the director is obliged to ensure not only the coordination of scientific research, but also comfortable living conditions on its territory for more than 150 scientists and members of their families. Nevertheless, he found time to defend his second scientific degree (D. of Sci.) in 1988.

In 1991, Oleg resigned to devote most of his time to science, and had a position of principal researcher. He was also a professor at Kazan University for almost two decades (1996 – 2014). Oleg was a member of the International Astronomical Union from 1966, and in 1982 he was elected as President of Commission 22 IAU for the following triennium.



Figure 2 – An historic photo of IAU Commission 22 Chairmen taken during the first Meteoroids conference at Smolenice, Slovakia in July 1992. From l. to r. Lubor Kresak, Pulat Babadzhanov, Zdenek Ceplecha, Ian Williams, Oleg Belkovich, Bertil Lindblad, Graham Elford, Colin Keay and Jan Stohl (credit unknown photographer).

As a professional astronomer, Oleg Belkovich had been focusing on the study of radar observations of meteors. He began with the development and improvement of

equipment for radar observations of meteors and took a direct part in the observations. The work started originally as military research on communications via meteors, but later evolved into the study of radar meteors themselves. Later Oleg became more involved with theoretical work regarding the interpretation of radar observations. Oleg proposed a new, probability-based approach to processing and interpreting the radar observations of meteors. For the first time in the world, he obtained the distribution of the amplitudes and durations of meteor echoes in an analytical form, considering the random positions of the reflecting points on the meteor trails. The method allows calculation of the incident flux density for a meteor shower, which is one of the basic problems of meteor astronomy. Asteroid 179595 Belkovich (2002 MK4) is named in his honor for his work in radar observations of meteors.



Figure 3 – During the excursion of the IMC in 1991, in Potsdam Germany. From l. to r. Gennadij Andreev, Oleg Belkovich, and Alexandra Terentjeva at right (photo by Paul Roggemans).

It would not be an exaggeration to say that Oleg Belkovich was an eminent meteor astronomer. Some of his numerous students are now doctors and professors and continue his work in astronomy. He always had time for collaboration with amateur meteor astronomers, highly appreciating the scientific value of their efforts. In 1994, he organized the Meteor Summer School in EAO, inviting several amateur astronomers from Europe to participate. In co-authorship with amateur meteor astronomers from Crimea, he published research papers in WGN (journal of the International Meteor Organization, IMO), and participated in several annual International Meteor Conferences, organized by IMO. In 2005, IMO organized a Radio Meteor School in Oostmalle, Belgium, where Oleg, being the main invited lecturer, presented a series of lectures covering his theoretical work on radio meteors. For five days participants, listened to lectures, alternated with “study time” and Q&A sessions. As a result, the 130-pages volume of RMS2005 Proceedings appeared. At this occasion Oleg was nominated as IMO honorary member.

Until the end of his life Oleg lived and worked in EAO, and here he was buried. He found his peace, and we lost a teacher, colleague, friend and just a good man.



Figure 4 – Malcolm Currie, Ralf Koschack and Oleg Belkovich during his lecture at the International Meteor Conference in 1991 in Potsdam, Germany (photo by Paul Roggemans).



Figure 5 – From l. to r. Subhon Ibadov, Alexandra Terentjeva, Oleg Belkovich and Detlef Koschny at the IMC in 1993 in Puimichel, France (photo by Casper ter Kuile).



Figure 6 – Oleg Belkovich (in front) being celebrated as honorary IMO member in Belgium during the IMC in September 2005, after the radio meteor school (photo by Casper ter Kuile).

Possible upcoming return of the chi Cygnids in September 2020

P. Jenniskens

SETI Institute, 189 Bernardo Ave, Mountain View, CA 94043, USA.
pjenniskens@seti.org

In late August 2020, a cluster of meteor radiants was detected by CAMS stations in Australia, South Africa, Namibia and Chile consistent with the return of the chi Cygnid meteor shower (IAU #757). If so, that shower may be ongoing and be an interesting target for observations in the coming month of September. The shower was last seen in 2015, when it peaked in mid and late September.

1 Introduction

In the night of August 20–21, 2020, the CAMS low-light video surveillance networks in Australia, South Africa, Namibia and Chile recorded an outburst of slow meteors from a compact radiant located between the constellations Delphinus and Aquila (Jenniskens et al., 2020). The CAMS automated software identified this shower as the chi Cygnids (IAU 757), first detected by CAMS in 2015 during the period September 14–25 (Jenniskens, 2015; Roggemans et al., 2016; Koukal et al., 2016).

2 Methods

The Cameras for Allsky Meteor Surveillance (CAMS) project triangulates the trajectories of visible +5 to -5 magnitude meteors recorded in different networks of camera stations spread over the globe in order to calculate their radiant and speed. Each day, over a thousand radiant positions are measured which are displayed at the website¹.

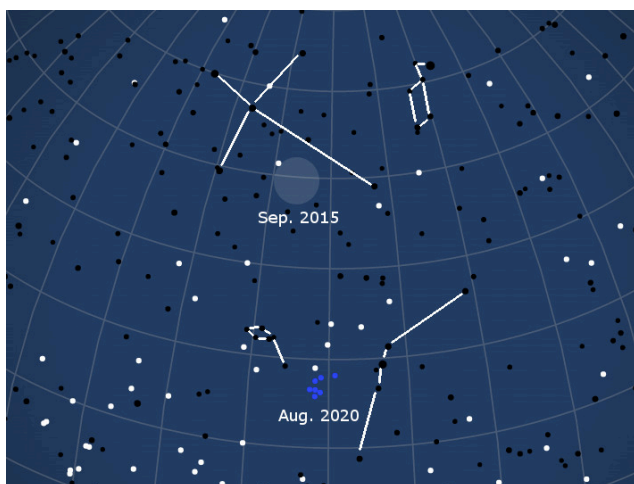


Figure 1 – Blue points mark the radiant of meteors identified as chi Cygnids in CAMS data of August 21, 2020, plotted in sun-centered ecliptic coordinates. White points are sporadic meteors. The radiant position of the shower in mid September 2015 is shown as a light circle.

Each radiant and speed are compared to a look-up table of past identified showers to obtain its shower association, which are shown by colors representing speed (red is fast, blue is slow).

3 A possible chi Cygnid shower in 2020

The outburst of possible chi Cygnids can be seen as a blue cluster in the map after selecting the date of Aug. 21, 2020 (Figure 1). The map covers the solar longitude interval 147.59–148.55 degrees (equinox J2000.0). The geocentric radiant was at R.A. = 304.7 ± 1.0 deg, Decl. = $+8.5 \pm 1.0$ deg, and meteors had a slow speed $v_g = 17.0 \pm 0.4$ km/s. The 8 measured orbits have median orbital elements $a = 2.95 \pm 0.17$ AU, $q = 0.830 \pm 0.008$ AU, $e = 0.716 \pm 0.017$, $i = 12.7 \pm 0.6$ deg, $\omega = 235.3 \pm 1.3$ deg, and $\Omega = 148.0 \pm 0.3$ deg. The longitude of perihelion of the median orbit is $\Pi = 23.5 \pm 1.3$ deg.

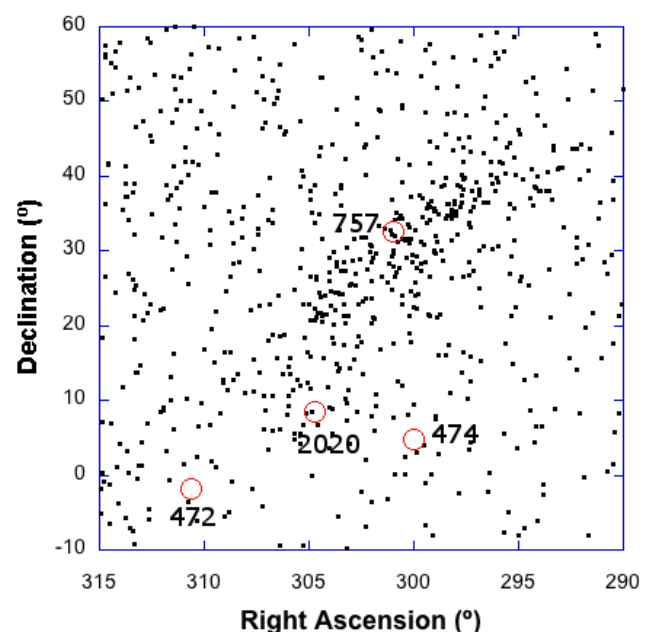


Figure 2 – 2015 chi Cygnids. The radiant position of all meteors observed from August 15 to October 2, 2015. The circle with label “757” marks the median orbit of the chi Cygnids. Showers 472 and 474 are discussed in the text.

¹ <http://cams.seti.org/FDL/>

Table 1 – Radiant and orbit of showers discussed here.

	λ_0 (°)	α_g	δ_g	v_g	q	e	i	ω	Ω	Π	References
	J2000	(°)	(°)	km/s	AU		(°)	(°)	(°)	(°)	
2020 shower	148.0	304.7	8.5	17.0	0.830	0.716	12.7	235.3	148.0	23.3	Jenniskens (2020)
757 CCY	171.6	301.0	32.6	15.1	0.949	0.655	18.6	209.9	171.6	21.5	Jenniskens (2015)
474 ABA	148.7	300.0	4.7	15.1	0.872	0.701	10.2	228.1	148.7	16.8	Rudawska & Jenniskens (2014)
472 ATA	147.3	310.6	-1.8	15.9	0.790	0.648	7.4	243.5	147.3	30.8	Rudawska & Jenniskens (2014)

Looking back at previous dates, the shower was first detected on August 18 (4 meteors) and one or two meteors were identified in the period August 19–22. The meteors are at higher ecliptic latitude and have a different longitude of perihelion than the late alpha Capricornids (labeled as shower 692). The map of August 18 shows both showers.

4 Discussion

At first sight, the association with the chi Cygnids (CCY, IAU#757) is not obvious. The median orbit of this shower has a much higher inclination of $i = 18.6 \pm 1.6$ deg with a radiant in the constellation Cygnus (Table 1, Figure 1). Figure 2 is a graph showing all CAMS detected radiants in that part of the sky between August 15 and October 2, 2015. The 2020 meteors had a radiant position below the main of the chi Cygnid shower, but in what appears a faint onset of the main cluster at lower latitudes.

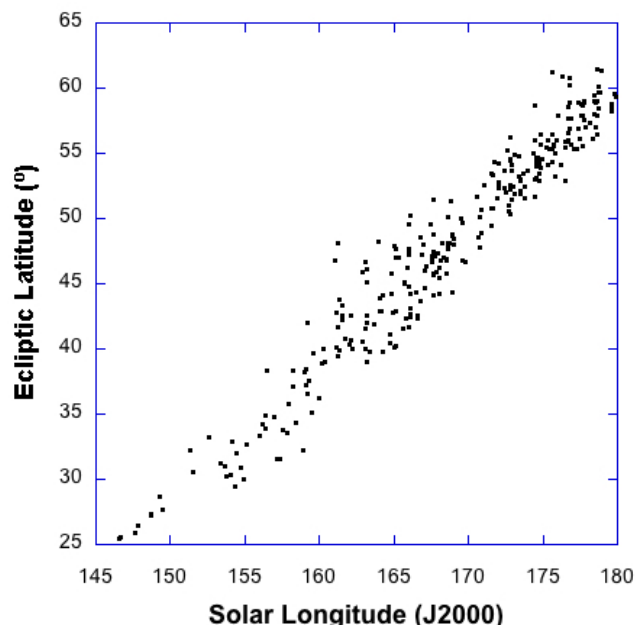


Figure 3 – 2015 Chi Cygnid meteors.

Indeed, the median orbit is not representative for the shower as a whole and the early detection of the shower in Aquila/Delphinus in 2020 does appear to be the return of the chi Cygnids. The chi Cygnids in 2015 had a moving radiant that changed a lot over the activity period throughout September. Figure 3 shows the Sun-centered latitude of the radiant as a function of solar longitude. The shower was first detected at solar longitude 147° , when the ecliptic radiant latitude was 26° . The 2020 meteors had an ecliptic latitude of $27.1 \pm 1.1^\circ$, in good agreement. The Sun-

centered ecliptic longitude was $161.7 \pm 0.9^\circ$ for the 2020 shower and 161.8° for the 2015 chi Cygnids.

The 2020 shower has the same longitude of perihelion as that of the chi Cygnids ($\Pi = 21.5 \pm 1.9$ deg.). Nearby (now removed) showers 472 (August theta Aquilids) and 474 (August beta Aquariids) do not: 474 has a lower Π , 472 a higher value (Table 1). Especially shower 474 has a radiant that is not so far from that of the observed meteors. However, the radiant and speed are significantly off from those of the radiant cluster (Figure 2). They were detected in a D-criterion search in an early CAMS sample (Rudawska and Jenniskens, 2014; Kornos et al., 2014). Both showers are currently in the List of Removed Showers, after we found that the showers were not recognized as a density cluster when more data became available (Jenniskens et al., 2016).

It will be interesting to see what happens the coming month. If we are now seeing the beginning of shower 757, we might expect more of these meteors the coming weeks and the radiant will gradually shift north into Cygnus, peaking in mid and late September. Based on their orbital elements, the meteoroids appear to originate from an unknown Jupiter Family comet and the observations of the stream may assist in identifying the parent body.

Acknowledgments

Many thanks to *John Greaves* for pointing out the similarity of the 2020 meteors to shower 474. CAMS Namibia is coordinated by *T. Hanke* (the H.E.S.S. Collaboration), CAMS Chile by *S. Heathcote* (AURA/Cerro Tololo) and *E. Jehin* (University of Liege), CAMS Australia by *M. Towner* (Curtin University), and CAMS South Africa by *T. Cooper* (Astronomical Society of Southern Africa - Meteor Section).

References

- Jenniskens P. (2015). “New Chi Cygnids meteor shower”. CBET 4144. IAU Central Bureau for Astronomical Telegrams. D. W. E. Green (ed.), 1pp.
- Jenniskens P., Nénon Q. (2016). “CAMS verification of single-linked high-threshold D-criterion detected meteor showers”. *Icarus*, **266**, 371–383.
- Jenniskens P., Hanke T., Heathcote S., Jehin E., Towner M., Cooper T. (2020). “Chi Cygnid meteor shower

- 2020". CBET 4837. IAU Central Bureau for Astronomical Telegrams. D. W. E. Green (ed.), 1pp.
- Kornos L., Matlovic P., Rudawska R., Toth J., Hajdukova M., Koukal J., Piffel R. (2014). "Confirmation and characterization of IAU temporary meteor showers in EDMOND database". In: T. J. Jopek, F. J. M. Rietmeijer, J. Watanabe, I. P. Williams, editors, *Proceedings of the Astronomical Conference Meteoroids 2013*, held at A. M. University, Poznan, Poland, Aug. 26-30, 2013. A. M. University Press, pages 225–233.
- Koukal J., Srba J., Toth J. (2016). "Confirmation of the chi Cygnids (CCY, IAU#757)". *WGN, Journal of the IMO*, **44**, 5–9.
- Roggemans P., Johannink C., Breukers M. (2016). "Status of the CAMS-BeNeLux network". In: Roggemans, A.; Roggemans, P., editors, *Proceedings of the International Meteor Conference*, Egmond, the Netherlands, 2-5 June 2016. IMO, pages 254–260.
- Rudawska R., Jenniskens P. (2014). "New meteor showers identified in the CAMS and SonotaCo meteoroid orbit surveys". In: T. J. Jopek, F. J. M. Rietmeijer, J. Watanabe, I. P. Williams, editors, *Proceedings of the Astronomical Conference Meteoroids 2013*, held at A. M. University, Poznan, Poland, Aug. 26-30, 2013. A. M. University Press, pages 217–224.

Meteors and 2018 LF₅

John Greaves

cpmjg@tutanota.com

Meteor orbits with D criterion similarity to the comet like orbit Amor Asteroid 2018 LF₅ are presented and their potential association with known meteor showers discussed.

1 Method

A list of known Near Earth Objects (NEOs) was obtained from the Minor Planet Center² and the 618 objects with inclinations of 40 degrees or greater were filtered out for assessment via the Jopek (1993) variation of the Southworth and Hawkins (1963) D criterion against publicly available meteor orbits from various sources utilizing a threshold value of 0.1.

Resultant orbits were then assessed in the cases where any particular NEO had ten or more meteor orbits matching with D criteria less than this value. The list of NEOs were also tested against themselves as a simple way of trying to avoid the situation of objects similar in orbital characteristics simply because of the commonality of being injected into their current orbit via interactions with Jupiter, although the selection of such a high inclination cut off point should have removed that selection effect. Similarly, the meteoroid orbits were also further tested against the NEO list again to ensure that they did not match any other object in the NEO dataset. The original agglomeration of publicly available datasets also contained the elements for all comets with perihelion distances of 1.3 AU or less.

Finally, the resultant stream particulars were assessed against showers detailed by the International Astronomical Union Meteor Data Center³ (Jopek and Kaňuchová, 2017) for known streams.

2 Result

The meteoroids

Although a handful of NEOs returned more than ten meteoroid orbits per object, the vast majority only just did so with only the Amor Asteroid 2018 LF₅ having markedly more.

This had a total of 42 orbit matches for $D < 0.1$ predominantly classified as sporadic and consisting of 2 from the Croatian Meteor Network (CMN) (Korlević et al., 2013), 3 from SonotaCo (e.g. SonotaCo, 2009), 16 from EDMOND (e.g. Kornoš et al., 2014) and 21 from CAMS 3.0 (Jenniskens et al., 2018), spread across the period 2009 to 2016. *Figure 1* demonstrates the spread in D criterion in 0.01 steps whilst *Figure 2* shows the number per year which is a reflection of the observing regimes rather than the

shower activity. It should be noted that all these surveys bar CAMS, exactly half of the orbits, use the same analysis software which reports to a higher precision than CAMS and that despite the CAMS precision is reflecting better the reality, the rounding off of the numeric data before a mathematical analysis will give different results than rounding off after analysis. The surveys also use different technology and to some extent observing methodologies, with the EDMOND dataset being a combination of many different groups. Nevertheless, the differences in the mixed data were considered negligible and their results were analyzed as equivalent.

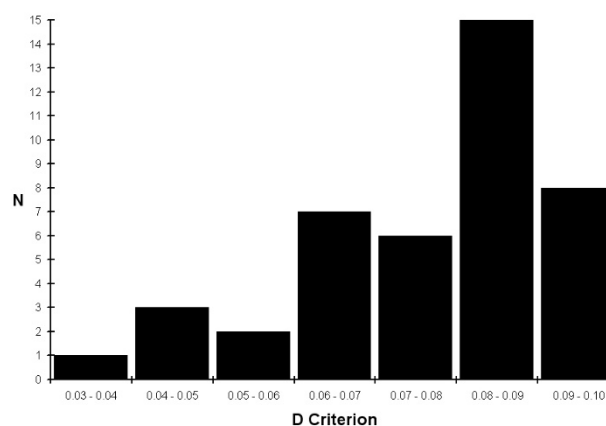


Figure 1 – Frequency of D Criterion values for the 42 meteor orbits matched to 2018 LF₅ in bin sizes of $D = 0.01$.

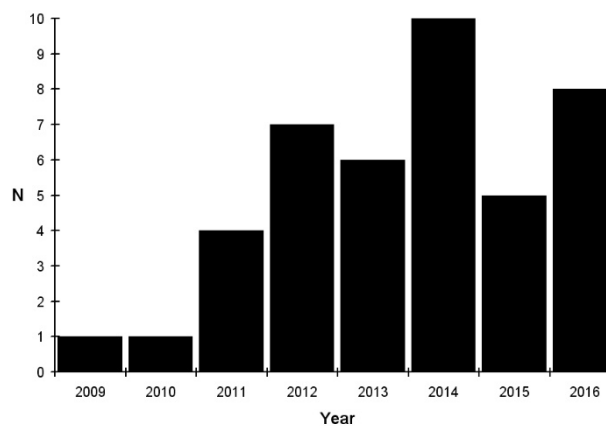


Figure 2 – Number of matched meteor orbits to 2018 LF₅ per calendar year.

² <https://www.minorplanetcenter.net/iau/lists/MPLists.html>

³ <https://www.ta3.sk/IAUC22DB/MDC2007/>

Table 1 – The identifier, perihelion distance (q) in Astronomical Units, eccentricity (e), inclination (i), argument of perihelion (ω), ascending node (Ω) all in degrees and D criterion values for the 42 video meteors. Their mean and median values are also included as are those for 2018 LF₅.

ID	q (A.U.)	e	i (°)	ω (°)	Ω (°)	D
CAMS9943	1.0102	0.63091	42.08	190.3	94.271	0.095
ED20150629_233145	1.010665	0.656853	40.593	189.843	97.693	0.092
ED20140629_021808	1.011745	0.608199	38.46	189.129	97.095	0.087
ED20140628_033231	1.013242	0.585325	42.446	187.654	96.19	0.079
ED20120628_210658	1.01332	0.55582	38.723	187.714	97.378	0.097
ED20120709_020332	1.01396	0.64719	38.585	173.353	107.105	0.096
070910MLA0004	1.014	0.6271	41.524	173.314	107.371	0.086
ED20160706_003120	1.014195	0.616748	43.932	173.426	104.159	0.088
20140630_233622	1.014388	0.681372	41.742	186.007	98.538	0.082
070506MLA0021	1.014653	0.630086	44.291	174.1	103.38	0.089
ED20150626_022848	1.014999	0.63334	41.746	184.964	93.996	0.085
CAMS10690	1.0152	0.59889	37.88	185.22	100.842	0.078
ED20130705_220933	1.01525	0.6158	42.998	175.032	103.843	0.068
CAMS196067	1.0155	0.6289	41.49	175.51	104.859	0.061
CAMS120926	1.0155	0.6182	42.62	184.2	94.738	0.08
CAMS122205	1.0155	0.6282	40.18	184.61	104.177	0.083
CAMS379772	1.0155	0.6534	43.26	175.65	98.74	0.098
CAMS325931	1.0156	0.6013	38.48	175.49	100.64	0.081
ED20140703_023707	1.01576	0.594394	43.785	183.992	100.923	0.067
CAMS396522	1.0158	0.609	38.61	183.57	94.631	0.088
CAMS194281	1.0159	0.6204	42.55	183.34	95.511	0.073
CAMS396683	1.0162	0.6483	36.37	182.99	102.31	0.098
CAMS122401	1.0163	0.5899	44.25	177.15	105.122	0.085
CAMS11396	1.0163	0.64749	41.7	177.45	107.603	0.09
20130709_220504	1.016341	0.58785	39.039	177.632	107.298	0.092
CAMS66019	1.0164	0.5869	43.09	178.19	97.7	0.084
20090629_025551	1.016429	0.635551	39.591	181.729	97.033	0.062
CAMS325782	1.0165	0.6292	45.53	181.78	99.567	0.083
ED20120630_213443	1.01652	0.61961	44.034	181.431	99.303	0.06
ED20120706_231323	1.01659	0.59902	40.169	178.867	105.086	0.061
ED20140703_221110	1.016598	0.587962	39.87	181.206	101.7	0.046
CAMS67107	1.0166	0.6352	43.06	178.81	103.455	0.055
CAMS67697	1.0166	0.6189	38.1	178.74	106.345	0.087
ED20160704_002939	1.016636	0.599036	41.185	181.395	102.25	0.038
ED20140707_010433	1.016652	0.584315	38.246	179.656	104.675	0.079
ED20150704_232410	1.016666	0.649469	40.959	180.382	102.453	0.044
CAMS326146	1.0167	0.6287	42.98	179.28	101.748	0.045
CAMS195794	1.0167	0.5702	41.85	180.48	103.13	0.063
CAMS265600	1.0167	0.6412	39.65	180.17	104.718	0.065
CAMS122593	1.0167	0.6045	39.52	180.44	106.059	0.08
CAMS195087	1.0167	0.558	37.48	179.9	99.29	0.094
ED20160703_011620	1.016714	0.564945	38.658	179.292	101.327	0.073
Mean	1.015439	0.614945	40.983	180.795	101.292	
Median	1.01605	0.61855	41.337	180.411	101.724	
2018 LF ₅	1.064285	0.61874	41.046	181.079	100.749	

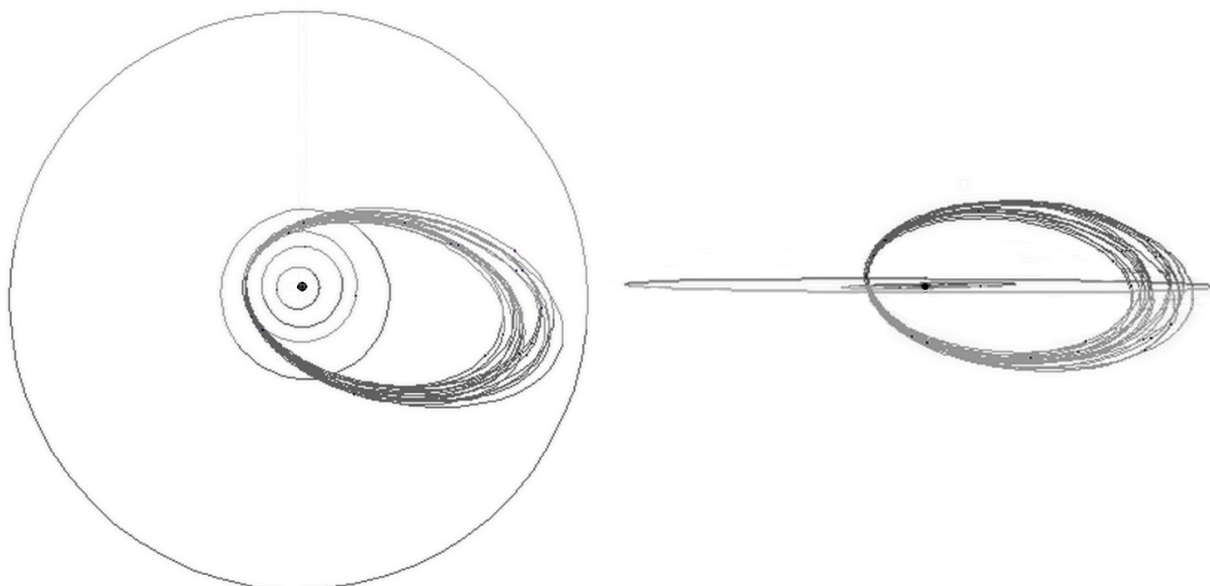


Figure 3 – The orbit of 2018 LF₅ and the 20 matched orbits with $D \leq 0.080$ as seen from the Ecliptic North with Ecliptic Longitude zero towards the top of the images (left) and from the Ecliptic Plane with Ecliptic Longitude zero into the image (right). Planetary orbits out to and including that of Jupiter are also shown.

Table 2 – The Right Ascension (R.A.), Declination (Dec.), Solar Longitude (λ_{\odot}), geocentric velocity (v_g), perihelion distance (q) in Astronomical Units, inclination (i), argument of perihelion (ω), ascending node (Ω) all in degrees for mean and median of the 42 meteor orbits as well as those for the zeta Draconids (ZDR#073), omicron Draconids (ODR#088) and July zeta Draconids (ZED#279).

ID	R.A. (°)	Dec. (°)	λ_{\odot} (°)	v_g (km/s)	q (A.U.)	i (°)	ω (°)	Ω (°)
Mean	276.2	65.9	101	25	1.015	41	180.8	101.3
Median	276.3	66.5	101	25	1.016	41.3	180.4	101.7
ZDR#073	269	59	122	24	1.015	33	183.5	149.5
ODR#088	285	61.3	115.5	28.6	1.006	46.2	192.2	115.5
ZED#279	251.6	66.5	115.7	20.6	1.016	32.5	176.7	115.7

The 20 orbits with D criterion values of 0.080 and less along with that for 2018 LF₅ are presented in Figure 3 for illustrative purposes. The meteor orbits' individual elements, their mean and median, and the same elements for 2018 LF₅, are presented in Table 1.

The asteroid

The particulars of 2018 LF₅'s orbit are derived from 239 observations spanning 149 days from May to October 2018 as provided in MPO 529360⁴ led to the object being identified as an Amor type asteroid. However, both the inclination of 41 degrees and the Tisserand parameter with respect to Jupiter (T_J) of 2.7 are more representative of a comet. However, an examination of the few publicly available images for the object during its apparition (Deen S., pers. comm.) gave no indication whatsoever of anything other than a point like object, although this is not surprising given its apparent magnitude barely rose above 18.

Examination of the Asteroid Lightcurve Photometry Database (e.g. Warner et al., 2011) revealed somewhat noisy data except for a short run near opposition where a

handful of peaks very roughly 1.5 hours apart are suggested, which for a non-spheroidal object could represent a periodicity around 3 hours or so. However, the irregular shape and on occasion tumbling motion of such objects often lead to multiple peaks per rotation period, not just the two expected per rotation from an elongated object. Further such a rotation rate would not necessarily distinguish between a comet and a fast-rotating asteroid throwing off fine debris

In summary it can be said that varying degrees of circumstantial evidence can hint at 2018 LF₅ being more cometary than asteroidal, especially the orbital parameters, but no definitive evidence exists.

The showers

The mean particulars for the derived meteors were checked against the IAU MDC list of showers both numerically and visually via plotting in the astronomical charting software Guide 9.0⁵ to check for any relation to known showers. No evident association appeared to exist, and the nearest representative star would be 42 Draconis (although the

⁴ <http://minorplanetcenter.net>

⁵ <http://projectpluto.com>

more well-known Cat's Eye Planetary Nebula lies very adjacent, and of course the mean radiant also lies very close to the North Ecliptic Pole, however such things are not included in the nomenclature guidelines).

However, three relatively adjacent showers in terms of radiant position and solar longitude do exist, namely ZDR#073 (zeta Draconids), ODR#088 (omicron Draconids) and ZED#279 (July zeta Draconids). The surveys providing the meteor orbit data all assess shower association via radiant clustering algorithms and predominantly identified their objects as sporadic meteors with no known association, albeit with EDMOND matching 4 to ODR#088, 1 to ZDR#073 and 1 to ZED#279, 6 out of the total of 16. A CMN meteor that was included in the EDMOND dataset but removed to avoid duplication before analysis had however been identified by CMN as sporadic despite being classified as ZDR#073 by EDMOND (see Koseki, 2019 with respect to SonatoCo, which is also used by CMN, and EDMOND shower look up table differences). Table 2 provides the mean particulars for this study's orbits as well as those for the other three showers as derived from the IAU MDC database or literature search.

The shower ZDR#073 results from Lindblad (1971) and was obtained from a small handful of photographic orbits yet those orbits had been included in the analysis having been obtained from the IAU MDC (Neslušan et al., 2014), yet none from that dataset were matched to 2018 LF₅. The ODR#088 Sekanina (1976) are again originally from a small number of orbits, which are in fact radar orbits, and although those orbits were also included in the analysis only one matched to 2018 LF₅, although Jenniskens (2016) has cross identified CAMS meteor orbits with this shower and provided new particulars. The ZED#279 (Jenniskens, 2006) are from an assessment of potential asteroidal showers but again based on little data, certainly predating the modern era of plentiful double station video meteor orbit datasets.

In other words, none of the showers as originally presented are well defined in orbit elements, being based on few meteors, and indeed in that context are not particular that different from each other given the low and to some extent happenstance sampling rate upon which radiant positions and solar longitudes were based upon. Unfortunately, the classical minor meteor streams are often ill defined, more or less unique to their discovery papers and consequently difficult to relate to other surveys thus at times inflating the IAU MDC shower list with duplication which could well all be manifestations of the same entity. Yet on the other hand these same reasons are why there is insufficient information to show that these three classical showers and the meteors associated via *D* criteria with 2018 LF₅ are assuredly the same. The data are insufficient to outright connect or outright reject an association between any and all of the showers or the current orbits connected to 2018 LF₅, yet this would represent four not particularly different near coincidental showers in a relatively small area of the sky about at the same time of year.

Whether 2018 LF₅ is associated with an unknown meteor stream with a radiant lying near the star 42 Draconis, or whether it is associated with one of the three known meteor streams, which in turn may all be themselves manifestations of the same stream only appearing different due to selection effects and limited data, is more a matter for the IAU Meteor Group nomenclaturists and taxonomists than for this paper. Within zoological and botanical nomenclature, the naming of a taxonomic group usually follows priority, that is which one was published first, which would favor the zeta Draconids of the Lindblad (1971) study.

3 Conclusion

Examination of a large number of publicly available meteor orbits revealed that 42 video survey orbits matched well with Amor Asteroid 2018 LF₅'s orbit based on the results of Jopek (1993) modified Southworth and Hawkins (1963) using a *D* criterion threshold of 0.1. Meanwhile the same orbits revealed no association between them and neither other known NEOs nor comets. Despite a comet like orbit there was no direct evidence for 2018 LF₅ being a comet so the nature of that object is not entirely clear. Assessment of the derived mean shower details with respect to known showers revealed no strong candidate but that there were three not completely dismissible showers adjacent in both time and space. These showers themselves appeared to be potentially the same entity only differentiated because of the limited datasets they were based upon, yet this same limitation ensured there was insufficient information to either confirm or dismiss them being all aspects of the same shower or stream, let alone associated with 2018 LF₅, despite this circumstantial evidence.

The author decided that this however would be a parsimonious solution over declaring yet another new shower and that in terms of publication priority the ZDR#073 zeta Draconids would be the choice.

Acknowledgment

Sam Deen is acknowledged for kindly finding and pointing out archival asteroid survey images of 2018 LF₅.

References

- Jenniskens P. (2006). "Meteor Showers and their Parent Comets", Cambridge, U.K.: Cambridge University Press.
- Jenniskens P., Nénon Q., Gural P. S., Albers J., Haberman B., Johnson B., Holman D., Morales R., Grigsby B. J., Samuels D., Johannink C. (2016). "CAMS confirmation of previously reported meteor showers". *Icarus*, **266**, 355–370.

- Jenniskens P., Baggaley J., Crumpton I., Aldous P., Pokorny P., Janches D., Gural P. S., Samuels D., Albers J., Howell A., Johannink C., Breukers M., Odeh M., Moskovitz N., Collison J., Ganju S. (2018). “A survey of southern hemisphere meteor showers”. *Planetary Space Science*, **154**, 21–29.
- Jopek T. J. (1993). “Remarks on the meteor orbital similarity D-criterion”. *Icarus*, **106**, 603–607.
- Jopek T. J. and Kaňuchová Z. (2017). “IAU Meteor Data Center-the shower database: A status report”. *Planetary and Space Science*, **143**, 3–6.
- Korlević K., Šegon D., Andreić Z., Novoselnik F., Vida D., and Skokić I. (2013). “Croatian Meteor Network Catalogues of Orbits for 2008 and 2009”. *WGN, Journal of the International Meteor Organization*, **41**, 48–51.
- Kornoš L., Koukal J., Piffel R., and Tóth J. (2014). “EDMOND Meteor Database”. In: Gyssens M., Roggemans P., Zoladek, P., editors, *Proceedings of the International Meteor Conference*, Poznań, Poland, Aug. 22-25, 2013. International Meteor Organization, pages 23–25.
- Koseki M. (2019). “Problems in the meteor shower definition table in case of EDMOND”. *eMetN*, **4**, 265–270.
- Lindblad B. A. (1971). “A computerized stream search among 2401 photographic meteor orbits”. *Smithson. Contrib. Astrophys.*, **12**, 14–24.
- Neslušan L., Porubčan V., Svoreň J. (2014). “IAU MDC Photographic Meteor Orbits Database: Version 2013”. *Earth, Moon, and Planets*, **111**, 105–114.
- Sekanina Z. (1976). “Statistical model of meteor streams. IV. A study of radio streams from the synoptic year”. *Icarus*, **27**, 265–321.
- SonotaCo (2009). “A meteor shower catalog based on video observations in 2007-2008”. *WGN, Journal of the International Meteor Organization*, **37**, 55–62.
- Southworth R. R. and Hawkins G. S. (1963). “Statistics of meteor streams”. *Smithson. Contrib. Astrophys.*, **7**, 261–286.
- Warner Brian D., Stephens Robert D., Harris Alan W. (2011). “Save the Lightcurves”. *Minor Planet Bulletin*, **38**, 172–174.

Some Near Earth Objects and meteor associations

John Greaves

cpmjg@tutanota.com

The particular details of meteor orbits with D criterion similarity to Near Earth Objects 1999 LT₁, 2010 MU₁₁₁, (507716) = 2013 UP₈, 2015 RR₁₅₀ and 2020 BZ₁₂ are presented.

1 Introduction

A list of known Near Earth Objects (NEOs) was obtained from the Minor Planet Center⁶ and the 618 objects with inclinations of 40 degrees or greater were filtered out for assessment via the Jopek (1993) variation of the Southworth and Hawkins (1963) D criterion against publicly available meteor orbits from various sources utilizing a threshold value of 0.10. The meteor orbits are from a database of over a million compiled from the publicly available datasets of the SonatoCo Network (e.g. SonotaCo, 2009), CAMS (Jenniskens et al., 2018) and EDMOND (e.g. Kornoš et al., 2014) surveys.

Resultant orbits were then assessed in the cases where any particular NEO had ten or more meteor orbits matching with D criteria less than the threshold value. Amongst the many candidate associations many had few meteors involved, barely sufficient to suggest anything more than happenstance association. A handful had over a dozen meteors often from asteroids with Jupiter Comet Family like orbits according to their Tisserand Parameters relative to Jupiter as well as inclinations more appropriate for comets, although no cometary activity had ever been detected for them. One very recently discovered object has an orbit more like that of a long period comet and a high inclination that makes the orbit retrograde and despite only presenting against 8 meteor orbits is potentially of interest.

One, 2018 LF₅, is dealt with separately (Greaves, 2020). The others are the Amor 1999 LT₁, the Apollo 2010 MU₁₁₁, the numbered Apollo (507716) formerly known as 2013 UP₈, the Amor 2015 RR₁₅₀ and the long period comet-like orbit possessing 2020 BZ₁₂.

The associated meteors were assessed against the IAU MDC list⁷ (Jopek and Kaňuchová, 2017; Neslušán et al., 2014) of all showers to check if they matched any known showers.

2 Results

1999 LT₁

This object is listed as an Amor asteroid with a 2-opposition orbit from 64 observations and a total observational arc length of 1666 days (MPO 55865) at the time of writing. It's Tisserand Parameter with respect to Jupiter, T_J , is 2.6.

Table 1 carries the details for 19 meteor orbits matched to $D < 0.10$, with 5 of those having $D < 0.8$. *Table 1* also includes the mean and median values for the 19 as well as the orbital particulars for A/1999 LT₁ from the Minor Planet Center⁸.

Examination of the IAU MDC list of showers revealed no known shower fitting the results and the nearest bright star is ϵ Draconis, already used for the epsilon Draconids and the September epsilon Draconids. If a valid shower the name May epsilon Draconids is therefore tentatively suggested with the mnemonic code MED, neither of which appear to exist in the list at the time of writing.

2010 MU₁₁₁

This object is listed as an Apollo asteroid with a 2-opposition orbit from only 32 observations and a total observational arc length of 1582 days (MPO 460898) at the time of writing. It's Tisserand Parameter with respect to Jupiter T_J , is 3.0. *Table 2* carries the details for 12 meteor orbits all matched to $D < 0.09$ with 7 of them having $D < 0.08$. *Table 2* also includes the mean and median values for the 12 as well as the orbital particulars for A/2010 MU₁₁₁ from the Minor Planet Center³.

Examination of the IAU MDC list of showers revealed no known shower fitting the results and the brightest nearby star is 69 Draconis leading to the suggestion of the name 69 Draconids with mnemonic code SND.

(507716) = 2013 UP₈

This PANSTARRS discovered numbered object is listed as an Apollo asteroid with a 5-opposition orbit from 118 observations and a total observational arc length of 1505 days (MPO 434870) at the time of writing. It's Tisserand Parameter with respect to Jupiter T_J , is 2.8. It is also classed as a Potentially Hazardous Asteroid (PHA). *Table 3* carries the details for 15 meteor orbits matched to $D < 0.10$ with 8 of them having $D < 0.08$. *Table 3* also includes the mean and median values for the 15 as well as the orbital particulars for (507716) from the Minor Planet Center³.

Examination of the IAU MDC list of showers revealed no known shower fitting the results and the brightest nearby star is 45 Draconis leading to the suggestion of 45 Draconids with mnemonic code FFD.

⁶ <https://www.minorplanetcenter.net/iau/lists/MPLists.html>

⁷ <https://www.ta3.sk/IAUC22DB/MDC2007/>

⁸ <https://minorplanetcenter.net/>

Table 1 – The identifier, D criterion value relative to A/1999 LT₁, radiant position as Right Ascension and Declination in degrees, Solar Longitude λ_{\odot} in degrees, Geocentric Velocity v_g in kms^{-1} , perihelion distance q in Astronomical Units, eccentricity e , inclination i in degrees, Argument of Perihelion ω in degrees and Ascending Node Ω in degrees are given for each associated meteor orbit followed by their mean and median value and finally the orbital details of the asteroid.

ID	D	R.A.	Dec.	λ_{\odot}	v_g	q	e	i	ω	Ω
20190530_002421	0.049	296.5696	72.046	67.7215	25.7	0.9859	0.6298	42.321	158.325	67.722
CAMS188716	0.067	298.87	70.94	64.863	27.2	0.992	0.6693	44.81	161.46	64.857
ED20160525_204839	0.067	290.6732	71.9113	64.8305	25.2	0.9912	0.599	41.982	160.484	64.83
20180525_021906	0.072	296.5613	69.2908	63.2411	25.5	0.9939	0.6032	42.547	161.909	63.241
20140601_014519	0.080	301.3887	74.678	69.9599	24.7	0.9782	0.6268	40.2	155.317	69.96
20160527_211318	0.083	287.692	69.1166	66.4065	26.5	1.0003	0.6184	44.285	165.112	66.407
CAMS188593	0.087	295.88	75.41	63.9979	24.2	0.9868	0.6374	39.36	159.02	63.993
20190524_201937	0.088	290.2266	73.3848	62.7575	25	0.986	0.6063	41.253	158.502	62.758
CAMS60880	0.089	302.94	69.79	62.3837	27.3	0.9871	0.6401	45.5	159.29	62.379
ED20150602_222632	0.090	299.1996	73.8487	71.8569	25.3	0.98	0.5941	42.102	155.445	71.857
CAMS187944	0.091	294.33	70.17	60.1432	25.9	0.996	0.6304	42.94	163.49	60.137
20190527_010414	0.092	295.4971	70.4791	64.8685	24.6	0.9908	0.571	41.087	160.001	64.869
CAMS61352	0.093	307.86	77.9	68.1759	24.9	0.971	0.659	39.92	153.38	68.173
CAMS188411	0.095	307.02	70.22	63.7675	27.8	0.9807	0.6472	46.15	156.82	63.759
CAMS117211	0.096	296.68	67.95	61.2209	27	0.9975	0.6113	45.36	164.03	61.212
CAMS261002	0.098	298.82	67.59	62.7285	28	0.9966	0.6359	46.97	163.59	62.726
ED20140530_004838	0.099	306.0914	69.6913	68.3634	27.1	0.9857	0.5732	46.041	157.543	68.364
ED20140525_232754	0.099	300.715	72.1303	64.469	24.8	0.9867	0.5653	41.508	158.167	64.469
20180521_215101	0.099	289.2593	67.9863	60.178	26.5	0.9983	0.6115	44.515	164.58	60.178
Mean orbit		297.7	71.3	64.8386	25.9	0.9887	0.6173	43.097	159.814	64.836
Median orbit		296.7	70.5	64.469	25.7	0.9871	0.6184	42.547	159.29	64.469
1999 LT ₁						1.0797	0.6406	43	158.658	66.942

Table 2 – The identifier, D criterion value relative to A/2010 MU₁₁₁, radiant position as Right Ascension and Declination in degrees, Solar Longitude λ_{\odot} in degrees, Geocentric Velocity v_g in kms^{-1} , perihelion distance q in Astronomical Units, eccentricity e , inclination i in degrees, Argument of Perihelion ω in degrees and Ascending Node Ω in degrees are given for each associated meteor orbit followed by their mean and median value and finally the orbital details of the asteroid.

ID	D	R.A.	Dec.	λ_{\odot}	v_g	q	e	i	ω	Ω
CAMS119201	0.046	293.55	76.87	81.3434	24.7	0.9879	0.5975	40.9	158	81.336
CAMS262561	0.052	306.07	77.63	82.6673	26	0.9747	0.6107	43.06	153.32	82.66
CAMS323336	0.063	293.5	79.13	79.6551	23.7	0.9807	0.5949	38.85	155.29	79.651
CAMS366538	0.067	294.48	76.22	80.8635	26.1	0.9892	0.6559	42.79	159.2	80.86
CAMS119731	0.071	296.82	78.02	84.3372	25.8	0.9825	0.6393	42.42	156.34	84.331
CAMS323310	0.073	293.16	74.19	79.5454	26.1	0.9958	0.6384	43.21	161.91	79.539
ED060607MLA0042	0.074	292.4755	75.9827	76.0877	24.4	0.9887	0.6474	39.613	159.143	76.088
CAMS263009	0.080	305.24	79.4	85.6653	25	0.9705	0.5763	41.49	151.35	85.661
ED20150612_200334	0.081	292.7714	80.7285	81.3285	25.1	0.9655	0.6611	40.216	151.187	81.329
CAMS262293	0.082	281.43	75.87	80.013	23.9	0.9977	0.6152	39.13	162.63	80.008
CAMS119401	0.088	296.74	73.78	82.3868	26	0.9951	0.5877	43.77	160.96	82.38
20150608_000204	0.089	293.0258	71.4728	76.347	24.6	0.9945	0.5453	41.636	160.609	76.347
Mean orbit		294.9	76.6	80.8534	25.1	0.9852	0.6141	41.424	157.495	80.849
Median orbit		293.5	76.5	81.096	25	0.9883	0.613	41.563	158.572	81.094
2010 MU ₁₁₁						0.9236	0.6136	41.556	157.07	80.028

Table 3 – The identifier, D criterion value relative to (507716) = A/2013 UP₈, radiant position as Right Ascension and Declination in degrees, Solar Longitude λ_o in degrees, Geocentric Velocity v_g in kms^{-1} , perihelion distance q in Astronomical Units, eccentricity e , inclination i in degrees, Argument of Perihelion ω in degrees and Ascending Node Ω in degrees are given for each associated meteor orbit followed by their mean and median value and finally the orbital details of the asteroid.

ID	D	$R.A.$	$Dec.$	λ_o	v_g	q	e	i	ω	Ω
ED20140515_224742	0.029	277.5527	58.6422	54.8199	27.9	1.0087	0.6257	46.985	186.211	54.82
CAMS186887	0.037	274.71	57.37	53.3504	27.7	1.0053	0.6206	46.57	189.54	53.345
ED20130516_223157	0.049	274.9789	58.0514	56.0194	28.1	1.0075	0.6572	46.951	187.87	56.02
20180515_000427	0.054	272.6532	55.7486	53.5217	27.3	1.003	0.6019	46.106	191.601	53.522
20130517_235736	0.070	282.2388	55.1561	56.6789	29.7	1.0083	0.592	51.107	187.375	56.679
CAMS378672	0.071	273.18	54.9	51.6756	27.9	0.9987	0.5965	47.18	194.21	51.668
ED20120512_010417	0.075	274.4992	54.6666	51.5465	27.7	1.0003	0.5761	47.13	193.299	51.546
ED20140520_212501	0.079	282.7635	61.3374	59.5795	27.4	1.012	0.5997	46.424	180.289	59.58
ED20110518_004746	0.081	278.5779	58.4309	56.6116	26.5	1.0092	0.5547	45.257	186.246	56.612
ED20120510_231813	0.082	270.1031	54.4325	50.5097	28.1	0.9964	0.6327	47.058	195.139	50.51
ED20150517_233258	0.085	273.1841	57.654	56.5318	26.2	1.006	0.58	44.16	189.73	56.532
CAMS260770	0.090	271.61	55.17	55.0175	27.8	0.9975	0.6337	46.35	195.13	55.012
CAMS187374	0.092	279.45	54.07	56.2314	30.1	1.0015	0.623	51.18	192.88	56.224
20190512_213343	0.093	268.5764	58.2551	51.251	27.9	1.0056	0.686	46.026	188.539	51.251
ED20150510_013122	0.095	276.0887	54.7191	48.8887	29.6	1.0018	0.6418	49.914	191.38	48.889
Mean orbit		275.3	56.6	54.1489	28	1.0041	0.6148	47.226	189.963	54.147
Median orbit		274.7	55.7	54.8199	27.9	1.0053	0.6206	46.951	189.73	54.82
(507716) = 2013 UP ₈						0.9712	0.6176	47.775	187.331	55.187

Table 4 – The identifier, D criterion value relative to A/2015 RR₁₅₀, radiant position as Right Ascension and Declination in degrees, Solar Longitude λ_o in degrees, Geocentric Velocity v_g in kms^{-1} , perihelion distance q in Astronomical Units, eccentricity e , inclination i in degrees, Argument of Perihelion ω in degrees and Ascending Node Ω in degrees are given for each associated meteor orbit followed by their mean and median value and finally the orbital details of the asteroid.

ID	D	$R.A.$	$Dec.$	λ_o	v_g	q	e	i	ω	Ω
CAMS82383	0.044	247.89	74.57	172.6375	25.8	0.9978	0.4999	44.28	167.61	172.627
20070920_200856	0.051	257.4728	72.3115	177.0159	24.6	0.9986	0.485	42.156	169.217	177.016
ED20140916_030204	0.057	256.8135	71.6164	172.9829	24.5	1.0028	0.5306	41.449	172.892	172.983
ED20150921_211445	0.065	250.7663	71.1783	178.3557	24.6	0.9927	0.5345	41.322	165.432	178.355
20190918_213438	0.075	260.1872	74.4802	175.0426	26.4	0.9999	0.539	45.098	170.293	175.043
CAMS285290	0.077	256.07	72.76	170.8995	25.5	1.0028	0.5569	43.17	172.18	170.889
CAMS337741	0.079	247.73	68.03	176.4151	22.7	0.9957	0.5167	38.1	166.99	176.4
CAMS23764	0.091	257.42	72.1	171.8127	22.7	1.0033	0.4348	39.29	172.67	171.801
CAMS137830	0.091	259.16	73.86	172.3876	26.2	1.0038	0.5558	44.57	174.19	172.378
ED20160912_231210	0.093	269.5086	76.5899	170.2957	26.4	1.0051	0.4903	45.914	175.306	170.295
CAMS82463	0.095	250.9	72.71	172.903	26.3	0.9996	0.5842	44.1	169.73	172.894
CAMS214139	0.096	257.63	72.72	174.1129	25.9	1.003	0.5682	43.69	173.7	174.104
Mean orbit		256.0	72.7	173.7384	25.1	1.0004	0.5247	42.762	170.851	173.732
Median orbit		256.8	72.7	172.9829	25.5	1.0004	0.5306	43.17	170.851	172.983
2015 RR ₁₅₀						1.0234	0.498	42.146	167.287	174.23

Table 5 – The identifier, D criterion value relative to A/2020 BZ₁₂, radiant position as Right Ascension and Declination in degrees, Solar Longitude λ_\odot in degrees, Geocentric Velocity v_g in km s^{-1} , perihelion distance q in Astronomical Units, eccentricity e , inclination i in degrees, Argument of Perihelion ω in degrees and Ascending Node Ω in degrees are given for each associated meteor orbit followed by their mean and median value and finally the orbital details of the asteroid.

ID	D	$R.A.$	$Dec.$	λ_\odot	v_g	q	e	i	ω	Ω
20160116_030027	0.087	181.9745	-7.9802	294.7996	68.6	0.6767	0.9537	166.297	68.851	114.8
20120126_040025	0.089	190.4267	-10.7927	305.0414	67.3	0.6191	0.9023	167.126	77.44	125.041
ED20150119_032136	0.089	184.1106	-10.0283	298.5057	68.3	0.6562	0.9557	163.764	71.428	118.505
20100117_050453	0.093	184.5748	-7.7481	296.45	68.5	0.6805	0.9297	168.675	68.888	116.45
20170126_023227	0.095	189.8968	-11.7372	305.7104	67	0.6063	0.9089	164.895	78.868	125.711
20100118_031621	0.099	183.9011	-9.0527	297.3918	69	0.6744	0.9855	165.831	68.51	117.392
CAMS4076	0.100	190.59	-10.78	306.0152	68	0.616	0.955	168.21	76.5	126.012
20160117_015003	0.100	182.0922	-7.9284	295.7683	68.9	0.6648	0.9846	166.518	69.717	115.769
Mean orbit		185.9	-9.5	299.9603	68.2	0.6493	0.9469	166.414	72.525	119.96
Median orbit		184.3	-9.5	297.9488	68.4	0.6605	0.9543	166.407	70.572	117.949
2020 BZ ₁₂						0.6032	0.9217	165.541	57.613	105.723

2015 RR₁₅₀

This object is listed as an Amor asteroid with a 2-opposition orbit from only 56 observations and a total observational arc length of 1042 days (MPO 457018) at the time of writing. It's Tisserand Parameter with respect to Jupiter T_J , is 3.4. It is also classed as a Potentially Hazardous Asteroid (PHA). *Table 4* carries the details for 12 meteor orbits matched to $D < 0.10$ with 7 of them having $D < 0.08$. *Table 4* also includes the mean and median values for the 12 as well as the orbital particulars for A/2015 RR₁₅₀ from the Minor Planet Center³.

Examination of the IAU MDC list of showers revealed no known shower fitting the results and the brightest nearby star is ψ^1 Draconis, however there is already a psi Draconids shower (POD#754). As the shower occurs in September the name September psi1 Draconids is tentatively suggested as the mnemonic code of SPD doesn't appear to exist at this time.

2020 BZ₁₂

This object is listed as an Apollo asteroid with a 1-opposition orbit from only 135 observations but with a total observational arc length of only 56 days (MPEC 2020-E49) yet its highly retrograde orbit and semimajor axis with an aphelion between the orbits of Saturn and Uranus (14.8 A.U.) are more suggestive of a long period comet albeit of relatively short orbital period (21.4 years). At the time of writing (27th April 2020) it is just at perihelion and behind the Sun from the Earth's perspective, with the last MPC observation being for mid-March. If picked up again after its passage behind the Sun when it will again approach the Earth from a few weeks onwards the additional observations and extension of the orbital arc may well modify the derived orbit, and possibly even show some hint of cometary activity following perihelion if it shows any such at all. *Table 5* carries the details for 8 meteor orbits matched to $D < 0.10$ with none of them having $D < 0.08$. *Table 5* also includes the mean and median values for the 8 as well as the orbital particulars for A/2020 BZ₁₂ from the Minor Planet Center³.

Examination of the IAU MDC list of showers revealed no known shower fitting the results and the brightest nearby star is 21 Virginis, however there has been a shower in the IAU MDC bearing that name in and a mnemonic code in the past (now removed) so such a classification would be problematic. More importantly as the orbit of A/2020 BZ₁₂ is still not necessarily well defined and with the nodes not crossing near Earth's orbit, plus the number of meteor orbits being small in tandem with their D criteria all clustered in the range 0.087 to 0.100, this is a weak candidate for meteor asteroid association and no shower is going to be nominated here based on this current limited data.

Nevertheless, it is included here due to its recent journey through the inner Solar System in tandem with its current perihelion passage having the potential to lead to meteor enhancement in late January 2021 around Solar Longitude 300 degrees. On the other hand, with the relevant nodal point being at the pre-perihelion arc of the orbit and not being that near to Earth's orbit even if any fresh meteoroids are liberated during the current perihelion passage, they may take years to evolve into orbits likely to intersect the Earth itself.

3 Discussion

Given that these objects are not only observationally but, in some cases, intrinsically faint little is known of their nature there being no spectral reflectance or visual albedo data to speak of. Equally there are no data to distinguish between them being either comets or asteroids. Jupiter Family Comets and Near-Earth Objects may on the whole derive from different source populations yet their orbits have each evolved as a consequence of multiple interactions with Jupiter, which would also lead to some commonality in Jovian Tisserand Parameters. In recent times, as dramatically demonstrated by (101955) Benu, asteroids have also been shown to be potential sources of dust ejection and in the aforementioned case of (101955) Benu the YORP effect upon the asteroid in tandem with its

unconsolidated nature is a good candidate for the mechanism of dust ejection.

Neither do the orbital characteristics present any particular evidence to distinguish between comet and asteroid for it is not impossible for the Kozai cycle to pump up planar orbits into higher inclinations during their orbital evolution due to Jupiter's influence. Certainly, the higher inclination asteroid orbits are in the minority, the higher the inclination the more so.

Four of these showers, five if the one associated with 2018 LF₅ is included, have radiant clusters around the North Ecliptic Pole. There appears to be no great significance to this as in common with many NEOs all these objects have orbits with aphelia near Jupiter's orbit and perihelia near Earth's. They also have similar inclinations of just over 40 degrees, so despite having a range of Ascending Nodes (and correspondingly Solar Longitudes) and Arguments of Perihelia and the orbits being quite different the orbits do have similarity of shape. Not being an orbital dynamicist the author assumes that this is simply a geometric effect and that the showers are no more associated with each other than the asteroids are.

Over the years many meteor showers have been predicted for asteroids with next to no confirmation for any. However over the past decade or so various professional sky surveys have led to an explosion in both known asteroids and especially known Near Earth Objects down to fainter and fainter magnitudes and sometimes smaller and smaller sizes, increasing the number of candidates, whilst over a similar time period the availability of meteor orbits has increased far more impressively. Nevertheless, despite the explosion in data it seems candidate associations are still few and far between.

In these current predictions two of the objects are classed as Potentially Hazardous Asteroids, that is objects having the potential of Earth impact. If the predicted meteor shower associations are valid then in some ways they already have!

Acknowledgments

The online data services for the Minor Planet Center at the Harvard and Smithsonian Center for Astrophysics were utilized for obtaining the asteroid orbit details.

References

- Greaves J. (2020). "Meteors and 2018 LF₅". *eMetN*, **5**, 290–294.
- Jenniskens P., Baggaley J., Crumpton I., Aldous P., Pokorny P., Janches D., Gural P. S., Samuels D., Albers J., Howell A., Johannink C., Breukers M., Odeh M., Moskovitz N., Collison J., Ganju S. (2018). "A survey of southern hemisphere meteor showers". *Planetary Space Science*, **154**, 21–29.
- Jopek T. J. (1993). "Remarks on the meteor orbital similarity D-criterion". *Icarus*, **106**, 603–607.
- Jopek T. J. and Kaňuchová Z. (2017). "IAU Meteor Data Center-the shower database: A status report". *Planetary and Space Science*, **143**, 3–6.
- Kornoš L., Koukal J., Piffel R., and Tóth J. (2014). "EDMOND Meteor Database". In: Gyssens M., Roggemans P., Zoladek, P., editors, *Proceedings of the International Meteor Conference*, Poznań, Poland, Aug. 22-25, 2013. International Meteor Organization, pages 23–25.
- Neslušan L., Porubčan V., Svoreň J. (2014). "IAU MDC Photographic Meteor Orbits Database: Version 2013". *Earth, Moon, and Planets*, **111**, 105–114.
- SonotaCo (2009). "A meteor shower catalog based on video observations in 2007-2008". *WGN, Journal of the International Meteor Organization*, **37**, 55–62.
- Southworth R. R. and Hawkins G. S. (1963). "Statistics of meteor streams". *Smithson. Contrib. Astrophys.*, **7**, 261–286.

Results of spectral observations of meteor showers and sporadic meteors from October 2018 until May 2020

Takashi Sekiguchi

Nippon Meteor Society
SonotaCo network

ts007@mtj.biglobe.ne.jp

I present a survey of 1596 spectra obtained from October 2018 until May 2020. Meteor spectra that include sporadic meteors as well as members of minor and major meteor showers. These meteors are in the absolute magnitude range from +2.6 to -8 . The overall spectrum type for sporadic meteors showed mostly similar distributions. In addition, the Quadrantids, the Perseids, and the Geminids could be analyzed more in detail than other major meteor showers. The Quadrantids and the Geminids could be classified into four types. The types of other major meteor showers differed depending upon the meteor stream. Even minor meteor showers with three or more spectra showed differences. Na Free and Na Poor were observed in the Quadrantids and Geminids and Southern δ -Aquariids and several minor meteor showers. An Fe content rate with more than 50% is considered to be intermediate with Irons, we have several suspected Iron meteoroids and minor meteor shower parent bodies.

1 Introduction

Borovička et al. (2005) published a survey of the spectra of 97 sporadic meteors. The luminous intensity was obtained in high-sensitivity video, mainly in the magnitude range from +3 to 0. The spectra were classified into seven categories according to the relative line intensities of Mg, Na, and Fe. Moreover, three different populations of meteoroids without Na were identified. Vojáček et al. (2015) presented a catalog of 84 video spectra of both sporadic and shower meteors obtained for meteors from magnitude +2 to -3.5 . This is representative in the sense that it includes everything as a catalog of observed sporadic meteors as well as major meteor showers.

This study was started by an investigation of what can be obtained from a large amount of spectral data with many cameras compared to the studies made by Borovička et al. and Vojáček et al. Major and minor meteor shower as well as sporadic meteor results are considered for future research.

2 Observing equipment

The equipment to register spectra consists of a color SONY alpha 7s camera with a 50 mm f 1.4 lens with a transmission diffraction grating film of 500 lines per mm as spectrometer. From 2018 October 01 until 2019 December 03 Standard definition (SD) was used and from 2019 December 03 to May 2020 full high definition (FHD) was used. Furthermore, seven black and white cameras were used, four Watecs Neptune 100+ with CBC 6 mm lenses, one with a 12 mm f 0.8 lens, two Watecs 902H2U with CBC lenses of 6 mm and 8 mm with f 0.8. Some cameras had a spectrometer, from 2018 December 18 until 2020 May

these used SD. From the observations so far, the resolution for Fe is rather poor in SD. In FHD, the resolution increased and Fe became clearly visible (*Figure 1*).

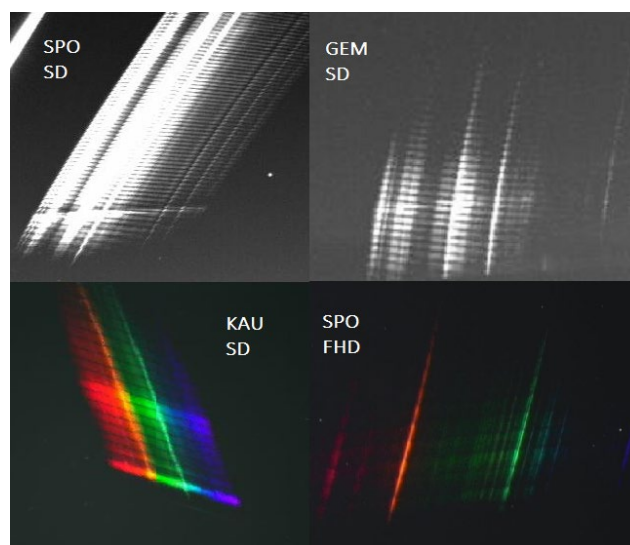


Figure 1 – Spectral photographs obtained with these cameras.

3 Observing and orbital calculation software

The author uses the software UFOCaptureV2, UFOCaptureHD2, UFOAnalyzer V2 and UFOOrbitV2⁹. These programs identify identical events and perform the triangulation calculations for the SonotaCo net's meteor data. Since each observing person has different conditions such as cameras and weather, there are variations in accuracy. For simultaneous events from three or more points, the orbit is determined based on the best fit solution.

⁹ <http://sonotaco.com/>

4 Spectral analysis software

The Japanese version of the spectral analysis software Rspec¹⁰ has been used. In each spectrum analysis, a triangular diagram is created with the peak ratios including rotation, tilt correction, background correction and sensitivity correction. There may be a difference of about 5 to 10% when comparing without sensitivity correction, also in the peak area ratio. This time, I am applying the sensitivity correction because I use many cameras. Most of them measure the whole path, but some of them include only a part of the emission point with either the part of the extinction point or the part with the explosion point.

Saturated meteors are measured in the unsaturated area.

5 Triangular diagrams

The software CKTriangle¹¹ is used to create the triangular or ternary diagrams for the 1596 spectral observations of October 2018 to May 2020 captured by eight cameras. The distribution of Na (5892 Å), Mg (5182 Å) and Fe (5269–5441 Å) is displayed by a triangle diagram. I refer for the classification to the article by Borovička et al. (2005):

- Iron meteoroids are these where the Na line is missing and the Mg line is much fainter than in normal spectra. Given that most of the light is emitted by Fe atoms (e.g. Figure 2).
- Na-free meteoroids are defined as those without the Na line but not classified as Irons. They fall into the region close to the left edge of the ternary diagram.

- Na-rich meteoroids are these dominated by the Na line. The Na/Mg and Na/Fe ratios are obviously higher than expected for chondritic meteoroids.

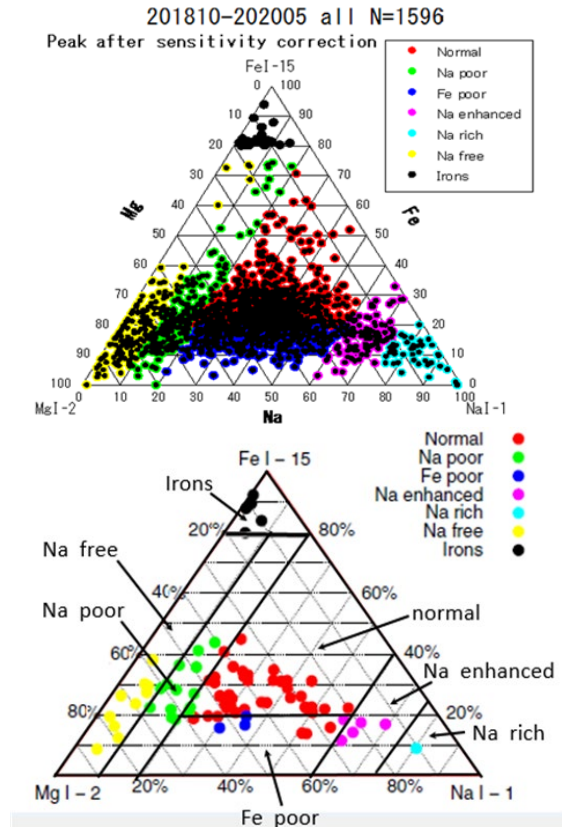


Figure 2 – The triangle diagram displaying the relative line intensities of Na, Mg and Fe. The triangle (top) is for the 1596 spectra, obtained from October 2018 until May 2020 for this work. The triangle (bottom) is taken from Vojáček et al. (2015).

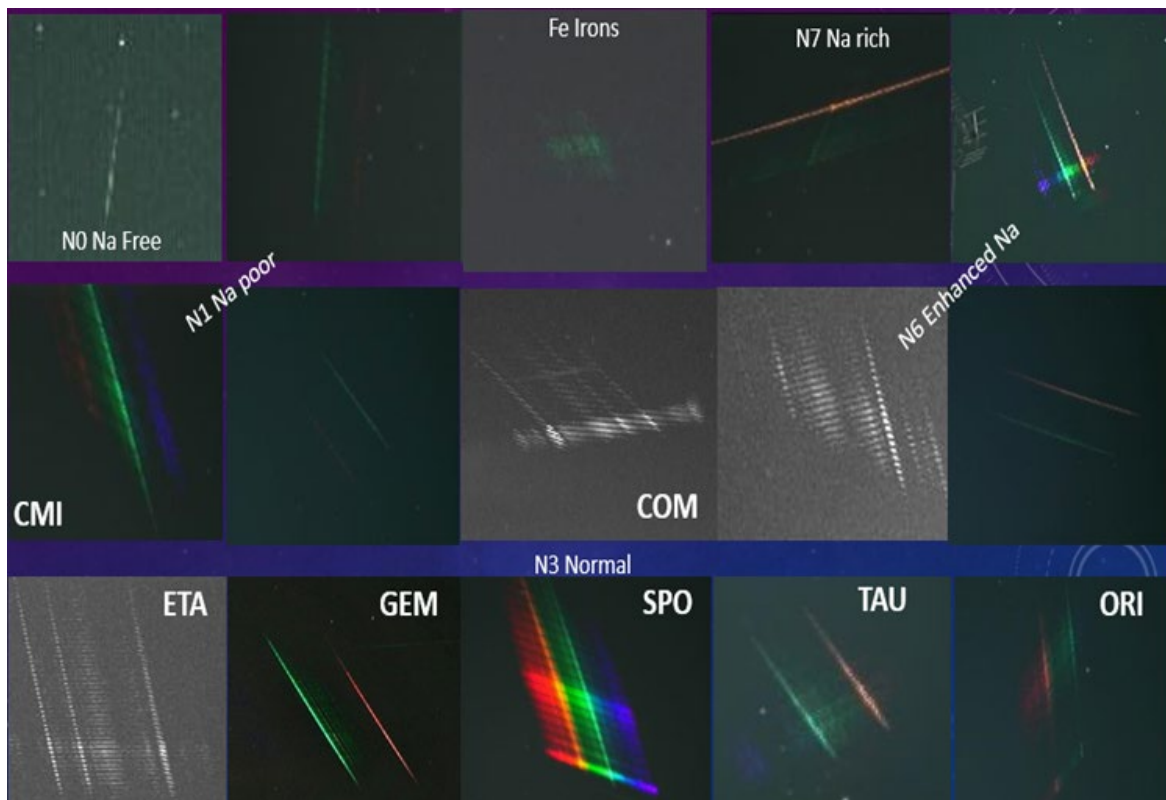


Figure 3 – Examples of spectrograms by type.

¹⁰ <https://www.rspec-astro.com/>

¹¹ <https://clikington-saito.com/CKTriangle/CKTriangle.html>

- Normal meteoroids are mainstream meteoroids lying near the expected position for chondritic bodies in the Mg–Na–Fe diagram or with somewhat lower Fe intensity.
- Na-poor meteoroids are mainstream meteoroids with the Na line significantly weaker than expected for the given velocity but still well visible.
- Enhanced-Na meteoroids are defined as those with the Na line obviously brighter than expected for the given meteor velocity but not so dominant as in Na-rich meteoroids.
- Fe-poor meteoroids are mainstream meteoroids having the expected Na/Mg ratio but with Fe lines too faint to be classified as Normal meteoroids. In this paper, Normal types with iron content of 20% or less are classified as Fe poor.

The 1596 meteor spectra include sporadic meteors and members of minor and major meteor showers. These meteors are in the absolute magnitude range from +2.6 to –8. There are many Normal types. There are only few Na rich meteoroids and Irons. Compared to the paper by Vojáček et al. (2015), there are many, about 50 to 80%, of the spectra of meteors with Na enhanced, Na rich, Fe poor and Fe contents. The distribution trends are similar (Figure 2). Examples of spectrograms are given in Figure 3.

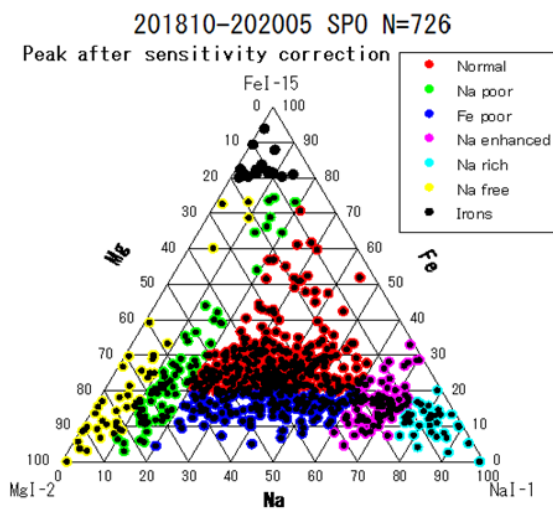


Figure 4 – The triangle diagram displaying the relative line intensities of Na, Mg and Fe for the 726 sporadic meteor spectra obtained from October 2018 until May 2020.

726 meteor spectra were obtained for sporadic meteors. Like for all meteors, there are many Normal types among these sporadics. Twenty-one Irons were analyzed. Nearly 25 meteors with 50% or more Fe are present, and there are many intermediate meteors in which the Fe component can be seen at the start of the light emission. In addition, the distribution of sporadic meteors is similar to the distribution of all meteors, except for some meteor showers. Therefore, we believe that this distribution is reliable (Figure 4).

The type differs depending on the meteor shower. The Quadrantids (QUA#010) and the Geminids (GEM#004)

spectra can be divided into four types. These are Na free meteoroids, Normal meteoroids, Na-poor meteoroids and Fe poor meteoroids. The Perseids (PER#007) are Normal meteoroids and Fe-poor meteoroids.

The Geminids had a different type of distribution from year to year¹², probably due to the difference in the dust trail distribution.

The Geminids have a higher proportion of Na free and Na poor meteoroids compared to the Quadrantids. (Figure 5).

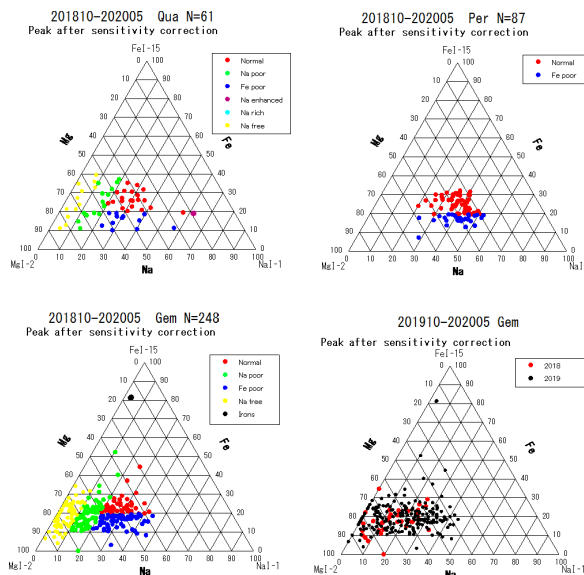


Figure 5 – The triangle diagrams displaying the relative line intensities of Na, Mg and Fe for the Quadrantids, the Perseids, and the Geminids spectra during the period October 2018 to May 2020.

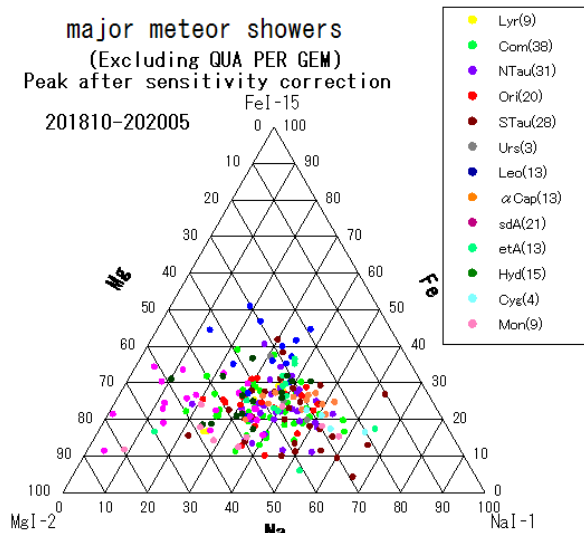


Figure 6 – The triangle diagram displaying the relative line intensities of Na, Mg and Fe for 13 major meteor showers excluding the Quadrantids, the Perseids and the Geminids spectra during the period October 2018 to May 2020.

A concentration can be seen in the Normal type. The σ -Hydrids (HYD#016), α -Capricornids (CAP#001), Ursids (URS#015) and η -Aquiriids (ETA#031) are Normal meteoroids. The Coma Berenicids (COM#020), April

¹² <http://sonotaco.jp/forum/viewtopic.php?t=4555>

Lyrids (LYR#006), Orionids (ORI#008) and the December Monocerotids (MON#019) are Normal meteoroids and Fe poor meteoroids. The Southern δ -Aquariids (SDA#005) were observed as Na free meteoroids, Na poor meteoroids and Normal meteoroids. The κ -Cygnids (KCG#012) are Normal meteoroids and Na enhanced meteoroids. The Leonids (LEO#013) are Normal meteoroids and have a higher Fe content than the others. Northern Taurids (NTA#017) and Southern Taurids (STA#002) cover a wider area than any other meteor showers. Most of them were Normal type, but no Irons (Figure 6).

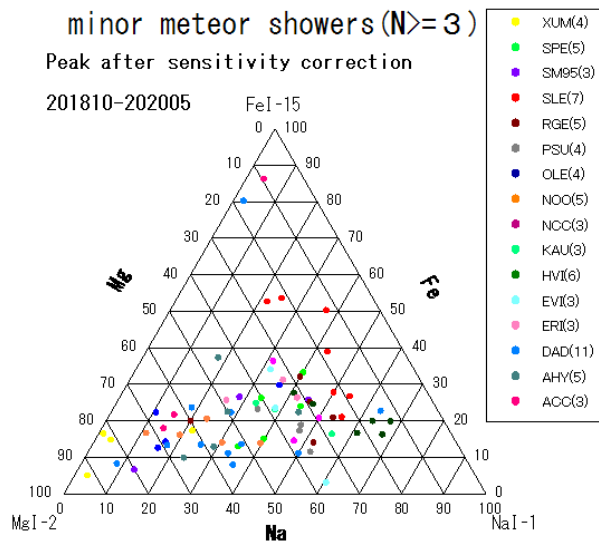


Figure 7 – The triangle diagram displaying the relative line intensities of Na, Mg and Fe for 16 minor meteor showers ($N \geq 3$) during the period October 2018 to May 2020.

(HVI#343) stream has mostly Enhanced-Na meteoroids. The σ -Leonids (SLE#136) stream has about half, from 40% to nearly 50%, of Fe. The ρ -Geminids (RGE#094) and α -Hydrids (AHY#331) streams contain mostly Normal meteoroids. The September ϵ -Perseids (SPE#208) shower has Normal meteoroids and Fe poor meteoroids. The o-Leonids (OLE#515) stream consists of Na poor meteoroids (Figure 7).

59 Iron meteoroids in which the Fe content was determined to be 50% or more, were identified from the graph of Mr. Maeda's classification (Figure 8). The areas N6 and N7 appear denser in the classification than in the study by Borovička (2005) (Figure 9).

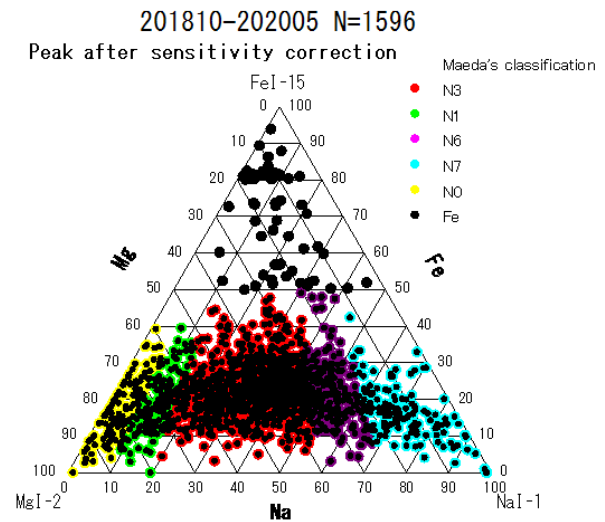


Figure 9 – Triangle diagram created by Maeda's classification.

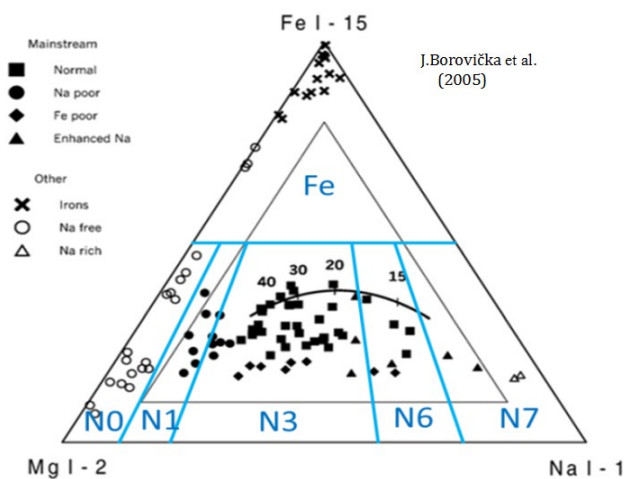


Figure 8 – The triangle diagram displaying Maeda's classification (Maeda and Yasunori, 2016).

6 Percentage of classification compared to Mr. Maeda

Normal meteoroids represent about half in both pie charts shown in Figure 10. Other types are slightly different, but this is assumed to be due to the observation period, the cameras, the lenses, etc. In this paper, the number of cases in N6 and N7 are larger and smaller for N1 because we used mainly lenses with a shorter focal length than Maeda, so there are many low speed fireball cases and less faint meteors can be captured. In addition, it seems that Mr. Maeda has a better resolution, so the difference in the number of Iron meteoroids is more apparent (Figure 10).

The minor showers cover a wider area than the major meteor showers. There are many Normal and Fe poor meteoroids everywhere. The January χ -Ursae Majorids (XUM#341) stream has mostly Na free meteoroids and Na poor meteoroids. The November Orionids (NOO#250) stream has mostly Fe poor meteoroids and Na poor meteoroids. The α -Cancriids (ACC#266) stream has mostly Na poor meteoroids and one Iron. The December α -Draconids (DAD#334) stream has Na free meteoroids and Na poor meteoroids and one Iron. The h-Virginids

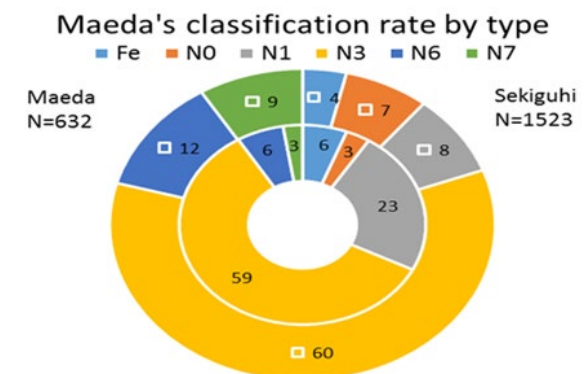


Figure 10 – Comparison of classification ratios for all meteors by Mr. Maeda. The inside is for Mr. Maeda. The outside is this paper.

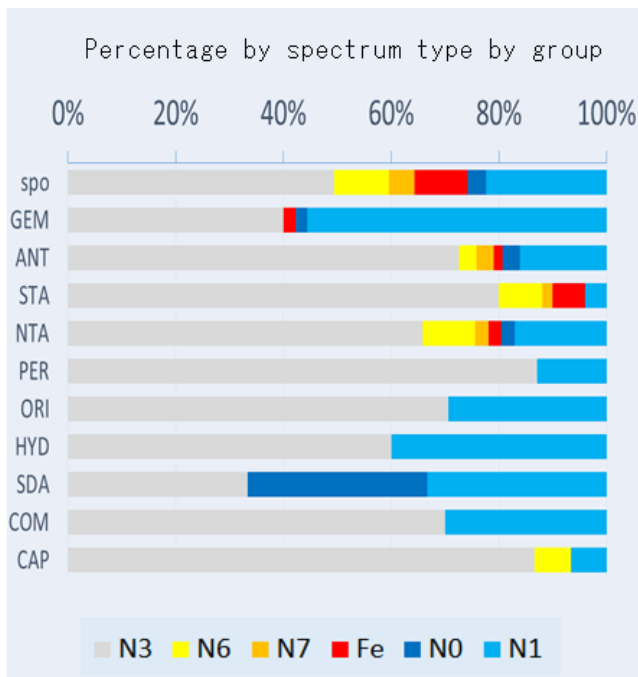


Figure 11 – Ratio by type by meteor shower according to Mr. Maeda.

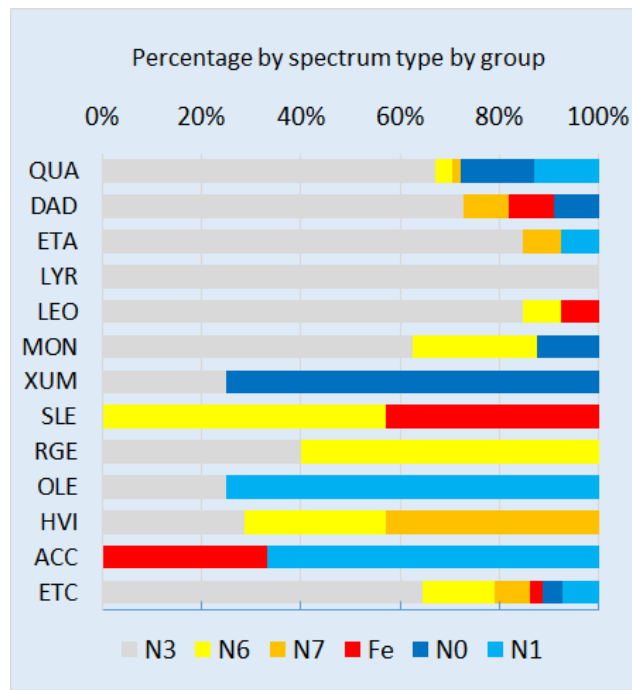


Figure 13 – Ratio by type by meteor shower according to this paper for minor meteor showers other than those in Figure. 12.

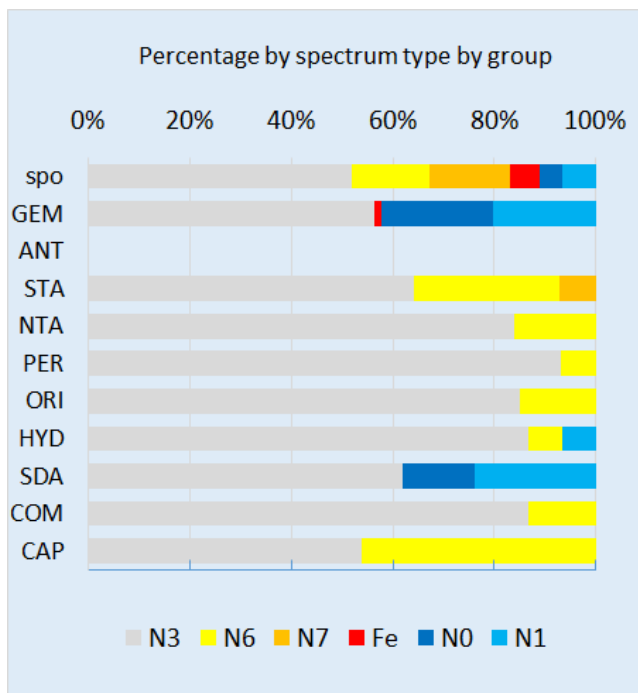


Figure 12 – Ratio by type by meteor shower according to this paper.

Figures 11 and 12 as a whole tend to show many Normal meteoroids for most of the meteor streams. Both SPO, GEM#004 and SDA#005 are very similar. The other streams are similar in the sense that these contain many Normal meteoroids, but differences can be seen for some types. Therefore, it can be concluded that there is a difference in composition depending on the meteor stream (Figures 11 and 12). The major meteor showers show mainly Normal meteoroids, but minor meteor showers display a clear difference in composition depending on the meteor showers (Figure 13).

The minor meteor showers XUM#341, OLE#515 and ACC#266 had a N0 + N1 ratio close to 70% (see Figure 14). In the major meteor showers, the Geminids, (GEM#004), the Southern δ -Aquariids (SDA#005) and the Quadrantids (QUA#010) have values of 30 to 40%. These meteor showers may be depleted of Na. Except for the QUA#010 and ACC#266, the perihelion distance q is 0.2 A.U. or less, which are Sun-approaching orbits. ACC#266 has a high value of two thirds for N0 + N1, one third are iron meteoroids, and the perihelion distance q is about 0.4 to 0.6 A.U. (Figure 14).

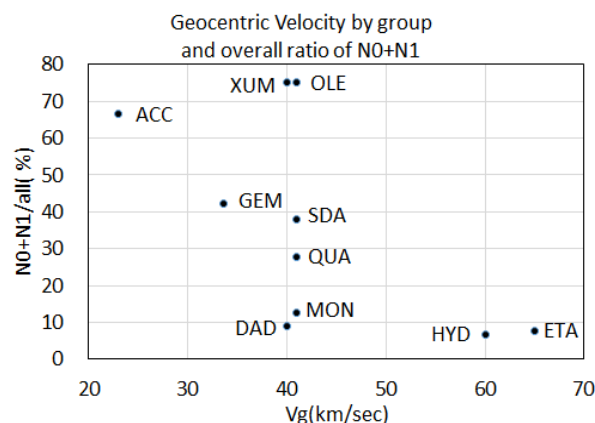


Figure 14 – Ratio N0 + N1 for each meteor shower (Number of spectra N >= 3) in the period October 2018 to May 2020.

7 Radiant point distribution

The radiant points of major and minor meteor showers appear as a number of concentrations. This can be seen at different positions for most of the velocity classes. (Figure 15).

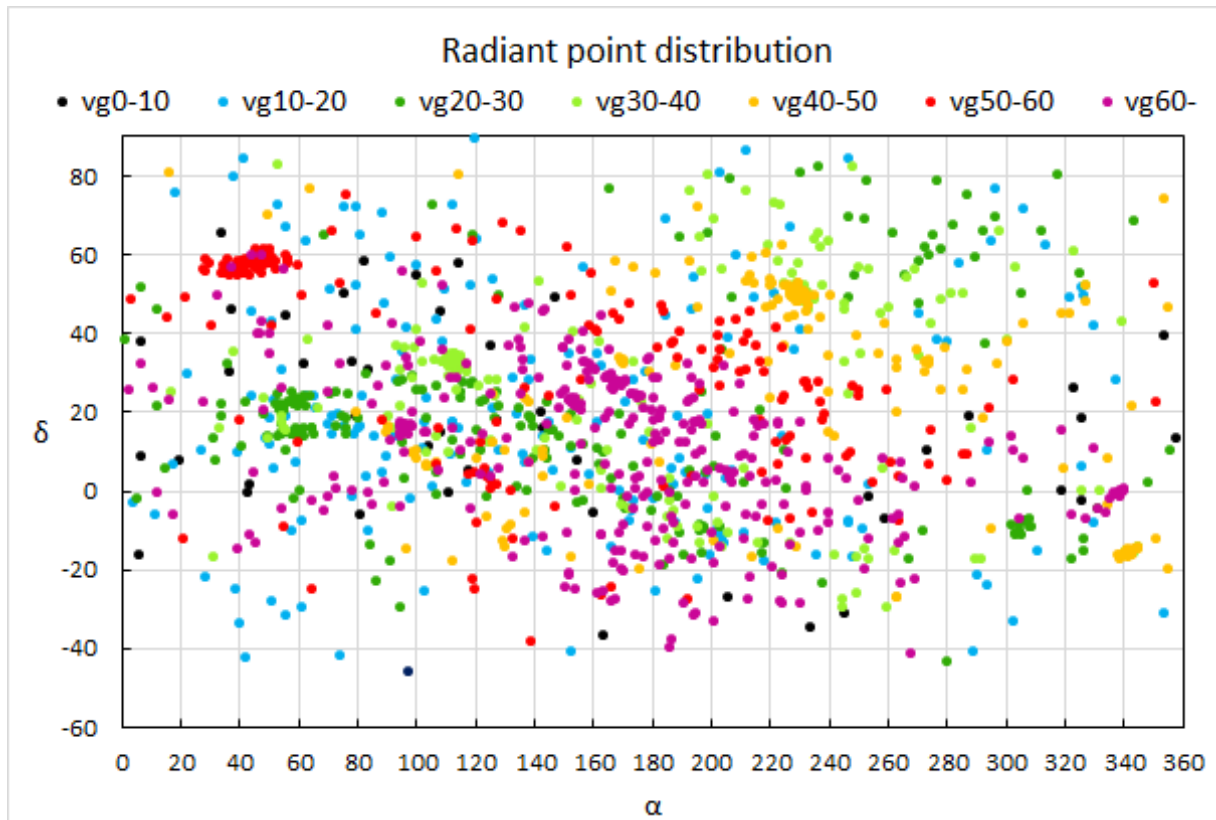


Figure 15 – Radiant distribution map in equatorial coordinates with a color code for the velocity.

8 Measured Na/Mg line intensity ratio

The Na/Mg line intensity ratio in function of the geocentric velocity v_g has been plotted in Figure 16. The overall trend changes with the same slope until about 30 km/sec, comparable to the result of Borovička (2005) and Vojáček (2015). Above 30 km/sec, there is no effect on the Na ratio visible in function of the velocity. It is the composition itself that changes. This graph also shows that the Quadrantids (QUA#010) with $v_g = 41$ km/s, the Geminids (GEM#004) with $v_g = 34$ km/s and the Southern δ -Aquariids (SDA#005) with $v_g = 41$ km/s have a large amount of Na free meteoroids and Na poor meteoroids (Figure 16).

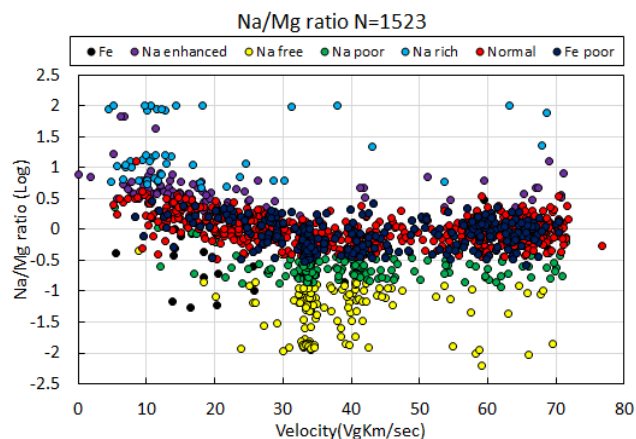


Figure 16 – The Na/Mg ratio (Log) plotted in function of the geocentric velocity for all spectra during the period October 2018 to May 2020.

According to Maeda’s classification, each type can be

clearly seen separately. The lower the speed, the more Na rich. The fact that a little higher speed can be seen is probably due to the difference in composition. There are a few numbers where the velocity is around 50 km/sec. There are only few Irons and all have a low velocity (Figure 17).

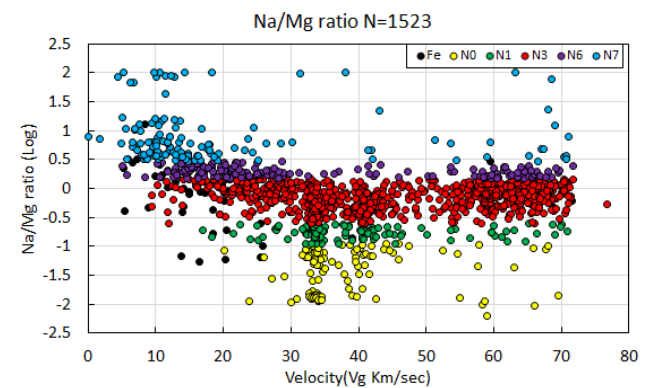


Figure 17 – The Na/Mg ratio (Log) plotted in function of the geocentric velocity for all spectra according to the classification by Maeda.

9 Measured O/Mg line intensity ratio

The O/Mg line intensity ratio in function of the geocentric velocity v_g (Vojáček et al., 2015) has been plotted in Figure 18, based upon 802 meteors obtained with a black and white camera. The proportion of O increased as the velocity increased, and the tendency is similar to the results obtained by Vojáček et al. (2015). The number of Na enhanced meteoroids and Na rich meteoroids is larger at velocities below 25 km/sec (Figure 18).

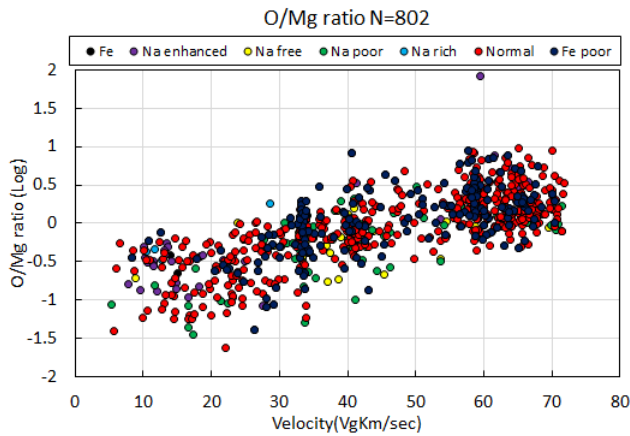


Figure 18 – O/Mg ratio (Log) in function of the geocentric velocity v_g for 802 meteors obtained with a black and white camera during the period from October 2018 to May 2020.

10 Relationship between meteor emission altitude and velocity

The tendency that the height of the beginning of light emission becomes lower as the speed becomes slower can be well seen in Figure 19. Looking by type, most of the iron meteoroids and the Na-free meteoroids start to ablate at lower heights than all other types. Na rich meteoroids and Na enhanced meteoroids are most common for meteors slower than 30 km/sec. Normal meteoroids can be seen throughout the entire distribution. Fe poor meteoroids are mainly found among medium-speed and high-speed meteors.

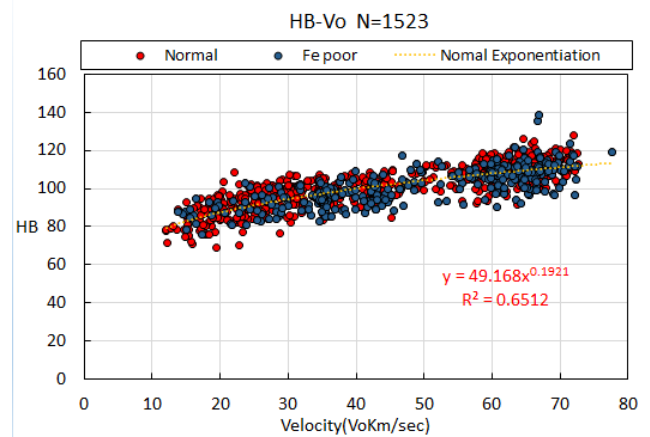
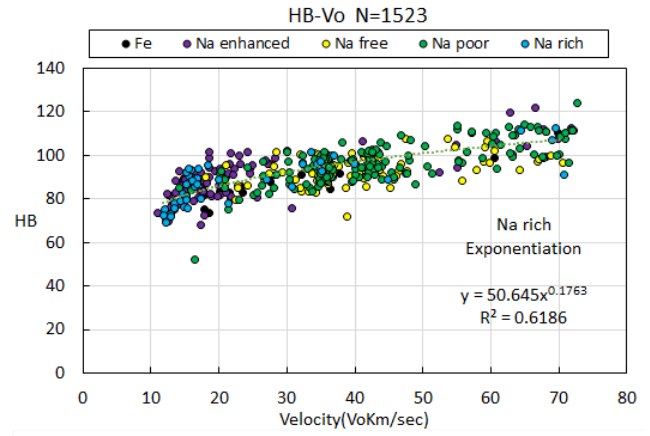


Figure 19 – Relationship between the meteor beginning altitude of light emission and the observed velocity for the different types.

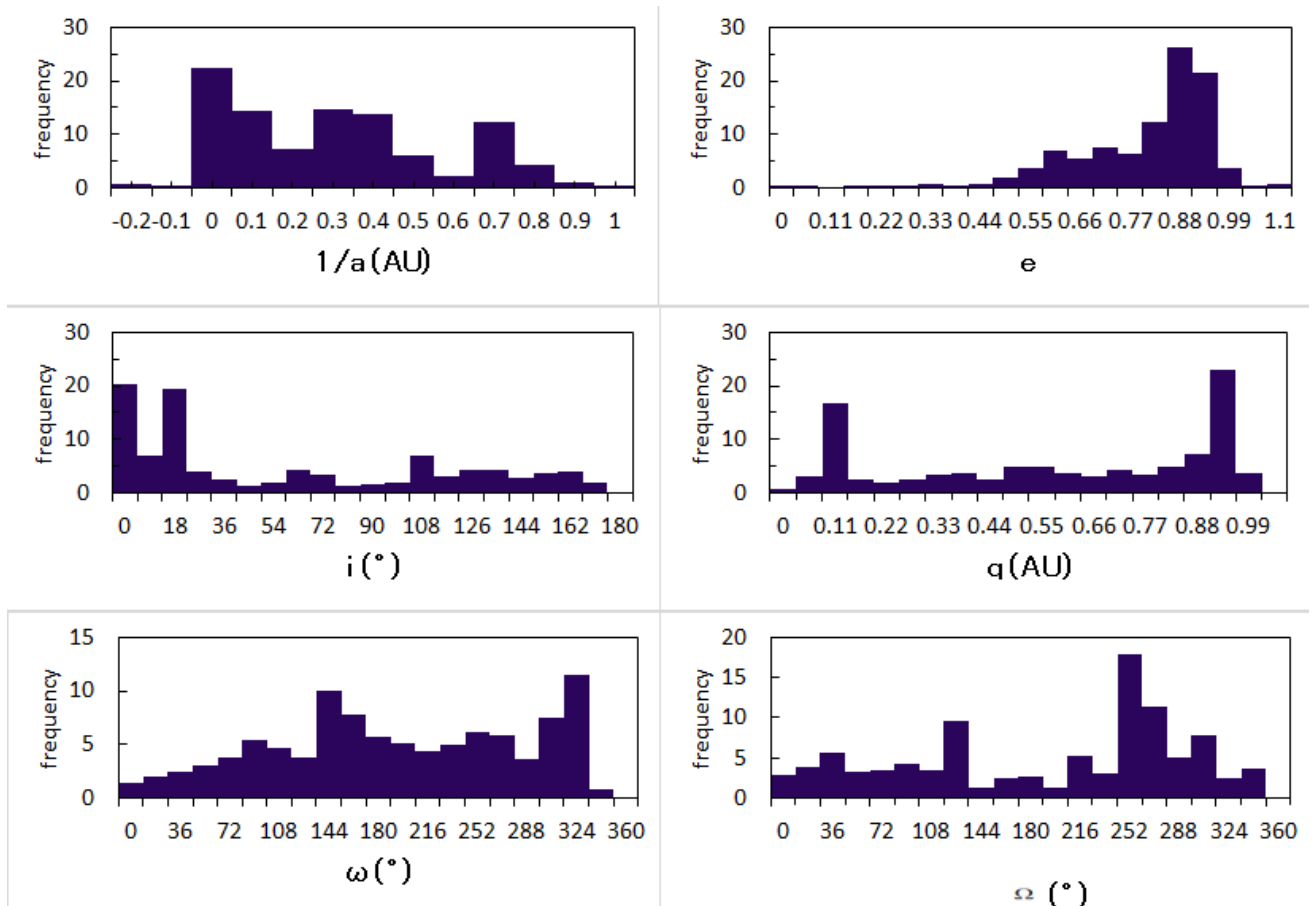


Figure 20 – Histograms for the orbital elements of meteoroids with a meteor spectra. a is the major axis of the meteoroid, e is the eccentricity, i is the inclination, q is the perihelion distance, ω is the argument of periaapsis and Ω is the ascending node.

11 Meteoroid orbits

The geocentric and heliocentric orbits are known for all 1523 meteors from double-station observations. This had been achieved for almost a year ago or more. Many orbit calculations were possible not only for sporadic meteors but also for the major and minor meteor showers. The distribution for each orbital element is displayed in *Figure 20*. Peaks can be explained by the presence of a large contribution by some major showers.

12 Relationship with orbital elements

In this section we consider the relationship with the orbital elements. The Tisserand parameter relative to Jupiter can be computed from;

$$T_J = \frac{a_J}{a} + 2 \cos i \sqrt{\frac{a(1 - e^2)}{a_J}}$$

Where $a_J = 5.2$ A.U. is the semimajor axis of Jupiter, a is the semimajor axis of the meteoroid and e is the eccentricity of the meteoroid. Five classes of meteoroid orbits were defined by Borovička et al. (2005):

- (SA) *Sun-approaching orbits* with $q < 0.2$ AU. Orbits with small perihelion distances are defined as a separate class.
- (ES) *ecliptic shower orbits*: Members of ecliptic meteor showers. For example, the Taurid meteors derived from the comet 2P/Encke and other showers with orbits close to the boundary between asteroids and Jupiter family comets.
- (HT) *Halley-type orbits*: $T_J < 2$ or $2 < T_J < 3$ and $i > 45^\circ$.
- (JF) *Jupiter-family orbits*: $2 < T_J < 3$ and $i < 45^\circ$ and $Q > 4.5$ AU.
- (A-C) *Asteroidal-chondritic orbits*: $T_J > 3$ or $Q < 4.5$ AU.

Most of the Na rich meteoroids are sporadic meteors with mainly Asteroidal-chondritic orbits. Many Na enhanced meteoroids are often sporadic meteors with Asteroidal-chondritic orbits. In addition, some meteors with ecliptic shower orbits were recorded. Other types are in general widespread. For Normal meteoroids and Fe poor meteoroids, the Halley-type orbits are often seen, more than the Asteroidal-chondritic orbits (*Figure 21*).

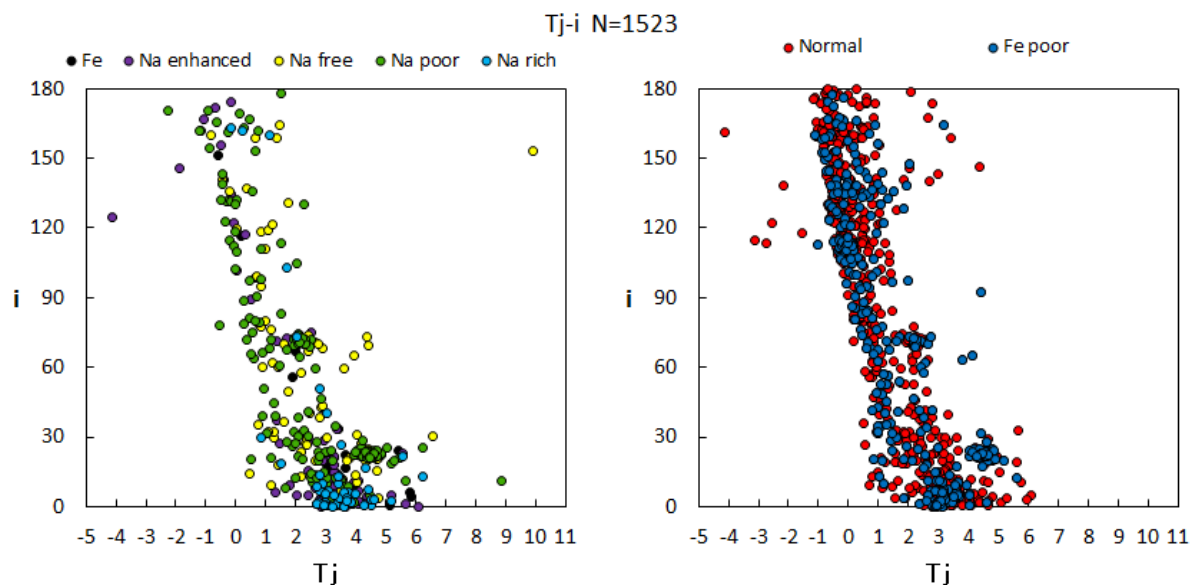


Figure 21 – Na distribution against inclination i and T_j .

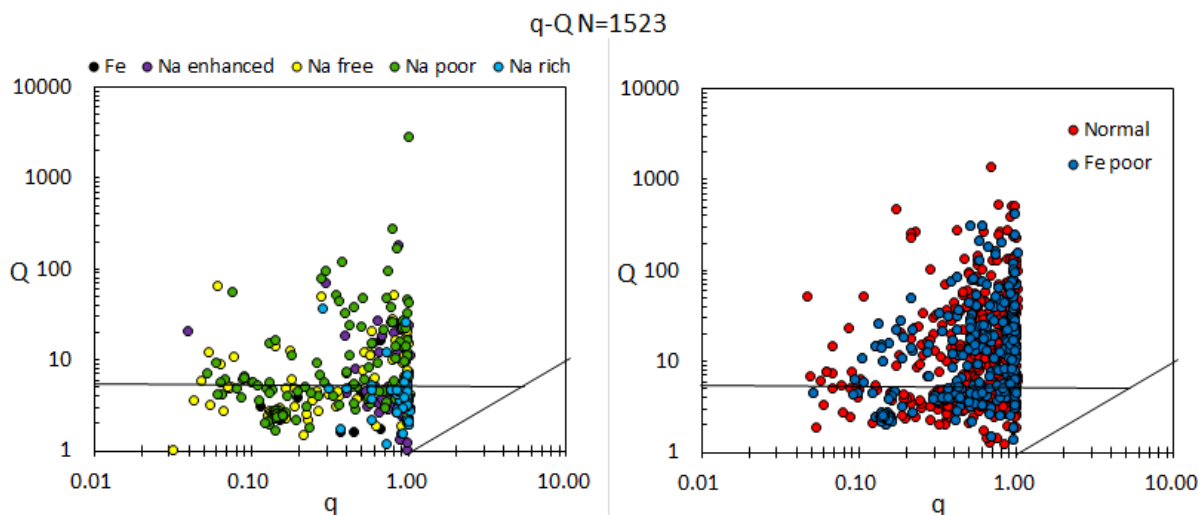


Figure – 22 Na distribution against aphelion Q and perihelion q .

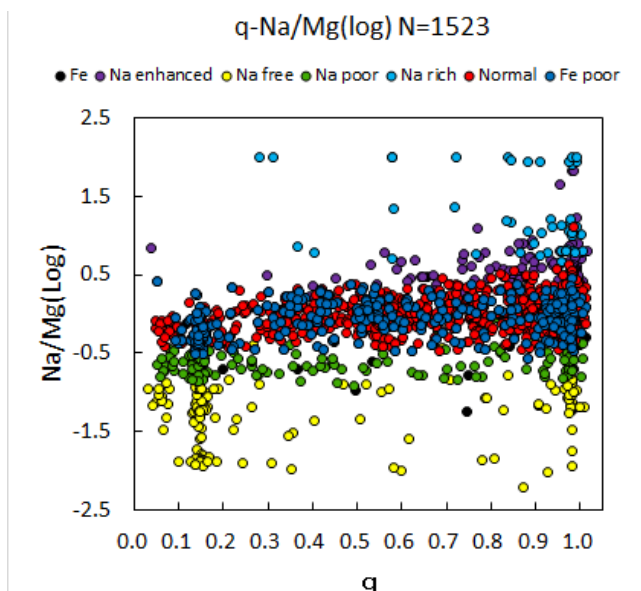


Figure 23 – Na/Mg ratio (Log) plotted in function of the perihelion distance q .

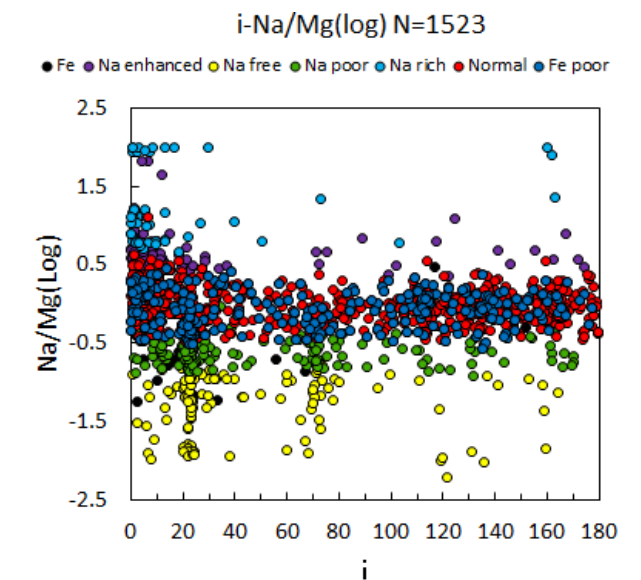


Figure 24 – Na/Mg ratio (Log) plotted in function of the inclination i .

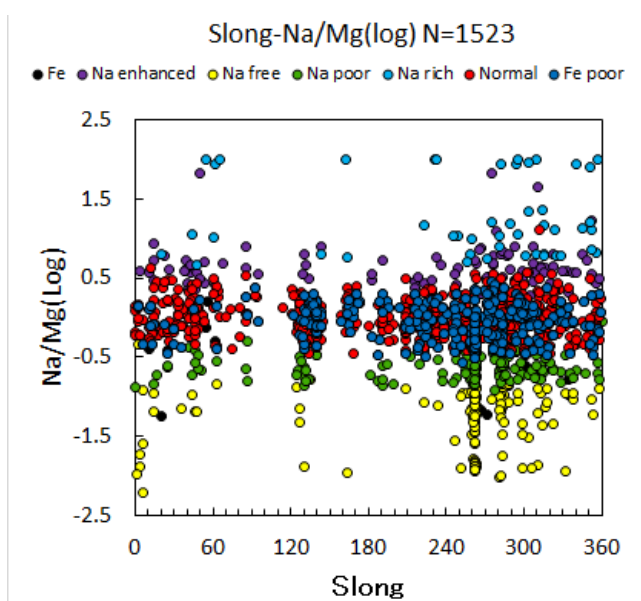


Figure 25 – Na/Mg ratio (Log) plotted in function of the solar longitude.

When q is 0.3AU or less, the numbers decrease for all types. Na rich, Na enhanced, Normal and Fe poor meteoroids are concentrated in the range of 0.3 – 1 A.U. Most of the meteoroids with Sun-approaching orbits with $q < 0.2$ AU are Na poor and Na free meteoroids (Figure 22).

Looking at Na rich meteoroids, it can be seen that the number decreases as q decreases and the amount of Na becomes less (Figure 23).

There is a split between the Jupiter-family orbits and the Halley-type orbits at an inclination $i \sim 45^\circ$ (Figure 24).

The number of spectra that can be obtained will change depending on the observation period. Irons are often slow, fainter meteors, not present between solar longitude 70° to 240° . This is probably due to bad weather and poor transparency of the sky (Figure 25).

Most of the Na free meteoroids and Na poor meteoroids have a mass less than 5 g. Masses of above 100 g are mostly Normal meteoroids (Figure 26).

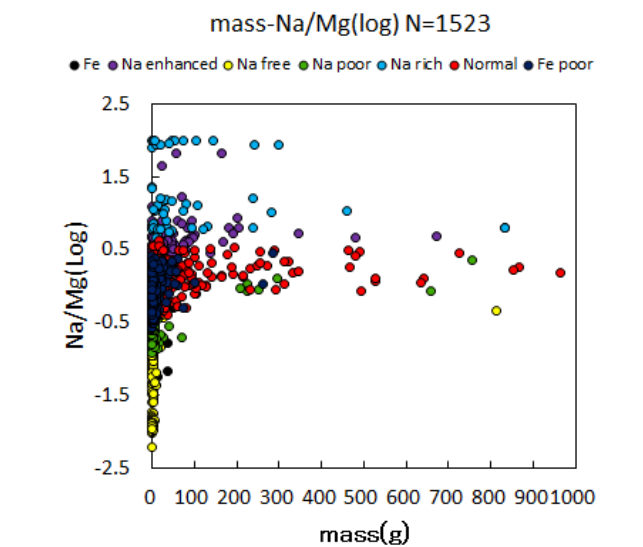


Figure 26 – Na/Mg ratio (Log) plotted in function of the mass.

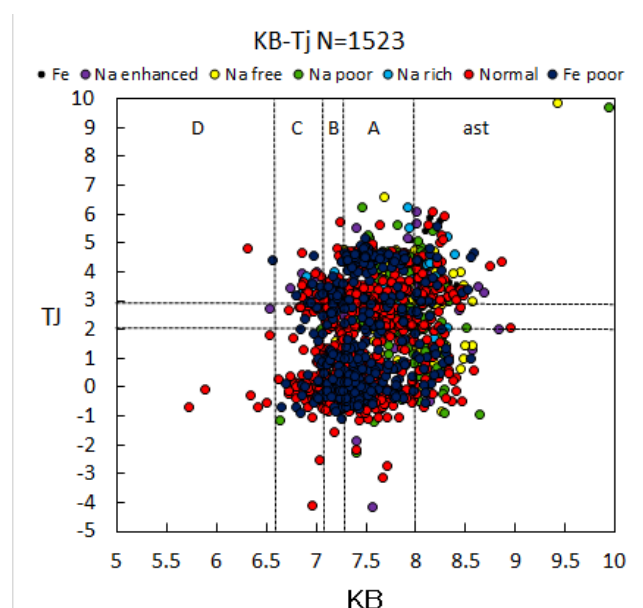


Figure 27 – Plot of Tisserand parameter and KB criterion space.

Looking at the overall relationship of the Tisserand parameter T_J and KB , the air density calculated from the altitude approximation (Ceplecha, 1988; Rudawska et al., 2016), we see many A types in *Figure 27*. There are few D types and Jupiter family comets. Irons are mostly asteroidal and A types. Na free meteoroids and Na poor meteoroids are often A types. Na rich meteoroids and Na enhanced meteoroids have less C and D types. Normal meteoroids and Fe poor meteoroids are considered to be mainly Halley cometary types and appear as a concentration of meteor showers (*Figure 27*).

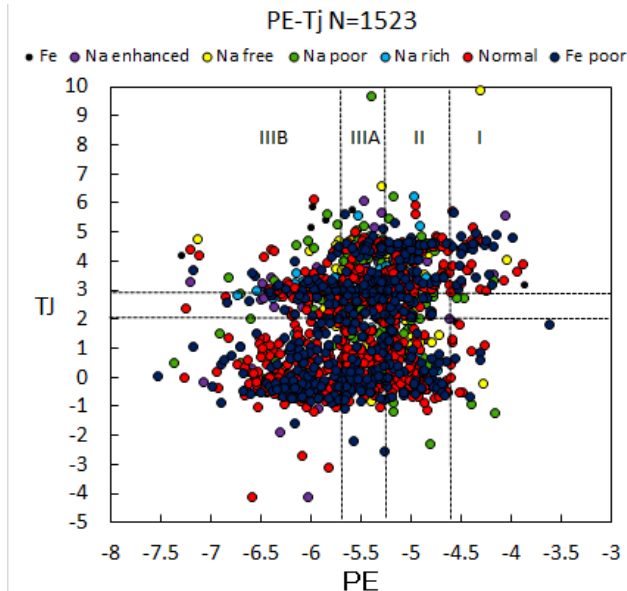


Figure 28 – Plot of the Tisserand parameter and the PE distribution.

Looking at the overall relationship between the Tisserand parameter T_J and PE (Ceplecha, 1988; Rudawska et al., 2016), there are many types II–III B and few types I. Na poor meteoroids have a lot of II and III A types. Na-free meteoroids and Fe-poor meteoroids are mostly II–III B types. Normal meteoroids and Na-enhanced meteoroids appear numerous as III A and III B types. Irons are mostly type III A (*Figure 28*).

13 Irons

I compared the Irons with the results of other researchers. First, the luminous intensity distribution is compared. There is a difference in the range captured by the type of camera and lens. My devices use multiple short focal length lenses which are brighter. Still, there are many faint meteors (*Figure 29*).

Regarding the relationship between the observed velocity and the luminosity, we see many faint meteors (magnitude -1 to $+4$) with low velocities v_o within the range 10 – 30 km/sec (*Figure 30*).

Regarding the relationship between the observed velocity v_o and the ablation altitude, Irons display a similar tendency for H_b in function of v_o , but the Fe 50–80% has no correlation. This is probably because the covered range is too wide (*Figure 31*).

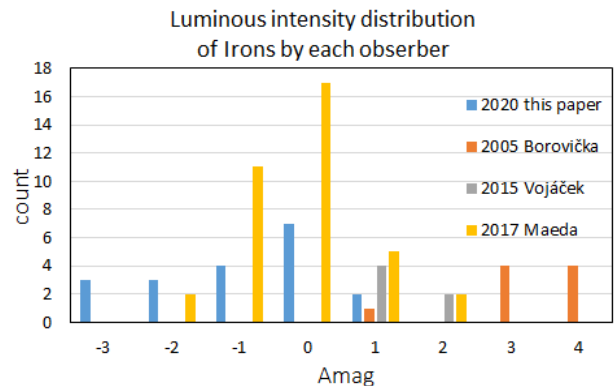


Figure 29 – Luminosity intensity distribution of Irons according to four different studies.

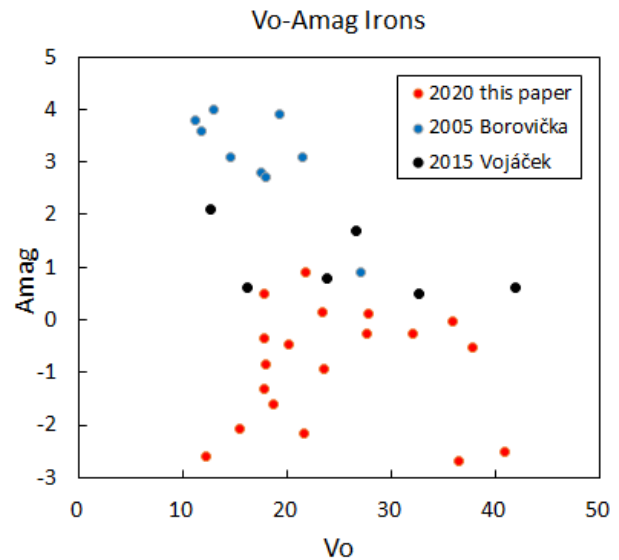


Figure 30 – Relationship between the observed velocity v_o and absolute luminosity of Irons in the different analyses.

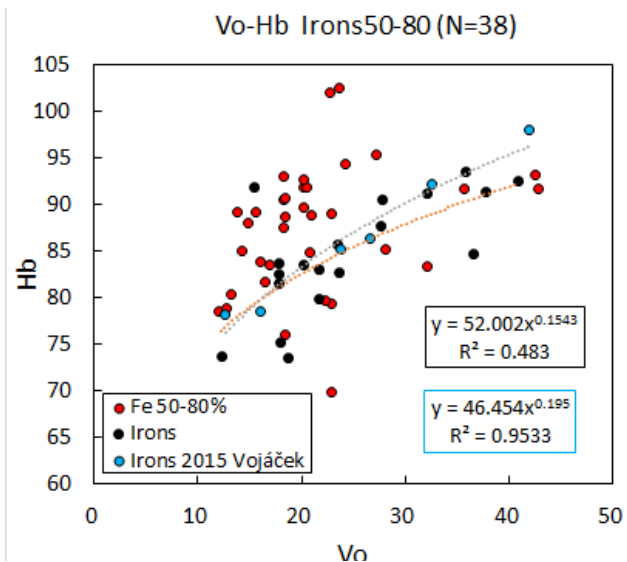


Figure 31 – Relationship between observed velocity v_o and the absolute luminosity of Irons and Fe 50–80%.

The relationship between the Tisserand parameter T_J and the inclination i (Vojáček et al., 2015) shows that most of the Fe 50–80% group belong to the Asteroidal-chondritic class (A-C) and Jupiter-family orbits (JF). There were three Halley-type orbits (HT). Irons had two Halley-type orbits (*Figure 32*).

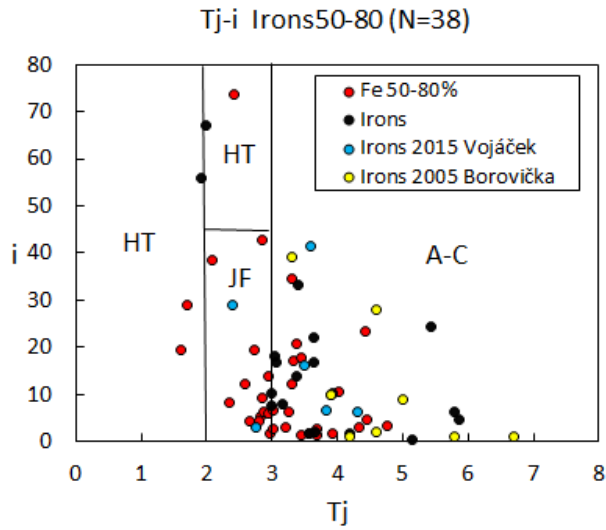


Figure 32 – Relationship between Tj and inclination i.

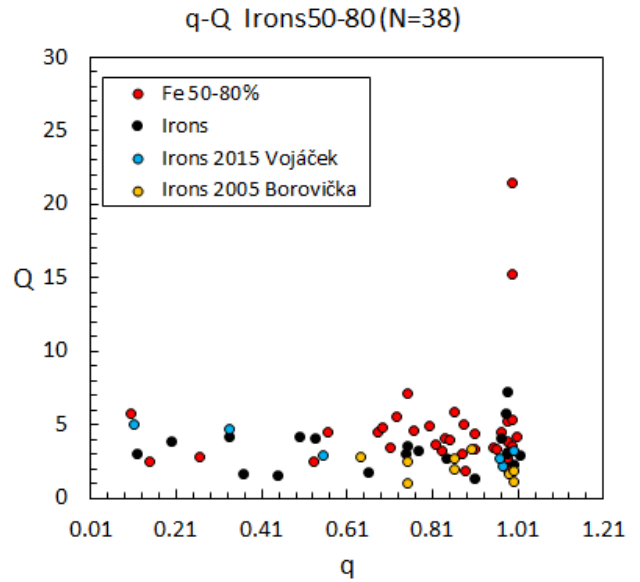


Figure 33 – Relationship between q and Q.

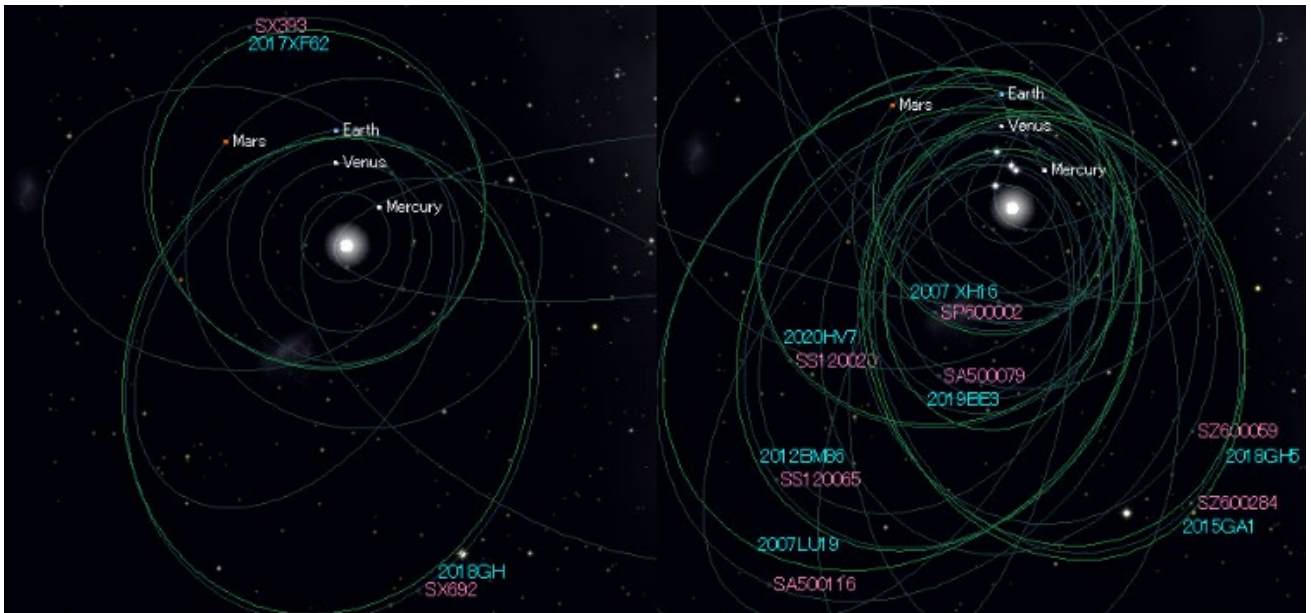


Figure 34 – The orbits of the Irons and their parent bodies comparing V-1 and V-2 (left) and S-1 to S-6 (right).

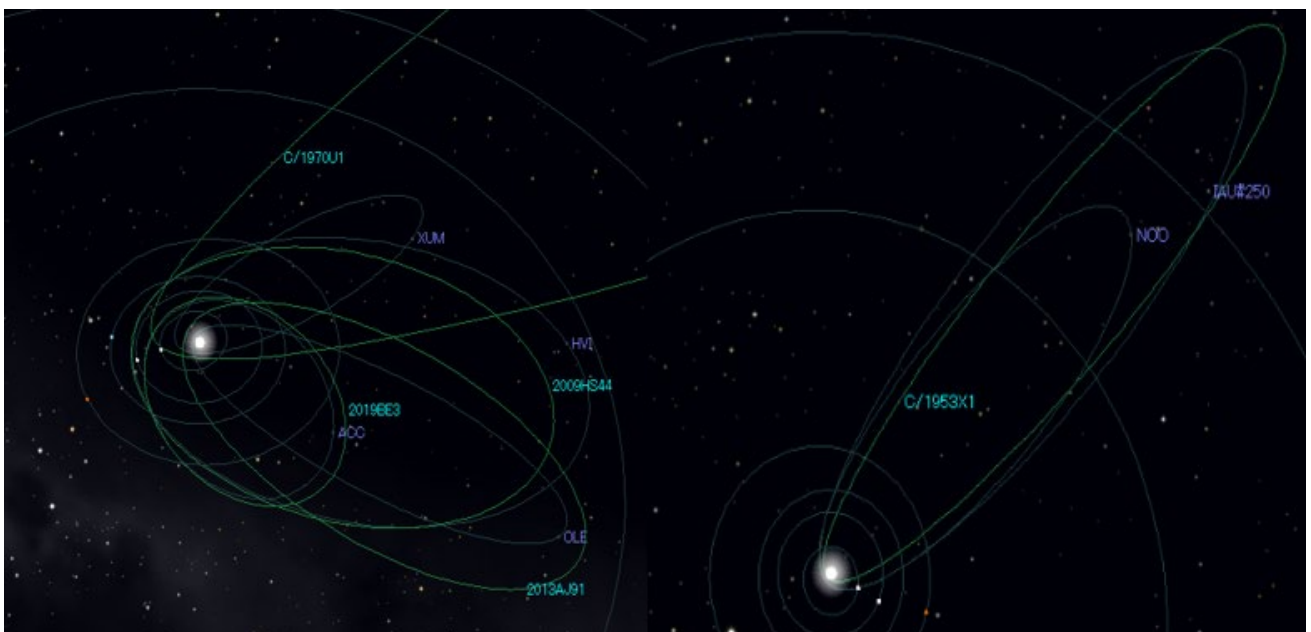


Figure 35 – The orbits of XUM, OLE, ACC,HVI and NOO and their possible parent body candidate.

Table 1 – Orbital elements of meteoroids classified as Irons compared to the orbits of the parent bodies.

	Name	e	q	i	ω	Ω	λ_{Π}	β_{Π}	D _{sh}	Remarks
V-1	SX393	0.38	0.98	6.40	194.10	262.70	96.73	-1.56		
V-1	2017XF62	0.34	1.00	5.45	203.92	254.07	97.89	-2.21	0.06	
V-2	SX692	0.52	1.00	16.00	194.00	45.80	239.28	-3.82		
V-2	2018GH	0.53	0.96	9.65	193.31	46.15	239.28	-2.21	0.12	
S-1	SP600002	0.20	0.91	24.30	58.40	86.40	142.40	20.51		
S-1	2007 XH16	0.23	0.91	27.43	58.30	91.29	146.46	23.08	0.08	
S-2	SS120020	0.40	1.00	1.80	359.20	190.20	189.44	-0.03		
S-2	2020HV7	0.40	0.99	1.55	354.36	194.25	188.61	-0.15	0.01	
S-3	SS120065	0.65	0.75	13.97	67.12	154.14	220.64	12.85		
S-3	2012BM86	0.63	0.79	11.40	56.35	164.15	219.98	9.47	0.07	
S-4	SZ600284	0.61	0.75	2.14	70.89	200.77	271.65	2.02		
S-4	2015GA1	0.61	0.78	5.17	69.55	202.58	272.06	4.85	0.06	
S-5	SA500079	0.57	0.45	6.30	120.80	121.00	241.89	5.40		ACC
S-5	2019BE3	0.59	0.50	8.51	111.01	130.11	241.33	7.94	0.07	
S-6	SA500116	0.62	0.97	8.00	153.10	55.30	208.59	3.61		
S-6	2008JD33	0.65	1.03	5.93	144.05	65.77	209.97	3.47	0.08	
S-7	SZ600059	0.52	0.84	10.10	238.00	25.20	262.72	-8.59		
S-7	2018GH5	0.55	0.85	5.07	248.76	21.84	270.52	-4.73	0.12	
S-8	SA500118	0.49	1.01	22.00	180.80	61.10	241.88	-0.30		
S-8	1999 FN53	0.46	0.94	20.16	191.71	50.59	241.60	-4.01	0.10	
S-9	SW600479	0.64	0.37	4.50	308.04	282.40	230.53	-3.54		
S-9	2013YL2	0.66	0.40	5.87	303.56	277.90	221.60	-4.89	0.11	
S-10	SA500064	0.53	0.98	33.20	177.70	271.70	89.76	1.25		
S-10	2019YA6	0.57	1.07	31.38	169.11	275.07	85.75	5.65	0.12	
S-11	SA500279	0.77	0.53	18.12	92.81	120.91	213.87	18.10		
S-11	2009 BJ58	0.71	0.53	13.03	85.60	131.46	216.94	12.99	0.12	
S-12	SS800036	0.46	0.66	0.40	93.50	138.40	231.85	0.35		
S-12	2019BV2	0.50	0.66	0.66	82.14	134.78	216.92	0.65	0.13	
S-13	SA500115	0.93	0.12	16.70	147.20	234.40	22.72	8.96		
S-13	2005 GL9	0.90	0.22	20.02	162.17	225.64	28.83	6.02	0.17	
S-14	SW600549	0.79	0.50	10.27	97.35	154.39	251.85	10.18		
S-14	2019DW1	0.78	0.50	4.87	97.38	164.86	262.26	4.83	0.17	
S-15	SA500259	0.90	0.20	16.66	313.20	281.48	235.90	-12.07		Gem?
S-15	Phaethon	0.89	0.14	22.26	322.19	265.22	229.53	-13.43	0.18	
S-16	SA500271	0.71	0.98	66.93	188.00	287.63	110.78	-7.35		Qua?
S-16	2003 EH1	0.62	1.19	70.84	171.34	282.98	100.12	8.18	0.33	

Table 2 – Orbital elements for XUM#341, OLE#515, ACC#266, HVI#343 and NOO#250, first the orbit for this study, compared with the reference orbit given by the IAU and compared with the orbit of the candidate parent body.

Name	v_g	e	q	i	ω	Ω	D_{sh}	λ_{II}	β_{II}	Remark
ACC#266	23.0	0.69	0.46	8.7	109.2	126.8	0.11	236.21	8.21	N=4
IAU	19.3	0.59	0.48	7.2	112.6	124.2	0.00	236.96	6.64	asteroidal
2019BE3		0.59	0.50	8.5	111.0	130.1	0.05	241.33	7.94	
OLE#515	40.1	0.94	0.11	26.5	146.8	114.9	0.11	264.55	14.16	N=4
IAU	41.5	0.97	0.08	23.0	151.0	116.0	0.00	268.97	10.92	
2013AJ91		0.93	0.18	33.3	165.8	95.4	0.27	263.45	7.73	?
XUM#341	40.7	0.84	0.23	66.8	312.5	299.3	0.03	276.01	-42.65	N=5
IAU	40.9	0.86	0.22	66.8	313.2	298.0	0.00	275.24	-42.07	
C/1970 U1		1.00	0.41	60.8	318.5	293.7	0.27	270.34	-35.32	?
HVI#343	17.7	0.71	0.77	0.9	64.6	219.9	0.02	284.59	0.80	N=7
IAU	18.1	0.73	0.76	0.6	64.1	220.4	0.00	284.50	0.54	
2009HS44		0.70	0.77	2.4	73.2	209.1	0.05	282.32	2.33	
NOO#250	40.7	0.97	0.12	19.8	140.4	67.0	0.08	209.17	12.45	N=5
IAU	42.5	0.99	0.12	24.4	140.4	67.6	0.00	210.61	15.27	
C/1953 X1		1.00	0.07	13.6	94.1	115.2	0.32	209.43	13.54	?

The Fe 50–80% group has two Sun-approaching orbits ($q < 0.2$ A.U.). A concentration appears at $0.6 < q < 1.1$ A.U. Irons had two Sun-approaching orbits. There is a lot of scatter. Except for the two meteoroids with $Q > 10$, it is very similar to the distribution for Irons obtained from other analyzes. Therefore, it is considered that the Fe50–80% group is related to Irons (Figure 33).

I investigated the parent bodies of the Irons. V-1 and V-2 in Table 1 are taken from Vojáček et al. (2015). Table 1 compares the orbits with their possible parent bodies, for S-1 to S-4 the association seems to be certain. From S-5 to S-15, D_{SH} is 0.2 or less, which are good candidates (Southworth and Hawkins, 1963). S-16 is supposed to be a Quadrantid, but there are errors on the velocity, etc., so it is a weak candidate only. Among the Irons, there was almost not a single one with the same orbit. Although some similar orbits are present, these cannot be identified as a meteor shower (Table 1 and Figure 34).

14 Five minor meteor showers

We investigated the mean orbits of XUM#341, OLE#515, ACC#266, HVI#343 and NOO#250 and parent candidates for the five minor meteor showers shown in Figures 7 and 14. As shown in Table 2, the ACC#266 and HVI#343 meteor shower are in very good agreement with the IAU mean orbit and the parent body. As for the other three, the average orbits are in good agreement, but it is possible that these are the closest candidates for the parent body, which may have changed due to perturbation, etc. The OLE#515 and the NOO#250 meteor showers have the perihelion

distance $q < 0.2$ A.U. which are Sun-approaching orbits (Table 2 and Figure 35).

15 Conclusions

The shower meteors and the sporadic meteors showed almost the same distribution. In addition, the Quadrantids, Perseids and Geminids could be analyzed in greater detail than the other major meteor showers. Quadrantids and Geminids could be classified into four types. Other major meteor shower types varied from shower to shower. Differences were also seen in minor meteor showers with more than three spectra. Na Free and Na Poor meteoroids have been observed in Quadrantids, Geminids and Southern δ -Aquariids and some minor meteor showers. The comet derived meteors have a heterogeneous composition, but most of the Halley-type orbits are Na-free, Na-poor, and Fe-poor meteors. Among the orbits of the Jupiter-family orbits, there are many Na-rich and Na-enhanced meteors. Many of the Normal types have a large mass. An Iron meteoroid with an Fe content of more than 50% was captured. There are some Irons with minor meteor shower association and parent body candidates. There were two Iron meteoroids in a typical orbit approaching the Sun.

Acknowledgment

We would like to thank the SonotaCo network for providing orbital calculation data for this study. We would also like to thank Paul Roggemans and Masahiro Koseki for their proofreading and advice.

References

- Borovička J., Koten P., Spurný P., Boček J., Štork R. (2005). “A survey of meteor spectra and orbits: evidence for three populations of Na-free meteoroids”. *Icarus*, **174**, 15–30.
- Ceplecha Z. (1988). “Earth's influx of different populations of sporadic meteoroids from photographic and television data”. *Bulletin of the Astronomical Institutes of Czechoslovakia*, **39**, 221–236.
- Maeda Koji and Fujiwara Yasunori (2016). “Meteor spectra using high definition video camera” In Roggemans A. and Roggemans P., editors, *Proceedings International Meteor Conference*, Egmond, the Netherlands, 2–5 June 2016. pages 167–170.
- Rudawska Regina, Tóth Juraj, Kalmančok Dušan, Zigo Pavol, Matlovič Pavol (2016). “Metorspectra from AMOS videosystem” *Planetary and Space Science*, **123**, 25–32.
- Southworth R. R. and Hawkins G. S. (1963). “Statistics of meteor streams”. *Smithson. Contrib. Astrophys.*, **7**, 261–286.
- Vojáček V., Borovička J., Koten P., Spurný P., Štork R. (2015). “Catalogue of representative meteor spectra”. *Astronomy & Astrophysics*, **580**, A67, 1–31.

The Lyrids and a minor antihelion outburst in 2020

Thomas Weiland

Ospelgasse 12-14/6/19, 1200 Wien, Austria

thomas.weiland@aon.at

A summary report is presented for the visual observations during the Lyrid activity from April 19–20 to 23–24 under exceptional favorable weather circumstances.

1 Introduction

Rarely does it occur that April presents five clear and moonless nights in a row, especially around the time when the Lyrid maximum is due. This was the case in 2020! Combined with exceptionally dry air and the effects of diminished human activity in the course of the Corona lockdown one got magnificent skies, even near major towns.

All the observations (April 19–20 to 23–24) were carried out from Atzelsdorf, Austria (16°33'11" E, 48°30'30" N, 220 m a. s. l.), some 30 km away from the capital Vienna. Limiting magnitudes were slightly varying between $m = 6.20$ and 6.30 before the onset of dawn (mean 6.28), and the effective observing time added up to $T_{\text{eff}} = 17.72$ hours, during which 210 meteors (78 Lyrids, 17 Antihelion and 115 sporadic meteors) were logged (*Table 1*).

2 2020 April 19–20

As expected, at the beginning of the campaign (April 19–20) observed Lyrid rates stayed on a rather low level (1–3/h), the brightest member reaching only magnitude 0 (*Table 1*). Based on an average population index of $r = 2.79 \pm 0.37$ for all Lyrids recorded (78 LYR; *Table 1* and *Figure 2*), corresponding ZHRs were fluctuating between 1 ± 1 and 5 ± 3 (*Figure 3*). For comparison, the mean population index for the sporadic background (excluding ANT) was found to be $r = 2.86 \pm 0.32$ (115 SPO; *Table 1*), in good agreement with values found in the literature for the current season (Rendtel and Arlt, 2014).

3 2020 April 20–21

During the following night (April 20–21) Lyrid rates saw only a modest increase (2–4/h), reflected by slightly raised ZHRs between 3 ± 2 and 6 ± 3 . Remarkably, observed Lyrids were fainter than on April 19–20, within the +2 to +5 magnitude range. To compensate for this, a yellow, star-like SPO of magnitude -3 showed up at $23^{\text{h}}08^{\text{m}}10^{\text{s}} \pm 5^{\text{s}}$ UT, travelling on a $> 40^\circ$ path and leaving a short train behind.

4 2020 April 21–22

As for the peak night (April 21–22), hopes were high that Lyrid activity would match the excellent conditions to a similar extent, though the predicted maximum time, April 22, $06^{\text{h}}40^{\text{m}}$ UT (Rendtel, 2019) did not favor my location in Central Europe.

Observations started at $21^{\text{h}}30^{\text{m}}$ UT, at a time when the Lyrid radiant had already a useful elevation of $h_{\text{Rad}} = 29.87^\circ$, but first rates remained rather low (2/h; ZHR 5 ± 3). Once more, sporadic meteors stole the show with an impressive yellow-blue, star-like member of magnitude -4 at $22^{\text{h}}25^{\text{m}}35^{\text{s}} \pm 5^{\text{s}}$ UT, moving on a 40° path across the northern sky.

After $22^{\text{h}}30^{\text{m}}$ UT, Lyrid activity showed signs of going up, resulting in modest rates during the next two hours (6–7/h; corresponding ZHRs 11 ± 5 and 11 ± 4 respectively), though the majority of meteors was rather faint (of magnitude +4 and +5). Again, to my pleasure, a fine SPO of magnitude -4 appeared at $23^{\text{h}}45^{\text{m}}40^{\text{s}} \pm 5^{\text{s}}$ UT, slowly travelling on a 25° path almost parallel to the northeastern horizon. Its bulbous, drop-like head sported a distinctive orange/red color, focusing in a thread-like train.

A further increase of Lyrid rates to 12/h between $00^{\text{h}}30^{\text{m}}$ and $01^{\text{h}}30^{\text{m}}$ UT yielded the highest ZHR of this night (17 ± 5), but with the exception of 3 LYR of magnitude -1 , 0 and -2 most of the meteors were still in the +3 to +5 range. That seemed all the more striking since a sharp descent during the last observing hour to 2/h (ZHR 3 ± 2) could be observed. My hopes for an impressive Lyrid maximum (as in 2012) were gone!

5 2020 April 22–23

With that in mind, I did not expect too much for the forthcoming night (April 22–23). Nevertheless, appropriate to my 25th anniversary of active meteor observing (I started on 1995, April 22–23), I felt I had a wish open.

Table 1 – Magnitude distribution of Lyrids and sporadic meteors logged from 2020 April 19–20 to 23–24.

Shower	Date	lm	-6	-5	-4	-3	-2	-1	0	+1	+2	+3	+4	+5	+6	Tot.
LYR	19/20	6.30	0	0	0	0	0	0	1	0	1	0	4	1	0	7
LYR	20/21	6.30	0	0	0	0	0	0	0	0	1	4	2	2	0	9
LYR	21/22	6.23	0	0	0	0	1	3	1	0	2	1	10	11	0	29
LYR	22/23	6.28	0	0	1	0	0	1	0	4	3	4	6	5	0	24
LYR	23/24	6.30	0	0	0	0	0	0	0	0	1	0	4	4	0	9
Total			0	0	1	0	1	4	2	4	8	9	26	23	0	78
Mean		6.28														
ANT			-6	-5	-4	-3	-2	-1	0	+1	+2	+3	+4	+5	+6	Tot.
19–24 April			1	0	0	0	1	0	1	1	0	7	5	1	0	17
SPO excl. ANT			-6	-5	-4	-3	-2	-1	0	+1	+2	+3	+4	+5	+6	Tot.
19–24 April			0	0	3	1	0	1	3	9	11	15	35	37	0	115



Figure 1 – Antihelion meteor of magnitude -6 (brightest flash), recorded from Pinkafeld, Austria on 2020 April 22, $23^{\text{h}}29^{\text{m}}45^{\text{s}} \pm 5^{\text{s}}$ UT (Photo © and courtesy Christa Plassak).

Already a few minutes after the start of my observations, at $22^{\text{h}}15^{\text{m}}$ UT, a flash lit up the sky in the west, but I could not detect any meteor. Apart from that, with 5 Lyrids logged during the first hour (ZHR 10 ± 4), the brightest one of magnitude -1 , and 9 sporadics as well, overall meteor activity looked more promising than the night before.

Shortly after the beginning of the second interval ($23^{\text{h}}15^{\text{m}}-00^{\text{h}}15^{\text{m}}$ UT), remarkable things commenced. The kick-off made a beautiful orange ANT of magnitude 0 at $23^{\text{h}}20^{\text{m}}05^{\text{s}} \pm 5^{\text{s}}$ UT, which slowly travelled some 10° from

northeastern Virgo to southeastern Bootes showing a drop-like head with a short train, followed by another one of magnitude $+3$ a few minutes later. At $23^{\text{h}}25^{\text{m}}15^{\text{s}} \pm 5^{\text{s}}$ UT a yellow -4 LYR flashed up near the horizon at the border of Crater and Hydra; it could photographically be traced over a distance of 250 km to the west¹³.

The absolute highlight of the night and even the entire session came at $23^{\text{h}}29^{\text{m}}45^{\text{s}} \pm 5^{\text{s}}$ UT – a white/blue/green ANT of magnitude -3 , showing up in northwestern Libra and culminating with two flashes of -5 and -6 in

¹³ <http://www.astromethyst.at/meteore.html>

southeastern Virgo; it left three glowing fragments and a train behind (see *Figure 1*). The fireball was also registered from another location and both pictures give an impression of the changing perspective from the two locations lying some 125 km apart, the latter resembling the appearance from my observation point (path length $> 10^\circ$). Unfortunately, no permission could be obtained to use this picture¹⁴.

On top of that, less than 3 minutes later, at $23^{\text{h}}32^{\text{m}}25^{\text{s}} \pm 5^{\text{s}}$ UT, another ANT of magnitude -2 and blue/green color took its course from northwestern Scorpius to southeastern Ophiuchus; once more it showed a drop-like head with a short train. Finally, a star-like ANT of magnitude $+3$ appeared shortly before the end of the interval.

Five Antihelion meteors within one hour – I do not recall ever seeing more of them at my location, not even in winter, when their radiant is culminating high in the sky!

As for the Lyrids, their rates remained fairly constant for the rest of night ($5\text{--}7/\text{h}$; corresponding ZHRs 7 ± 3 to 11 ± 4).

Forty-five seconds before official observations ended ($02^{\text{h}}14^{\text{m}}15^{\text{s}} \pm 5^{\text{s}}$ UT) my “anniversary night” delivered a worthy final – a yellow-blue SPO of magnitude -4 , travelling on a 25° long path from the Ursa Major / Bootes border to southwestern Bootes. Great!

6 2020 April 23–24

Despite top level sky quality, observed Lyrid rates during the last night (April 23–24) were more or less comparable to those at the beginning of the campaign ($1\text{--}4/\text{h}$; corresponding ZHRs 1 ± 1 to 7 ± 3); this applies for the Antihelion and sporadic meteors, too.

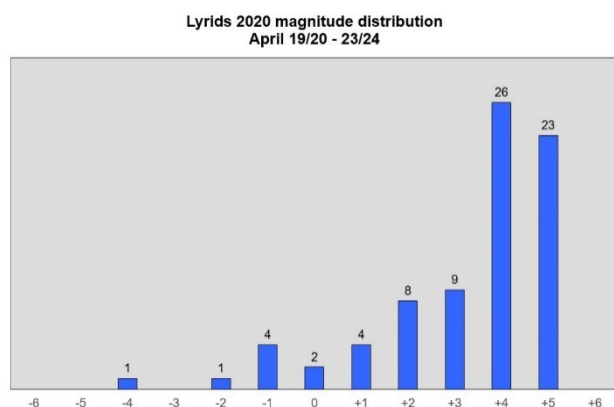


Figure 2 – Lyrids magnitude distribution logged from 2020 April 19–20 to 23–24.

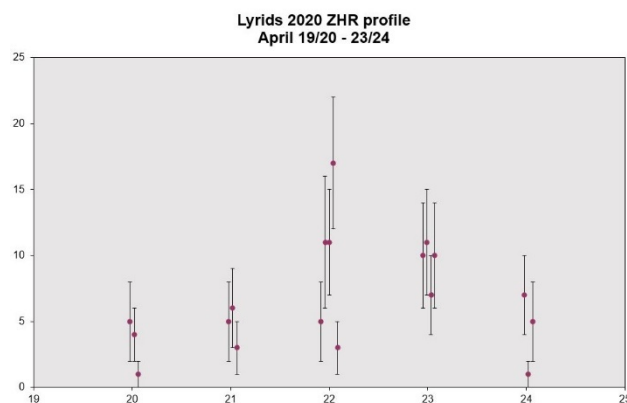


Figure 3 – Lyrids ZHR profile from 2020 April 19–20 to 23–24.

7 Conclusion

In 2020 both lunar and meteorological circumstances were top notch for observing the Lyrids. Nonetheless, they delivered only a modest return for Central European observers, mainly because the maximum occurred after sunrise on April 22, as predicted (ZHR 18 ± 3 around 08^{h} UT, according to www.imo.net).

Apart from that, most of the Lyrids observed in 2020 were rather faint, with nearly two-thirds (62.82 %) belonging to the $+4$ and $+5$ magnitude class respectively; only 1 LYR (1.28 %) was classified as a fireball (magnitude -4). The relatively high population index of $r = 2.79$ reflects that as well. 50 % of the Lyrids ≥ 0 mag showed a yellow color; additionally, white and orange tints were observed. Nearly 18 % of the Lyrids left a (short) train, less than in previous years.

However, the sporadic, in particular the Antihelion meteors can be called the undisputed “stars” of the entire observing session. Four members of magnitude -4 up to -6 within less than 20 hours of observing time seem to be a lone record of usually “low-tide” April nights!

References

- Rendtel J. (2019). 2020 Meteor Shower Calendar. International Meteor Organization.
- Rendtel J. and Arlt R. (2014). Handbook for Meteor Observers. International Meteor Organization, Potsdam.

¹⁴ https://spaceweathergallery.com/indiv_upload.php?upload_id=161590

Lyrids 2020: successful campaign!

Koen Miskotte

Dutch Meteor Society

k.miskotte@upcmail.nl

A report is presented about the observations of the author during the Lyrids 2020.

1 Introduction

Due to climate change, winters in western Europe are becoming softer, wetter and cloudier, while spring has become drier and sunnier in recent years. Like in 2018, April in 2020 excelled in many clear nights with record numbers of hours of sunshine during the day. The author was able to observe for 7 nights. For the Lyrids, the maximum was expected to take place around 08^h00^m UT on April 22, 2020, but this could also be some hours earlier or later (Rendtel, 2019). I made a report of all observing activities.

Air traffic has decreased considerably thanks to the lockdown imposed in the Netherlands and much of the rest of the world. This was also noticeable at the starry sky by the low numbers of aircrafts that were visible, but also there was much less cirrus and dust in the atmosphere. The nights during which it was clear were therefore very transparent! The first clear moonless night was Wednesday on Thursday night April 15–16.

2 2020 April 15–16¹⁵

This night I was observing from the meteor roof at home and observed between 00^h22^m and 02^h53^m UT. A cold night: the temperature on the roof dropped to 3 degrees Celsius. Initially I had a beautiful transparent sky, but from 2^h05^m UT onwards thin cirrus moved through the field of view from the south causing the limiting magnitude to drop from 6.3 to 6.1 (SQM decreased from 20.16 to 20.08). In April there is usually not much meteor activity, except for the Lyrids, of course. Thanks to the very clean and dry air now some more meteors were visible, in 2.50 hours effective observation time I counted 23 meteors, including my first two Lyrids (+3 and +1 respectively) of this year. The most beautiful meteors were the +1 Lyrid and a bright red +1 Antihelion with a long wake. Furthermore, a double satellite of the type NOSS or its Chinese clone was seen.

The nights 16–17, 17–18 and 18–19 April were clear, but there was often haze or cirrus passing over. However, in the predictions of the KNMI (our Dutch weather institute) we could get a series of beautiful clear nights in the week of the Lyrids maximum. In other words, another Lyrid return comparable to 2018. Indeed, it cleared up nicely on Sunday 19th April. I also decided to take one day off from work on Wednesday April 22 so that I could observe the Lyrids extensively that night.

3 2020 April 19–20¹⁶

During the coming nights I would observe from the Groevenbeekse Heide. When I cycled to the heath around 23^h UT, I saw that the sky was crystal clear. A relatively large number of stars could also be seen low on the horizon. The session started at 23^h12^m UT and continued until dusk at 02^h50^m UT. The limiting magnitude was 6.4. That was a top value for this location, the SQM was around 20.47. The hourly counts were good with 8 (1.00 hours), 13 (1.00 hours) and 11 (1.383 hours) meteors. The Lyrids were only very sparingly present, only three were noticed. Also, few bright meteors, at 1^h44^m UT a sporadic +1 in Cepheus with a short persistent train was the brightest meteor. So, in total 32 meteors, of which 4 ANT, 3 LYR and 25 SPO. This night was also a bit chilly; the temperature went down to 3 degrees Celsius at clog height.

From 01^h13^m UT onwards, satellites regularly appeared low in the southeast, which followed roughly the same track. These were the starlink satellites I imagined; I saw them for the first-time during observations. First there was one satellite every 3 or 4 minutes, but from 01^h56^m UT entire groups became visible. Sometimes 6 were visible at a time with a distance of 5 or more degrees. Brightness around magnitude +2 a +3. It was also clearly visible how the satellites floated out of the Earth's shadow and that this happened increasingly earlier as a result of the rising Sun. From 2^h15^m UT they also rose and moved through my field of view, fortunately, now again in smaller numbers.

¹⁵ https://www.imo.net/members/imo_vmdb/view?session_id=80192

¹⁶ https://www.imo.net/members/imo_vmdb/view?session_id=80319



Figure 1 – Part of the fish eye image of the Earth grazer captured in twilight with the all sky camera on April 20, 2020 at 19^h55^m UT. The image has been heavily edited to make the meteor more visible. Camera: Canon 6d with Sigma 8 mm F 3.5. The shutter was set to 16 breaks per second.

4 2020 April 20-21¹⁷

Again, a very dark clear night with Lm 6.4 and an SQM that even went up to 20.55! That was close to the record at this location from 2018, when I reached 20.65 once. I kept the session a bit shorter because I still had to work that day. In the evening, the all sky camera had captured two meteors.

Between 00^h13^m and 02^h50^m UT I counted 31 meteors. The Lyrids finally gained some strength this session with resp. 3 (T_{eff} 0.867 hours), 5 (T_{eff} 0.917 hours) and 6 meteors (T_{eff} 0.817 hours). So, in total 14 LYR, 1 ANT, 1 ETA and 15 SPO. For several years, observers such as Michel Vandeputte and Jurgen Rendtel had sometimes observed eta Aquariids around the Lyrid maximum. That is why I keep going a little longer during the twilight. This time it worked: a +3 ETA shot through Bootes.

Fortunately, I also saw some beautiful meteors this night:

- 01^h18^m UT: a nice magnitude 0 orange Antihelion in Bootes.
- 01^h45^m UT: +1 Lyrid with a short persistent train in the Big Dipper.
- 02^h12^m UT: +1 Lyrid in Cassiopeia.

During the second hour, occasional Starlink satellites (I call them Mosquitos) were seen low in the southeast. However, during the third hour, a stretched starlink train passed right through my field high in the southeast. The satellites were very bright, approximately magnitude +1 a +2. Sometimes 6 were visible at the same time, I saw 25 in total. If you followed the satellites with your eyes, this combined with the dark and clear starry sky gave a sort of 3D effect. However, it is also a significant concentration-breaker for the observation. I cannot rule out missing some (weak) meteors because of these satellites.

But, all in all it was a nice night. Thanks to the fairly strong east wind, the temperature remained around 6 degrees.



Figure 2 – 25 minutes later (April 20, 2020 at 20^h20^m UT), this meteor was captured in the constellation Leo. Camera: Canon 6d with Sigma 8 mm F 3.5. The shutter was set to 16 breaks per second.

¹⁷ https://www.imo.net/members/imo_vmdb/view?session_id=80320

5 2020 April 21–22¹⁸

Yes! The Lyrids have their maximum this night and the sky was clear and I was free from work the 22nd and 23rd of April! That meant a long session from the heath. I could observe from 22^h30^m to 02^h50^m UT. The quality of the sky was slightly less than the 2 previous nights. This was mainly due to the somewhat lighter sky background. Limiting magnitude again 6.4 and an SQM that sometimes reached at 20.45. Only after fifteen minutes I saw my first Lyrid, but quickly after that more Lyrids followed. The Lyrid counts went up from 8 to 17 an hour, so everything went very well. This time also more brighter meteors appeared:

- 00^h24^m UT: a beautiful white 0 Lyrid with 1 second persistent train in Cepheus.
- 00^h48^m UT: pats! A beautiful orange colored –4 or –5 Lyrid appears near Scorpius low south. Unfortunately, the all sky camera did not work well this night and did not capture this Lyrid.
- 01^h40^m UT: –1 Lyrid in Cygnus with 1 second persistent train.
- 01^h51^m UT: a white 0 Lyrid with a 2 second persistent train in Serpens Caput. One minute later;
- 01^h52^m UT: again, a white 0 Lyrid in Hercules with 1 second train.
- 02^h12^m UT: Beautiful white –1 Lyrid in Cassiopeia with 1 second persistent train.
- 02^h19^m UT: again, a –2 Lyrid in Cassiopeia with a 2 second persistent train.
- 02^h35^m UT: +1 Lyrid in Cygnus.

A total of 83 meteors were actually seen in 4.20 hours, of which 47 LYR, 5 ANT, 1 ETA ($M_V +2$ with persistent train) and 30 sporadic meteors. Also, this night a Starlink train was visible. This time they moved through the zenith reaching magnitude 0 to +1! And by temporarily keeping my field of view a little lower I largely kept them outside the FOV.

It was very nice on the heath, especially at the end of the session. Jupiter, Saturn and Mars were low in the southeast, Scorpius in the south-southwest. The Milky Way was beautifully visible between Cepheus and Sagittarius. The first bird sounds were audible. Nature awakened, always a beautiful moment! The wind blew through and ensured that the temperature did not dip below 7 degrees. Nevertheless, the author was quite cold after this session!

6 2020 April 22–23¹⁹

During the day the sky was deep blue again. I was curious what the Lyrids would deliver. After all, the maximum was expected on April 22 during the day. So, this night a bit more bright meteors and declining activity were expected. Due to fatigue, I decided to start a little later at 23^h00^m UT.

Again, a dark sky (and better than the previous night!), L_m 6.4 and SQM 20.50. The wind blew a little less hard. The Lyrids indeed showed less activity, but relatively more bright ones. During the night of April 21–22 I estimated most Lyrids were magnitude +4, now that was the magnitude +3 class. The Lyrid hourly counts were as follows:

- 23^h00^m–00^h00^m UT: 6 LYR
- 00^h00^m–01^h00^m UT: 11 LYR
- 01^h00^m–02^h00^m UT: 7 LYR
- 02^h00^m–02^h47^m UT: 4 LYR

So, after 1^h00^m UT decreasing activity. The brightest meteors appeared at:

- 00^h21^m UT: white –1 Lyrid in Cygnus with a 2 second persistent train.
- 00^h26^m UT: +1 Lyrid in Aquila with 1 second persistent train.
- 00^h31^m UT: white 0 Lyrid from Hercules to Corona Borealis with 1 second persistent train.
- 01^h18^m UT: White 0 Lyrid in Cygnus
- 01^h46^m UT: again a 0 Lyrid in Cygnus, 1 second persistent train.
- 02^h11^m UT: during the last hour another Starlink train was visible. At one point, three Starlink satellites moved in formation through Bootes. Pats! A nice –3 to –4 Lyrid put a brief end to the Starlink hegemony (*Figure 3*)! A persistent train remained visible for 4 seconds.
- 01^h44^m UT: a +1 SPO seen in Ophiuchus

A total of 59 meteors were seen, of which 28 LYR, 5 ANT, 0 ETA and 26 SPO. The average magnitude of the Lyrids was 0.6 magnitude lower this night than in the previous night. This was another beautiful session. This was followed by 2 nights with a lot of cirrus and clouds.



Figure 3 – Cropped image of the bright Lyrid from 22 April 2020 02^h11^m UT with a number of the Starlink train above it. Camera: Canon 6 D with Sigma 8 mm F 4.5 fish eye lens. The LC Shutter was set a 16 breaks per second.

¹⁸ https://www.imo.net/members/imo_vmdb/view?session_id=80321

¹⁹ https://www.imo.net/members/imo_vmdb/view?session_id=80322

7 2020 April 25–26²⁰

This night however, the sky was clear again! I had overslept, so I started an hour later than planned. Lm was 6.4 again and SQM rose again to 20.50. Transparency was excellent and because the wind had disappeared, the temperature could drop to -7 degrees Celsius at clog height! Few Lyrids this time, only 2 meteors. In total, 19 meteors were seen in 2.25 hours effective, of which 2 LYR, 3 ANT and 14 SPO. In the last hour low fog banks appeared here and there.

8 2020 April 26–27²¹

This was the last night in a beautiful series of clear nights. The Moon would soon be disturbing but the weather would also become more changeable after 6 dry weeks. I could observe 3.2 hours. Lm 6.4 and SQM 20.46 at maximum. Only 1 Lyrid was seen. Two ANT meteors were striking.

The first one moved on the Virgo / Bootes border and seemed to come more from the Spica area. But because the ANT radiant is very large, I keep it on an ANT. Shortly afterwards, a slow 0 ANT appears just above Scorpius. A rather long track. In retrospect, it appeared that these two meteors belong to the h-Virginids which radiant is to the left of Spica. In total I saw 24 meteors this night, 1 LYR and 3 ANT (2 times h-VIR). This source of meteors was more active than in previous years according to CAMS observations (Roggemans et al., 2020).

References

Rendtel J. (2019). IMO Meteor Shower Calendar 2020.

Roggemans P., Johannink C., Sekiguchi T. (2020). “h Virginids (HVI#343) activity enhancement”. *eMetN*, **5**, 233–245.

²⁰ https://www.imo.net/members/imo_vmdb/view?session_id=80323

²¹ https://www.imo.net/members/imo_vmdb/view?session_id=80334

Meteor observations from Midden-Eierland on the Dutch island of Texel

Koen Miskotte

Dutch Meteor Society

k.miskotte@upcmail.nl

A report is presented of the meteor observations by the author during May 2020.

1 Introduction

Already in September 2019, me and my wife decided that we would go on holiday to northern France in May 2020. Life is relaxed there, there is peace, a beautiful landscape and beautiful nature. And we can take all our four dogs with us. And when the sky is clear, we are in a region with a sky that (measured in 2018) can reach at least SQM 21.60 and Im 6.6 (Miskotte, 2018; 2019). Unfortunately, due to the corona pandemic we had to cancel this holiday in early May.

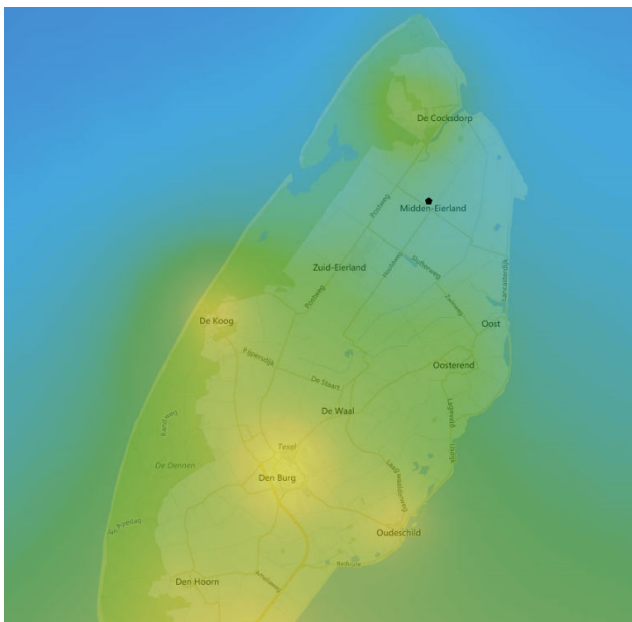


Figure 1 – Light pollution map of Texel 2019. My observation location is marked with a black star.

Fortunately, it turned out that a holiday in the Netherlands still was possible, and luckily, I was able to book at an address where we have often been guests with our dogs. This was in Midden Eierland (south of the little village of De Cocksdorp) on the island of Texel. Since 2012 we have been several times to Middle Eierland. Unfortunately, the weather was not so cooperative at the time, but when sky got clear you are immediately in a prime location. As mentioned, little could be observed during those previous visits, only in 2013 two nights permitted visual observing (Miskotte, 2013).

The village of Midden Eierland is actually not more than a crossing of two roads and 10–15 houses around it. On Texel people are very concerned about dark sky and light pollution. A few years ago, the public lighting on the entire island was adapted to dimmed LED lampposts. At some roundabouts, all lighting has even been removed and replaced by LEDs built into the road. The light pollution maps²² show that the area north of the villages of Den Burg and De Koog in particular is very dark to Dutch standards.

2 Observations in 2020

This year we were guests on Texel between May 20 and 29. Given the short preparation time, I decided not to bring any equipment, just a digital voicerecorder, a sleeping bag, DCF-77 clock and observation forms. We arrived on Texel on Wednesday 20 May, but visited astrophotographer Marco Verstraaten in Twisk on the way, to discuss the new all-sky housing that he will make for me. We were warmly welcomed and shown around his impressive back yard observatory and studio. Then we headed quickly to Texel.



Figure 2 – View from the garden towards the north. The lighthouse is left outside of the picture behind a row of trees.

The weather forecast was good for the Netherlands with lots of sun (and clear nights). However, during the weekend temporarily some rain and clouds were expected. The first night was clear but with some cirrus clouds. After the clouds on Friday and Saturday it got better on Sunday with blue almost Provencal skies during the day. Unfortunately, in the evening on the North Sea, middle high clouds and cirrus formed and moved over the island. Fortunately, the

²² <https://www.lightpollutionmap.info/>

next night (Monday on Tuesday) had a clear sky so I could do some observations.



Figure 3 – View to the south. The tall tree gives some obstruction.

May 25–26, 2020

The lampposts on the south side of our house were also adapted to (low!) full cut off luminaires with LED lighting. However, from the 2nd evening these were no longer turned on. Well I didn't think that was a disaster of course. The observations were done far back in the backyard. There is a small meadow with unobstructed views up to the northern horizon. De Cocksdorp lighthouse is 5 km away and hardly disturbs. There are also trees that way so you do not see direct light from the tower. Only the wall of a building a little further lit up weakly when the beam of light came by. To the south there is a little bit of obstruction of small trees and the houses.

I started at 21^h53^m UT when the SQM is 20.18. A small crescent moon was low in the west and set after one hour. In 2013 I did not have an SQM meter so I was curious about what it would eventually be. However, I kept in mind we were now at the beginning of the gray nights season and

here and there also was some sharply defined small tufts of cirrus... I was still surprised when I read the SQM measurements during the night, around 23^h30^m UT I even measured 21.53. The limiting magnitude was then 6.5!

Soon after the start of the meteor observations I saw the ISS, it always remains impressive when it passes. Unfortunately, a group of Starlink satellites also passed by around 22^h26^m and 00^h00^m UT. They were not as bright as in April (Miskotte, 2020), usually they were about magnitude +4 or +5.

I was observing meteors between 21^h53^m and 00^h50^m UT. The first hour was pretty tame with only 8 meteors, most of which were weak. The second hour was much better with 15 meteors, but during the last 50 minutes things started to settle down a bit with 8 meteors. So, a total of 31 meteors in 2.92 hours effective of which 6 ANT. Three of them in the second hour. The most beautiful meteors were at 23^h39^m UT (a short +1 orange ANT near the star alpha Libra), at 00^h03^m UT a beautiful fast bluish-colored –1 sporadic meteor in Lyra and Cygnus with a persistent 4-second train and later an orange +2 Antihelion. At 23^h01^m UT I was startled by a flash of light from the north. Turns out to be a very bright satellite that gave flashes up to magnitude –6.

All in all, a nice session! The combination of the beautiful clear starry sky with the planets Jupiter and Saturn from 0^h UT, with the rest (barely car traffic), the sounds of the birds and frogs remains great!

The next night, there was an alternation of clear gaps and fields of medium and high clouds. Fortunately, it cleared up very nicely later in the day and a clear night awaited!

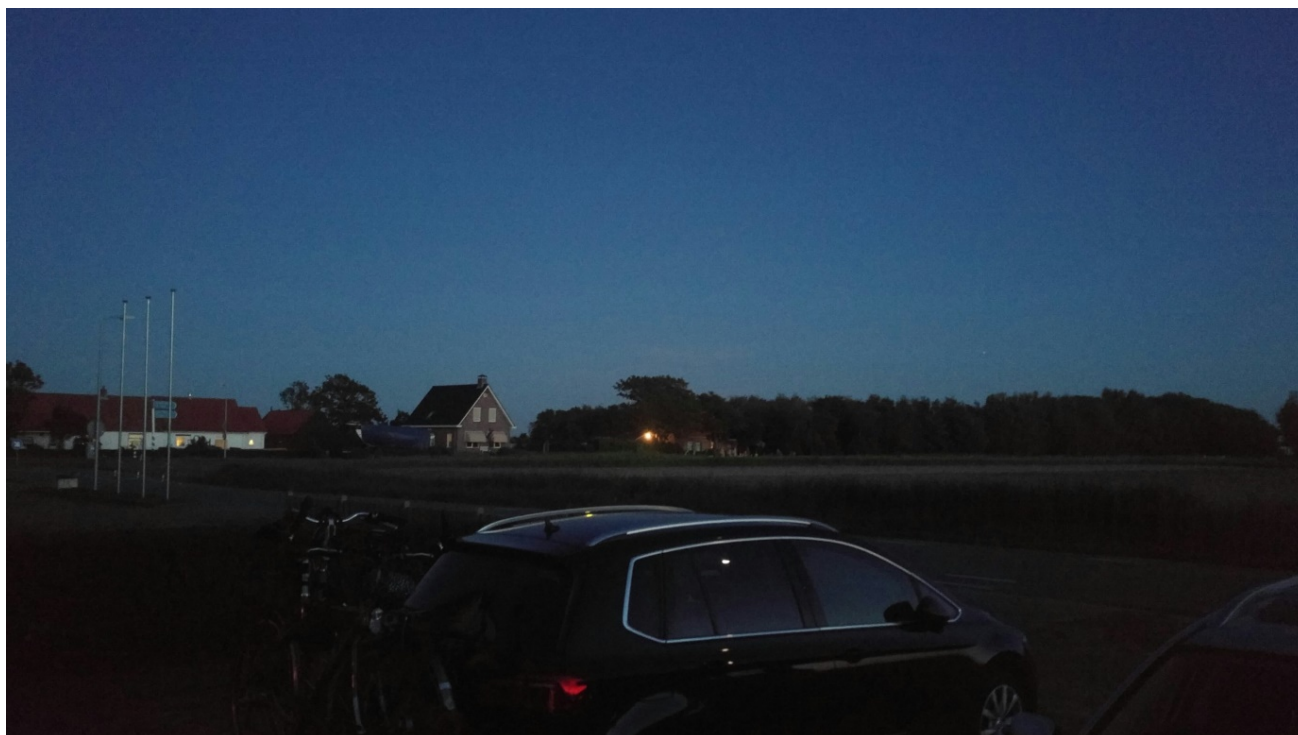


Figure 4 – Evening twilight Midden-Eierland. The street lights were off.

May 27–28, 2020

Unfortunately, the Moon would disturb much longer his night. The Moon would set at 00^h06^m UT, when twilight was beginning. Indeed, this was clearly visible in the SQM measurements. After an increase to a maximum of 21.40 around 00^h00^m UT it slowly started to decline again. Still, an SQM measurement of 21.20 at 23^h00^m UT is quite impressive if you take into account the Moon and the gray nights. The maximum limiting magnitude reached 6.4.

Also this night, again 31 meteors were counted in 2.73 hours effective. Of those, 4 were Antihelions. Also, this time an ISS passage and later a Starlink train. Slightly less bright meteors, a nice magnitude –1 moved through Hercules with a wide wake. A bright meteor that was recorded at 00^h43^m UT with the all sky camera at Twisk (Marco Verstraaten) was not seen, it appeared behind my back. All-in all this visual session was very successful.

28–29 May 2020

Although the Moon would disturb all night, I did another observational session. This time from the small garden on the street side. There, you could look over the meadows. There was a small light dome in the south, this will be probably the city Den Helder. The Den Helder lighthouse was also visible as a small rotating light beam up to 10 degrees in the south. The advantage of this location tonight was that the Moon stayed hidden behind the house of the owners. The street lights were also off, otherwise the story

would have been different. I was surprised again when I read the SQM measurements, it still reached 21.15 around 00^h12^m UT.

I was able to observe between 23^h35^m and 01^h03^m UT. During 1.45 hours I counted 9 meteors, 1 ANT. Two +2 sporadic meteors were the brightest.

Three successful observations under very dark skies this time was a great score! On the way back we paid a visit to Jos and Karin Nijland, who showed us their new impressive house. Thanks for the hospitality Jos and Karin!

References

- Miskotte K. (2013). “Meteoren en satellieten vanuit Texel”. *eRadiant*, **35**, 55–56.
- Miskotte K. (2018). “Midsummer nights 2018. Meteor observations at Any Martin Rieux, Northern France”. *eMetN*, **3**, 201–203.
- Miskotte K. (2019). “Meteor observations from the very dark village Buzancy in northern France”. *eMetN*, **4**, 241–243.
- Miskotte K. (2020). “Lyrids 2020: another great campaign!”. *eMetN*, **5**, 317–320.

Observations January 3-4, 2020

Pierre Martin

Ottawa, Canada

meteorshowersca@yahoo.ca

An overview is given of the 2020 meteor observations by the author, covering the Quadrantid meteor shower.

1 Introduction

The Quadrantids (QUA) are usually as strong as the more widely observed Perseids and Geminids, but have a short peak, making them tricky to see at their best. For 2020, it appeared to be promising with an ideal timing of the shower's narrow peak for North American longitudes, as well as favorable viewing conditions (setting first quarter moon before the prime viewing time). Raymond Dubois decided to join me for an attempt to observe and photograph the shower. The big question was the weather which can easily be poor (and very cold) at this time of the year. Up until just a day or two before the peak, the forecasts were dismal and would show just a few possible clear holes several hours of drive from Ottawa. We wanted to setup at a local dark sky site, but the hope for that was quickly vanishing. Instead, it looked like a longer road trip would be necessary to catch this shower!

2 The observations

We found that the weather forecasts favored clearer skies up past Quebec city, along the Saint Lawrence River, we had only about a day to organize our gear and pack up. The road trip would be around 500 km into an unfamiliar area, so we also needed some extra time to locate an observing site (that is dark, quiet, secluded and with a wide open view of the sky) and then setup. We packed everything in Raymond's SUV, and we left early on the afternoon of the 3rd. After an uneventful trip, we checked out two possible sites. The first one had possibilities but would likely have lights from passing cars. The second site was much more secluded, deep in a field, well away from any traffic or lights. It was perfect! We unpacked the car and got busy with our setups.

Much of the evening had an overcast sky, and it wasn't until



Figure 1 – Composite image of 25 Quadrantids. January 3–4 2020. Canon 6D with 24mm lens at f/2.0, ISO 1600.

9 pm that it cleared enough to align our mounts. The clearing was short lived though, and clouds rolled in for another two hours. It was mild at only +1C but the windchill made it feel like -8C, and it was certainly felt in the wide-open space we were. Raymond found refuge behind the back of his SUV while I wrapped myself up in my thick sleeping bag and bivy sack. Near midnight, the sky cleared and a few really nice Quadrantid earthgrazers appeared, including a 50 degrees long colorful -2 moving up into Ursa Major (though not captured by any of our cameras). I made a few early attempts to sign on for formal counts, but that didn't last more than a few minutes before getting clouded over again.



Figure 2 – Cameras setups.



Figure 3 – Observing site.

At around 1^h00^m am EST, the sky became variable cloudiness but the Quadrantids were very active. Several meteors could be seen passing through the clear holes,

including a beautiful blue Quadrantid near Procyon. It appeared that the shower was near full tilt, but it was still too cloudy for formal counts.



Figure 4 – Observing site.



Figure 5 – Equipment.



Figure 6 – The observing set up.

The sky finally cleared almost completely at 1^h25^m am, and I could observe for the next two and a half hours with a high radiant. The shower's peak was expected around at 4^h00^m am, but instead of seeing a shower building up in intensity, the opposite effect was seen. The peak clearly came a few hours earlier than predicted. My QUA hourly rates were 26, 28 and 14 (for the final half hour) for a total of 71 Quadrantids. On top of that, I saw 3 December Leonis

Minorids, 2 Anthelions, 2 January Leonids, 2 lambda Bootids and 12 sporadics. The nicest meteor was a mag +1 QUA just after midnight that left a long wake on top of Orion.

Even though we missed the Quadrantids peak and the late-night rates were disappointing, it was still a great night.



Figure 7 – Composite image of 7 Quadrantids and 1 sporadic. January 3-4 2020. Canon 5D with 35mm lens at f/2.0, ISO 800.

Thank you to Raymond Dubois for joining me! Had the peak came by on schedule, we would have been in perfect position to have seen it! As it turns out, the European and Atlantic longitudes had a better view of it this time.

3 Visual report

Observer: Pierre Martin^{23,24}.

Session Date: January 3–4 2020, 05^h25^m–09^h10^m UT (00^h25^m–04^h10^m EST). Location: L'Islet, Quebec, Canada (lng: -70.4039; lat: 47.0690).

Observed showers:

- Anthelion (ANT) – 07:48 (117) +21
- alpha Hydrids (AHY) – 08:32 (128) -09
- January Leonids (JLE) – 09:55 (149) +24
- December Leonis Minorids (DLM) – 11:34 (174) +24
- lambda Bootids (LBO) – 14:00 (210) +51
- Quadrantids (QUA) – 15:23 (231) +49

05^h25^m–05^h50^m UT (00^h25^m–00^h50^m EST); partly cloudy; 3/5 trans; F 1.11; LM 5.80; facing N70 deg; t_{eff} 0.333 hr

- QUA: three: +1(2); +2
- Sporadics: one: +5
- Total meteors: Four

06^h25^m–07^h41^m UT (01^h25^m–02^h41^m EST); a few clouds early in the period; 3/5 trans; F 1.03; LM 6.20; facing NE60 deg; t_{eff} 1.00 hr

- QUA: twenty-six: +1(4); +2(6); +3(4); +4(5); +5(7)
- ANT: two: +4; +5
- JLE: one: +5
- LBO: one: +4
- Sporadics: one: +3
- Total meteors: Thirty-one

07^h41^m–08^h41^m UT (02^h41^m–03^h41^m EST); clear; 3/5 trans; F 1.00; LM 6.20; facing NE60 deg; t_{eff} 1.00 hr

QUA: twenty-eight: 0; +1(3); +2(5); +3(3); +4(7); +5(9)

- JLE: one: +2
- DLM: one: +4
- LBO: one: +5
- Sporadics: nine: +1; +2(2); +3; +4(4); +5
- Total meteors: Forty

08^h41^m–09^h10^m UT (03^h41^m–04^h10^m EST); increasing clouds; 3/5 trans; F 1.21; LM 6.20; facing NE60 deg; t_{eff} 0.48 hr

- QUA: fourteen: 0; +1(3); +2; +3(5); +4(3); +5
- DLM: two: +1; +2
- Sporadics: one: +4
- Total meteors: Seventeen

Dead time: 21 minutes (for breaks)

Breaks (UT): 05^h40^m–05^h45^m, 05^h50^m–06^h25^m, 06^h40^m–06^h56^m.

²³ IMO Profile:
https://www.imo.net/members/imo_user/profile/?user_id=8022

²⁴ Session Link:
https://www.imo.net/members/imo_vmdb/view?session_id=79859

June 2020 report CAMS BeNeLux

Paul Roggemans

Pijnboomstraat 25, 2800 Mechelen, Belgium

paul.roggemans@gmail.com

A summary of the activity of the CAMS BeNeLux network during the month of June 2020 is presented. 6122 multiple station meteors were captured which allowed to calculate 1834 orbits. June 2020 was better than the average for this month, but less favorable than June 2019 which remains a record month of June.

1 Introduction

The last weeks of May and first weeks of June display very low meteor activity combined with short nights with between 7 hours and less than 6 hours of capture time. Therefore, no spectacular numbers of orbits are to be expected. Collecting orbits under these circumstances remains a challenge. What did June 2020 bring us?

2 June 2020 statistics

June is the most difficult month for CAMS BeNeLux because of the short observing window of barely 5 hours dark sky each night. June 2020 brought better weather conditions than usually for this time of the year, although the weather was not as good as in June 2019. Three nights remained without any double station meteors. Eight nights resulted in more than 100 orbits in spite of the short duration of these nights while in 2019, 13 nights had more than 100 orbits and two nights got over 200 orbits each! The statistics for June 2020 are compared in *Figure 1* and *Table 1* with the same month in previous years since the start of CAMS BeNeLux in 2012.

Table 1 – June 2020 compared to previous months of June.

Year	Nights	Orbits	Stations	Max. Cams	Min. Cams	Mean Cams
2012	0	0	4	0	–	0.0
2013	16	102	9	12	–	7.0
2014	23	379	13	31	–	19.0
2015	20	779	15	44	–	32.9
2016	18	345	17	50	15	35.7
2017	26	1536	19	66	30	52.1
2018	28	1425	21	78	52	64.9
2019	28	2457	20	84	63	75.6
2020	27	1833	24	93	60	83.1
Total	186	8856				

While all CAMS stations in Belgium operate 7/7 with AutoCams, some CAMS stations in the Netherlands still operate occasionally when the weather is clear. This way the coverage of the northern part of the network area is a little bit less than the southern part. For the coverage of the

atmosphere by a camera network the chances for multiple station events especially during nights with variable weather depends on how many cameras are operational. The greatest progress for the CAMS BeNeLux network was the introduction of Auto CAMS by Steve Rau. Gradually more and more CAMS operators decided to make use of AutoCams to operate their system 7/7. As the weather proves often to be unpredictable, the only way not to miss unexpected clear sky is to have the camera systems running all nights, regardless the weather.

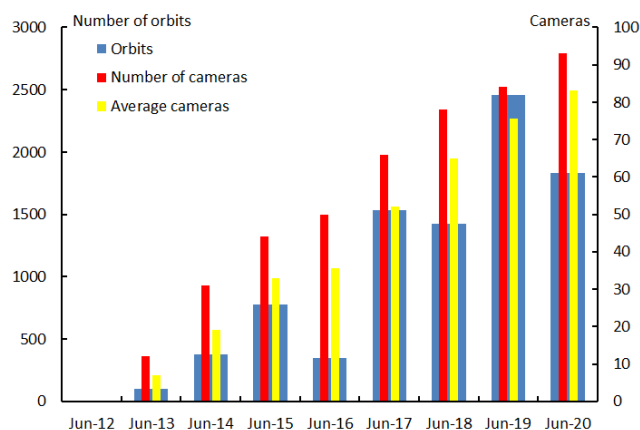


Figure 1 – Comparing June 2020 to previous months of June in the CAMS BeNeLux history. The blue bars represent the number of orbits, the red bars the maximum number of cameras running in a single night and the yellow bar the average number of cameras running per night.

During the best nights up to 93 cameras were operational (84 in June 2019 and 78 in 2018). Thanks to AutoCAMS at least 60 cameras were all nights operational (63 in 2019 and 52 in 2018). On average 89.4% of all available cameras were active, comparable to the 90% of last year. The ratio of multiple station coincidences depends on the number of stations with clear sky during the same time span. The more stable the weather conditions are network wide and the less technical problems, the better the chances to catch a meteor from at least two stations.

Two RMS cameras produced the best scores in terms of orbits of all cameras in the CAMS BeNeLux network. There is no competition to nominate any most successful camera in the network, but in this case, it is interesting to see how the RMS performs compared to the Watecs. Certain cameras are pointed at regions where the chances for

multiple station events is simply significant less, for instance towards the borders of the camera network coverage. However, to illustrate the order of difference for these RMS cameras, it is useful to compare these numbers with what the most successful Watecs obtained.

Table 2 – The ten cameras of the CAMS BeNeLux network with the best score in terms of orbits during June 2020.

Camera	Total orbits	Total nights
Grapfontaine BE (RMS 003814)	378	30
Genk BE (RMS 003815)	241	30
Kattendijke NL (RMS 000378)	178	30
Mechelen BE (RMS 003831)	143	29
Grapfontaine BE (000814)	141	30
Wilderen BE (000380)	133	30
Mechelen BE (RMS 003830)	130	29
Mechelen BE (000383)	116	30
Dourbes BE (000395)	115	30
Mechelen BE (000391)	113	30

3 Conclusion

June 2020 was a good month of June, but June 2019 remains the best month of June ever. The total number of orbits for the month of June rose to 8856 in 186 June nights that allowed to collect orbits. This way the month of June becomes the poorest covered month of the year for CAMS BeNeLux instead of March which had a record of orbits this year.

Acknowledgment

Many thanks to all participants in the CAMS BeNeLux network for their dedicated efforts. The data on which this report is based has been taken from the CAMS website²⁵. The CAMS BeNeLux team was operated by the following volunteers during June 2020:

Hans Betlem (Leiden, Netherlands, CAMS 371, 372 and 373), *Felix Bettonvil* (Utrecht, Netherlands, CAMS 376 and 377), *Jean-Marie Biets* (Wilderen, Belgium, CAMS 379, 380, 381 and 382), *Martin Breukers* (Hengelo, Netherlands, CAMS 320, 321, 322, 323, 324, 325, 326 and 327, RMS 328 and 329), *Guiseppa Canonaco* (Genk, RMS 3815), *Bart Dessoy* (Zoersel, Belgium, CAMS 397, 398, 804, 805, 806 and 888), *Jean-Paul Dumoulin*, *Dominique Guiot* and *Christian Walin* (Grapfontaine, Belgium, CAMS 814 and 815, RMS 003814), *Uwe Glässner* (Langenfeld, Germany, RMS 3800), *Luc Gobin* (Mechelen, Belgium, CAMS 390, 391, 807 and 808), *Tioga Gulon* (Nancy, France, CAMS 3900 and 3901), *Robert Haas* (Alphen aan de Rijn, Netherlands, CAMS 3160, 3161, 3162, 3163, 3164, 3165, 3166 and 3167), *Robert Haas* (Texel, Netherlands, CAMS 810, 811, 812 and 813), *Robert Haas / Edwin van Dijk* (Burlage, Germany, CAMS 801, 802, 821 and 822), *Kees Habraken* (Kattendijke, Netherlands, RMS 000378), *Klaas Jobse* (Oostkapelle, Netherlands, CAMS 3030, 3031, 3032, 3033, 3034, 3035, 3036 and 3037), *Carl Johannink* (Gronau, Germany, CAMS 311, 314, 317, 318, 3000, 3001, 3002, 3003, 3004 and 3005), *Hervé Lamy* (Dourbes, Belgium, CAMS 394 and 395), *Hervé Lamy* (Humain Belgium, CAMS 816), *Hervé Lamy* (Ukkel, Belgium, CAMS 393), *Koen Miskotte* (Ermelo, Netherlands, CAMS 351, 352, 353 and 354), *Tim Polfliet* (Gent, Belgium, CAMS 396), *Steve Rau* (Zillebeke, Belgium, CAMS 3850 and 3852), *Paul and Adriana Roggemans* (Mechelen, Belgium, CAMS 383, 384, 388, 389, 399 and 809, RMS 003830 and 003831), *Hans Schremmer* (Niederkruechten, Germany, CAMS 803) and *Erwin van Ballegoij* (Heesch, Netherlands, CAMS 347 and 348).

²⁵ <http://cams.seti.org/FDL/index-BeNeLux.html>

RMS cameras as alternative for Watec in CAMS

Paul Roggemans

Pijnboomstraat 25, 2800 Mechelen, Belgium

paul.roggemans@gmail.com

The new RMS cameras have been tested in Belgium since December 2018. From March 2019 onwards RMS cameras got fully operational within the CAMS BeNeLux network. The conclusion after months of testing is that the RMS is a valid alternative for the Watec camera. The RMS is significant cheaper, has a larger FoV and better positional accuracy, produces less false detections and has a slightly better score in percentage of orbits while the imaging quality is much better than that of the Watec camera.

1 Introduction

The CAMS BeNeLux network started in March 2012 with as standard equipment the relative expensive Watec H2 Ultimate cameras. Since all participants had to finance their own equipment, these costs seriously refrained amateurs to join the network. A camera with the required f/1.2, 12mm lens, frame grabber, power supply, video cables and camera housing requires a budget of about 650 Euro for each camera. A dedicated PC is also required for CAMS, regardless if one operates one single or several cameras. Since 2012 amateurs bought over a hundred of these camera units installed at about 25 camera stations of the BeNeLux network. A number of sites were equipped with 8 Watec cameras. Unfortunately, some amateurs quit and about 20 of these cameras are no longer used.

Since the CAMS standard equipment is based on 15-year-old technology, the hardware risks to become unavailable on the market. The EzCap frame grabbers tend to fail rather rapidly when being used permanently, but replacement becomes difficult to find. Windows 10 with its unavoidable updates caused some problems too. In recent years it became clear that we have to look for an alternative for the standard CAMS equipment. One possible alternative are the RMS cameras, introduced by Denis Vida and sold via the Croatian IStream²⁶. The first RMS cameras were offered for sale in October 2018 and the first such camera arrived in Belgium for testing in late November 2018. After some preliminary tests the first RMS got integrated in the CAMS BeNeLux network from 17–18 March 2019. After more than one and a half year of practice and testing, it is time for conclusions.

2 About the RMS camera

RMS stands for Raspberry Pi Meteor Station and has been developed in Croatia since 2014 when a Raspberry Pi was first used to record meteors (Zubović et al., 2015). Since then the project developed further into a more performant system that could be exported beyond Croatia. The software for the RMS cameras has been designed by Denis Vida, the registered meteor data is being collected and analyzed

within the Global Meteor Network²⁷ (Vida et al., 2019a; 2019b). Historically, the CAMS software has its roots in the video capture and detection methods and algorithms developed since 2006 in the Croatian Meteor Network project (Gural and Šegon, 2009). The new RMS software is to a large extent compatible with CAMS which is a major advantage on any other alternatives for the standard CAMS equipment. Some aspects were adapted in function of CAMS for instance the config file allows to define a CAMS ID number.

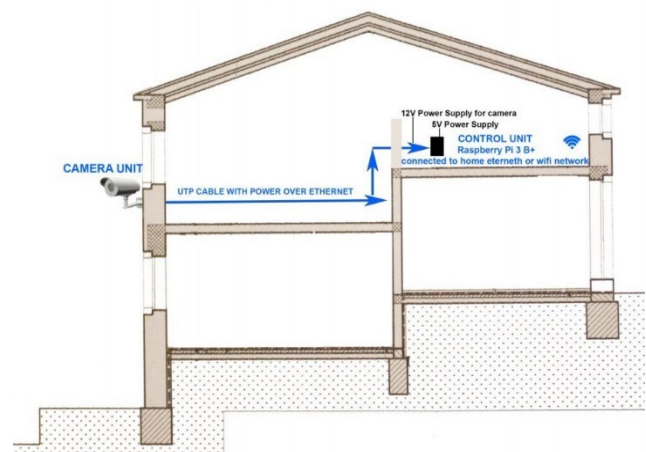


Figure 1 – Installing an IP camera controlled by its RPi connected to the internet (credit Denis Vida).

The first advantage of RMS is the required budget, purchased as plug and play, 450 Euro (price as advertised August 2020), ordering and assembling the components costs only ~200 Euro against 650 Euro + PC for a classic CAMS camera. Figure 1 shows the installation setup and Figures 2 and 3 display the camera components in detail. The RPi replaces the PC, no expensive video cables and no fragile frame grabbers are required. The images from RMS cameras show many more stars than those from Watecs (see Figure 6).

An excellent guideline can be found online²⁸ how to assemble all components to build your own RMS camera with a budget of about 200 Euro.

²⁶ <http://istrastream.com/rms-gmn/>

²⁷ <https://globalmeteornetwork.org/>

²⁸ <https://docs.google.com/document/d/18TT-Jm7z9kYsk1Sua07jQWD91OiyBemBnOosiNdW6nY/edit?usp=sharing>

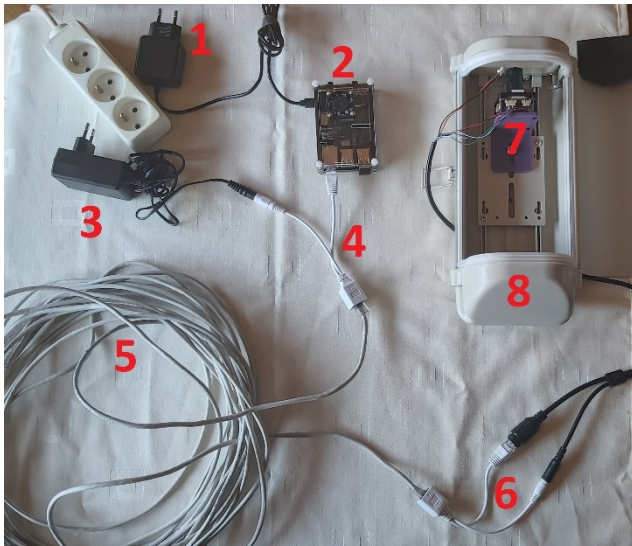


Figure 2 – Main parts of the RMS camera set up. (1) Power supply for the RPi, (2) RPi, (3) power supply for the camera, (4) Power over Ethernet connector, (5) ethernet cat.6 cable, (6), Power over Ethernet connector, (7) the camera itself and (8) the camera housing.

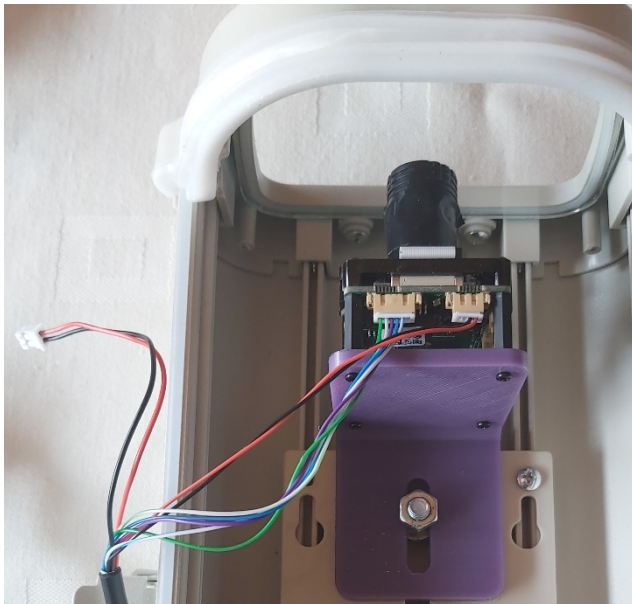


Figure 3 – Close up of the camera, note that the power supply to the camera has been split for in case an IR reflector is used.

While CAMS is running at most camera stations with a battery of Watecs, often 8 or even 16 cameras operated by a single PC, each RMS comes with its own small computer, the RPi. If a CAMS PC has a failure, all its cameras are affected, while a failure on an RPi affects only a single camera. The data reduction, removal of false detections and reporting of the data can be done for CAMS in a single procedure. Doing the same number of RMS cameras one by one takes significant more time.

The CAMS Watecs with the $f/1.2$, 12mm lenses and FoV of $22^\circ \times 30^\circ$ register many short faint meteors which are at the limit of detectability with poor chances to be multiple station. The RMS is a bit less sensitive and missing the faintest magnitude meteors captured by Watecs. The advantage of the RMS camera is that it can be combined with larger FoV optics with a good resolution, for instance

at dark sites the $f/0.95$, 3.6 mm lens covers more than 4 times the standard FoV of the CAMS Watecs. For light polluted areas the $f/1.0$, 8mm lens is recommended which has a FoV about 1.5 times that of the standard CAMS Watec.

The CAMS detection algorithm measures twice as many points on a meteor trail than the RMS software. However, the positional accuracy of the RMS is better because of the calibration for each detection while CAMS extrapolates from a single reference calibration for the entire night. Since the RMS requires the presence of a minimum of stars for each detection, it will not detect anything when the minimum of required stars is not available. While CAMS often detects meteors through thin clouds without any stars being visible, the RMS will detect nothing in such situation.

3 RMS in Belgium

The first RMS got installed in December 2018, with the large FoV $f/0.95$, 3.6mm lens at the light polluted camera station in the city of Mechelen. After initial tests this camera was replaced in March 2019 with a $f/1.0$, 8mm lens, identified as BE0002 in the Global Meteor Network and 003830 in CAMS. The first RMS got operational in Grapfontaine from 15–16 May 2019 identified as BE0001 with CAMS ID 003814. A third RMS followed 17–18 July 2019 in Genk with codes BE0003 and 003815. The fourth RMS had its first meteors 22–23 August 2019 in Mechelen, labelled BE0004 and 003831. Figure 4 shows the field of view (FoV) of the 4 cameras projected at an altitude of 100 km in function of the coverage required for the other cameras of the CAMS BeNeLux network.

Although each camera was focused, configured and tested in Croatia before being shipped as plug-and-play, all four RMS cameras required some finetuning after being installed. Without the assistance by Denis Vida, I would not have managed to get the RMS functioning. Luckily for me, Denis Vida solved the problems remotely or provided me with precise instructions what to do to help me out. Meanwhile the system got regularly updated and became far more stable than it was in the very beginning.



Figure 4 – The Belgian RMS cameras installed in Genk (BE0003), Grapfontaine (BE0001) and Mechelen (BE0002 and BE0004) with the FoV intersected at 100 km elevation.

4 Watecs versus RMS

The four RMS systems in Belgium have been successfully operational for a relevant period of time. There is enough data to compare some basic statistics to compare both systems, CAMS with Watecs versus CAMS with RMS, in order to answer the question whether or not the RMS cameras can be used as a valid alternative for the old Watec configuration for CAMS.

Table 1 – Comparison between RMS and Watecs in 2019. RMS BE0002 started 17–18 March 2019 (271 nights), BE0001 started 15–16 May (222 nights), BE0003 started 17–18 July (154 nights) and BE0004 started 22–23 August (132 nights). All 6 Watecs were running entire 2019 (365 nights).

Camera	Detect.	Meteors	%	Orbits	%
BE0001 3814	9993	7830	78.4%	5573	71.2%
BE0003 3815	11622	2871	24.7%	2021	70.4%
BE0002 3830	22504	4973	22.1%	3512	70.6%
BE0004 3831	22070	2947	13.4%	1098	37.3%
Total RMS	66189	18621	28.1%	12151	65.3%
Watec 383	39518	3654	9.2%	2322	63.5%
Watec 384	39520	4387	11.1%	3023	68.9%
Watec 388	39520	3462	8.8%	2503	72.3%
Watec 389	39516	3118	7.9%	1245	39.9%
Watec 399	39517	3575	9.0%	2724	76.2%
Watec 809	39500	3981	10.1%	1997	50.2%
Total CAMS	237091	22177	9.4%	13814	62.3%

Table 2 – Comparison between RMS and Watecs in 2020. RMS BE0002 (177 nights), BE0001 (177 nights), BE0003 (178 nights) and BE0004 (177 nights). All 6 Watecs were running during the entire period 1 January until 30 June 2020 (182 nights).

Camera	Detect.	Meteors	%	Orbits	%
BE0001 3814	6943	3880	55.9%	2710	69.8%
BE0003 3815	33513	2659	7.9%	1857	69.8%
BE0002 3830	23246	1753	7.5%	1344	76.7%
BE0004 3831	16617	1807	10.9%	1107	61.3%
Total RMS	80319	10099	12.6%	7018	69.5%
Watec 383	14989	1285	8.6%	866	67.4%
Watec 384	14989	1288	8.6%	884	68.6%
Watec 388	15001	1109	7.4%	807	72.8%
Watec 389	15002	1056	7.0%	409	38.7%
Watec 399	14996	1144	7.6%	892	78.0%
Watec 809	14999	1334	8.9%	794	59.5%
Total CAMS	89979	7216	8.0%	4652	64.5%

We split the available information in two sets, the first with the earliest RMS data mainly obtained during the second half of 2019 with the meteor rich season (*Table 1*) and the second during the first 6 month of 2020 (*Table 2*). Two trends can be spotted, RMS seems to have less false detections and a higher percentage of meteors that prove to be multi-station with a valid orbit. However, the results

differ a lot between the cameras and requires a look at each of them separately.

BE0001 f/0.95, 3.6mm lens (CAMS 003814)

This camera was first installed end 2018 in Mechelen but its optics proved to be unsuitable for light polluted sites. Therefore, the camera was moved to Observatoire Centre Ardennes, a public observatory in Grapfontaine, a dark region in the south-east of Belgium. The camera got reinstalled in April 2019, but it took a while before some technical issues were solved. From May till December 2019 this camera had 9993 detections of which 7830 were confirmed as meteors or 78.4%, good for 5573 orbits or 71.2%. The first six months of 2020 confirmed this trend with 3880 meteors out of 6943 detections or 55.9%. Stormy winter weather with fast moving clouds caused unusual numbers of false detections, but still the proportion remained much in favor of RMS compared to the Watec scores. The number of 2710 meteors (69.8%) with orbits is slightly lower due to poor coverage from the northern part of the CAMS network which had bad weather.

With these scores this camera performed as the best camera of the CAMS BeNeLux network. The camera is pointed low at 37° elevation so that its large FoV overlaps with almost 2/3rd of the network because of its large 47° × 88° FoV. The lens is very efficient at a dark sky, BE0001 often detects only meteors without any false detections which is a great advantage for a video meteor camera.

BE0002 f/1.0, 8mm lens (CAMS 003830)

This camera was purchased as replacement for BE0001 in Mechelen and got operational 17–18 March 2019. The lens was chosen because of the problematic light pollution in the city of Mechelen. Moreover, the camera is pointed low at 30° right into the worst light polluted part of the sky. With 22504 detections of which 4973 meteors or 22.1% the camera has substantial more false detections mainly caused by planes from the nearby Brussels airport. With 3512 orbits or 70.6% the camera scores very high. First three months of 2020 had huge numbers of false detections caused by rapid moving clouds in stormy weather. April, May and June had almost no false detections because of the Covid lockdown with almost no air traffic. With low meteor activity 92.5% of all detections were false. 1344 meteors of the 1753 resulted in an orbit, or 76.7% and that makes this camera one of the best performing in the CAMS network. With its f/1.0, 8 mm lens and FoV of 22° × 41°, this proves to be an ideal camera for light polluted areas.

BE0003 f/0.95, 3.6mm lens (CAMS 003815)

BE0003 got installed in July 2019 on the roof of Cosmodrome, a public observatory in Genk. The camera had to be pointed south and to avoid over exposure by moonlight a f/0.95, 6mm lens was ordered. Unfortunately, the camera was delivered with a wrong lens, the f/0.95, 3.6 mm. As a change would take several weeks, it was decided to try the camera with this lens. However, all nights around Full Moon proved to be ruined as no calibration is possible when the Moon is in the FoV and no detections can be recorded. Capturing since 17–18 July 2019, BE0003 had

11622 detections of which 2871 were meteors or 24.7%. Light pollution and planes caused many more false detections in Genk than at the darker location of Grapfontaine (BE0001). With 2021 orbits or 70.4% the camera still scores very well. The first 6 months of 2020 confirm these scores with 7.9% of all detections being meteors and 69.8% of all meteors resulting in an orbit.

One reason why the total number of meteors remained far less than that of an identical RMS in Grapfontaine was caused by humidity. During humid nights the camera housing gets covered with dew above the flat roof. To avoid dew the camera will be moved to a position at the edge of the roof. To reduce the problem with light pollution and the Full Moon in the FoV, the RMS will be replaced by a new camera with a f/0.95, 6mm lens and FoV $30^\circ \times 54^\circ$, a change that got postponed due to Covid and lockdown measures. We strongly recommend not to use the RMS with a f/0.95, 3.6mm lens with its $47^\circ \times 88^\circ$ FoV for cameras that must be pointed in Southern direction because the calibration fails during a few nights around Full Moon.

BE0004 f/1.0, 8mm lens (CAMS 003831)

Since BE0002 proved to be very efficient being pointed low to give coverage on a large part of the network in the Netherlands, an identical RMS was purchased to give coverage over Luxembourg and the south-eastern camera fields of the network. BE0004 got installed with some delay as it took a while to solve some technical issues. This camera got pointed South East at 32° elevation. The smaller FoV, $22^\circ \times 41^\circ$ is more suitable in the light polluted city of Mechelen. Even with Full Moon in the FoV, the camera registers meteors. Started 22–23 August 2019, BE0004 had 22070 detections of which 2947 were meteors or 13.4%, many of the false detections being caused by planes and moonlight reflected on the edges of clouds. 1098 of the meteors combined with some other stations to obtain an orbit, or 37.3%. This percentage is much lower than for the three other RMS cameras since the region covered by this camera had poor coverage from other camera sites. The first 6 months of 2020 confirm the statistics for the camera. The significant increase in percentage of meteors with orbits happened because of some adjustments in the camera network to improve camera coverage on this area (*Table 2*).



Figure 5 – Some of the cameras at the authors' home.

5 Advantages of the RMS

CAMS is using the Watec H2 Ultimate with a small FoV of $22^\circ \times 30^\circ$ f/1.2, 12mm lenses (Jenniskens et al., 2011). These are very efficient with severe light pollution. When considering to use RMS cameras different optics can be chosen. The larger the FoV, the more meteors the camera may capture if the sky is dark enough. The choice for the optics depends on the light pollution.

Another important aspect is the resolution. A Watec H2 with f/1.2, 12mm lens has a resolution of 2.8 arc/pix in NTSC format and 2.5 arc/pix in PAL. The RMS with f/1.0, 8mm lens has a resolution of 1.9 arc/pix with a FoV of $22^\circ \times 41^\circ$ which is better than the Watecs. The option with f/0.95, 6mm lens has a resolution of 2.5 arc/pix, identical to the Watec in PAL format, but the FoV is $30^\circ \times 54^\circ$, significantly larger than that of the Watec. The f/0.95, 3.6mm lens has a resolution of 3.9 arc/pix but a FoV of $47^\circ \times 88^\circ$ which is huge compared to the Watecs.

The positional accuracy on video meteor cameras depends on the astrometric accuracy of the calibration which is based on a single calibration for an entire night or series of nights in the case of CAMS assuming that these remain stable for a fixed camera. However, the calibration parameters change during the night and the deviations are far larger than the resolution of the camera. The RMS comes with a detection and calibration algorithm which adjusts the general calibration for each single detection. This correction requires standard minimum 20 stars. In light polluted regions this can be lowered to 12 stars while the theoretical minimum to have a solution is 5 stars. This requirement means that RMS ignores meteors detected through clouds when not enough reference stars are present for the calibration correction. This is a major advantage in favor of the RMS with significant better-quality positional accuracy than the Watecs with the CAMS calibration.

Very bright meteors are problematic with CAMS as pixels get randomly detected in overexposed parts, RMS ignores overexposed detections in its standard detection algorithm. Fireballs got a separate solution which requires a manual procedure to determine the positions. This way unreliable positions are banned from the DetectInfo file for further automated data processing.

The significant better positional accuracy, less false detections with a much larger FoV with a good resolution definitely all favor the RMS above the Watecs of CAMS.

6 Disadvantages of the RMS

The concept of the RMS offers important advantages, but during the tests we encountered some problems too:

- While setting up a Watec to start recording meteors with the CAMS software was really plug-and-play, installing the RMS was less straight forward. These IP cameras connected with the RPi based on Linux had specific network problems that had to be solved. Resetting the router of your internet provider, changing

a switchbox or adding some new device may interfere with the local network and its IP addressing. If for some reason the camera gets another IP address allocated than the one foreseen in the config file, the RPi fails to connect to its camera.

- The RPi freezes every now and then. Without anyone checking the system, it would remain idle until someone reboots the RMS. Until 31 December 2019 during the 289 available nights, 46 incidents occurred that one of the four RMS cameras could not function due to some failure. The CAMS Watecs had zero incidents during this period. During 182 nights in 2020, each RMS camera lost 5 nights due to failures of the RPi while the Watecs functioned all nights without incidents. One way to reduce the number of failures is to reboot the RPi each day.
- While both Watecs and RMS capture 25 frames per second, the RMS detects one position for each frame while the Watecs with CAMS software detect two positions for each frame.
- CAMS video camera stations in most cases have 4, 6 or 8 Watecs running on a single computer. The DetectInfo files for all cameras are combined into a single DetectInfo file with a unified Archived folder for all detections of all cameras. The confirmation of meteors and elimination of false detections happen in a single procedure that may take 5 up to 10 minutes of work if no excessive numbers of false detections are caused. With the RMS cameras this procedure has to be repeated for each camera separately, which takes for each single RMS camera about the time required as for a whole battery of Watecs. To replace eight Watecs with f/1.2, 12mm lenses, six RMS cameras are required with f/1.0, 8mm lenses to have the same coverage at the sky. So far, I could not test with more than two RMS cameras installed within a single local computer network. To keep the confirmation routine workable an app is required to merge the archive folders and DetectInfo files of all RMS cameras at a camera site into a single DetectInfo which allows to do the confirmation for all cameras in a single procedure. Of course, this concerns only those who use RMS cameras within CAMS. GMN participants not involved with CAMS don't have to bother about confirmation procedures, for them all is running fully automated.

Like for every new project some child diseases occurred with the RMS cameras, most of which got solved meanwhile. The GMN is an open source project supported by a growing community, a concept which offers more flexibility than any existing video meteor observing project. Any problems encountered with the RMS cameras may be solved by this community itself. The purchase of an RMS is far cheaper than the CAMS set-up. At dark sites a large FoV can be applied with a single RMS replacing the FoV of more than 4 Watecs. Having these RMS cameras successfully operational as part of the CAMS BeNeLux network, we can safely conclude that these cameras offer a

decent alternative for the meanwhile old CAMS technology based on the Watecs.



Figure 6 – An example of a meteor picture obtained with an RMS camera with a f/0.95, 3.6 mm lens (BE0001, Grapfontaine). Notice the number of stars visible compared to the typical poor images obtained by Watecs.

7 GMN trajectory and orbit data

Although the topic of this report is about using RMS cameras within a CAMS network, the RMS and GMN offer a number of important extras, regardless whether these cameras are used within CAMS or not.

By using the RMS cameras with the GMN software, the user contributes video meteor data to the Global Meteor Network which computes trajectories and orbits that are made publicly available. All the final results can be downloaded from the website²⁹. For each RMS camera a status report³⁰ is compiled for each night including stacked images, thumbnails, radiant distribution, calibration report, astrometry report, photometry report and a time lapse³¹ of the night sky. The standard RMS output also provides the detection data in UFOCapture format (R91) of the SonotaCo network. To add the CAMS format output the only requirement is to define the CAMS camera ID in the RMS config file. With overlapping neighboring networks, the same meteors were often registered by different cameras from different networks. With RMS the data of a single meteor camera can now be delivered to different networks in the appropriate format. For the BeNeLux area this means that many meteors registered for CAMS, also got analyzed by the GMN as well as the French BOAM network which uses UFOCapture format.

One of the biggest advantages of the GMN is the public availability of the results. The trajectory and orbit data are available for anyone interested to make analyzes. CAMS orbit data is made public every few years, with the data until 2016 being public now. All CAMS data from 2017 and later is still under embargo which means that even the amateurs participating in the CAMS BeNeLux network are denied access to the orbit data obtained by their own cameras. For some amateurs the lack of feedback within CAMS has been a reason not to participate. It is a challenge to keep amateurs motivated when no results can be shared and feedback remains restricted to a minimum. Using the RMS gives

²⁹ <https://globalmeteornetwork.org/data/>

³⁰ <http://istrastream.com/rms-gmn/be0001/>

³¹ <https://youtu.be/i4TXFennJzE>

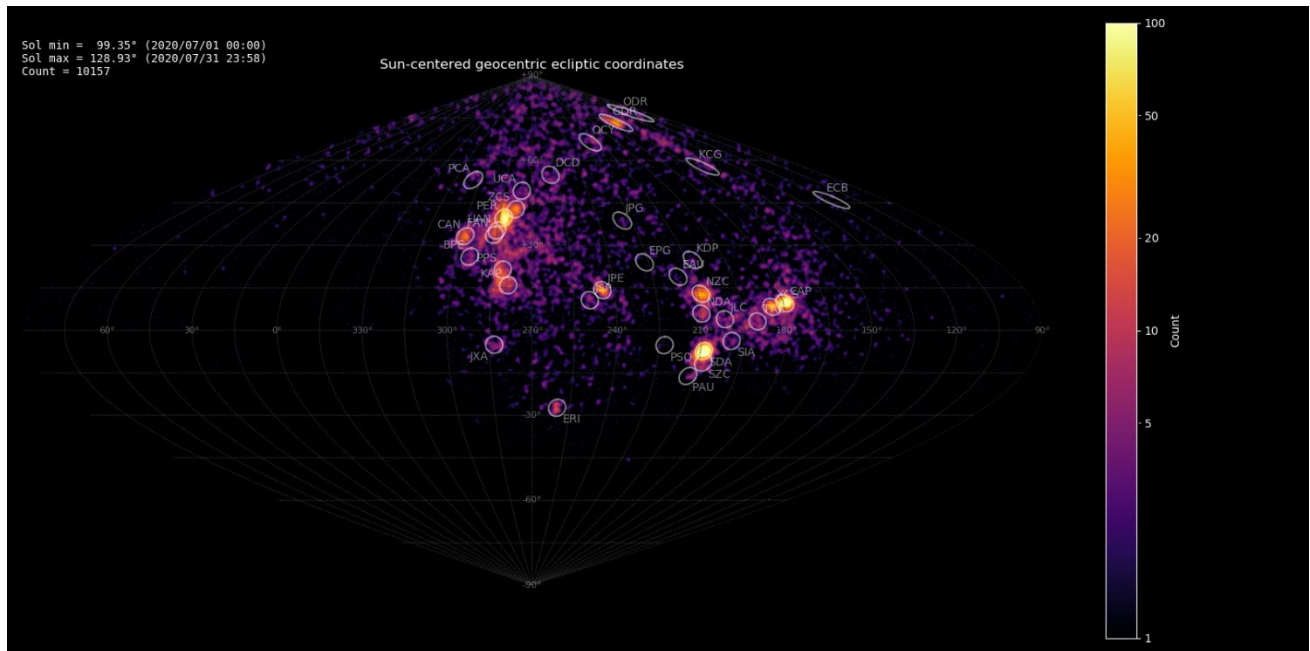


Figure 7 – Example of a heat map with the radiant density as obtained by GMN for July 2020.

direct access to its results which is far better for motivation than the data black hole policy applied for CAMS.

8 Conclusion

Since my first RMS camera got installed in Mechelen in December 2018, three more RMS cameras have been installed at three different sites in Belgium. After initial tests the RMS were successfully used for the CAMS BeNeLux network from 17–18 March 2019 onwards. Several shortcomings were solved during the testing period. The weak point in the RMS system remains the RPi which freezes too easily for no reason. A new OS for the RPi is expected to solve these problems.

Despite the encountered technical problems, the Belgian RMS cameras rank at the top as the best performing cameras in the CAMS BeNeLux network. Despite some frustrations with technical issues, the overall experiences are definitely positive. In my opinion the RMS cameras provide a valid alternative for the currently used Watecs in the CAMS networks. RMS cameras with 6 mm lenses are ideal to function at remote stations. The author hopes that more amateurs beyond the BeNeLux CAMS network will invest in video meteor work to expand the coverage of the Global Meteor Network. The RMS cameras have been developed for this purpose and will continue to expand our knowledge of meteor shower activity for the years to come.

Acknowledgment

The author thanks Denis Vida for his continuous support with the installation and operation of the RMS cameras. I thank Pete Gural for providing a conversion app to adapt the GMN DetectInfo to the CAMS format. Last but not least, I thank Martin Breukers and Damir Šegon for checking this article and for their valuable comments.

References

- Gural P. and Šegon D. (2009). “A new meteor detection processing approach for observations collected by the Croatian Meteor Network (CMN)”. *WGN, the Journal of the IMO*, **37**, 28–32.
- Jenniskens P., Gural P. S., Grigsby B., Dynneson L., Koop M. and Holman D. (2011). “CAMS: Cameras for Allsky Meteor Surveillance to validate minor meteor showers”. *Icarus*, **216**, 40–61.
- Vida D., Gural P., Brown P., Campbell-Brown M. and Wiegert P. (2019a). “Estimating trajectories of meteors: an observational Monte Carlo approach - I. Theory”. *Monthly Notices of the Royal Astronomical Society*, **491**, 2688–2705.
- Vida D., Gural P., Brown P., Campbell-Brown M. and Wiegert P. (2019b). “Estimating trajectories of meteors: an observational Monte Carlo approach - II. Results”. *Monthly Notices of the Royal Astronomical Society*, **491**, 3996–4011.
- Zubović D., Vida D., Gural P. and Šegon D. (2015). “Advances in the development of a low-cost video meteor station”. In: Rault J.-L. and Roggemans P., editors, *Proceedings of the International Meteor Conference*, Mistelbach, Austria, 27-30 August 2015. IMO, pages 94–97.

Delta Aquariids and Perseids 2020

Radio meteor observation report in the world

Hiroshi Ogawa

h-ogawa@amro-net.jp

The meteor activity of the delta Aquariids and Perseids has been observed by radio meteor observers worldwide. The delta Aquariids showed a peak time later than in previous years. The Perseids displayed the same usual activity level and also some unexpected activity.

1 Introduction

Radio Meteor Observations in the world covered the meteor shower activity of the delta Aquariids and the Perseids 2020. Worldwide radio meteor observation data were provided by Radio Meteor Observation (RMOB) (Steyaert, 1993) and by the radio meteor observations network in Japan (Ogawa et al., 2001).

2 Method

For analyzing worldwide radio meteor observation data, meteor activities are calculated by the “Activity Level” index (Ogawa et al., 2001). The activity profile was estimated by the Lorentz activity profile (Jenniskens, 2000).

3 Results

3.1. delta Aquariids

Figure 1 shows the result for the delta Aquariids with 33 observations in 12 countries. The activity peak was estimated to occur around 08^h UT on 28th of July (Solar Longitude $\lambda_{\odot} = 125.45^{\circ}$). Distinct activity was given by three components. The first peak was around 24th of July (Solar Longitude $\lambda_{\odot} = 121.8^{\circ}$). The main peak was 08^h UT on the 28th of July. The last component had a peak around the 4th of August (Solar Longitude $\lambda_{\odot} = 132.5^{\circ}$).

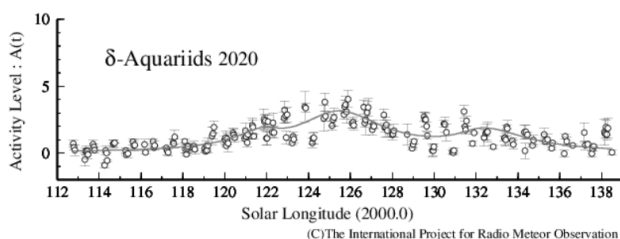


Figure 1 – Delta Aquariids 2020 using worldwide radio meteor observations.

The long-term activity profile for the delta Aquariids for 2005–2020 is shown in Figure 2. The peak in the long-term activity is at Solar Longitude $\lambda_{\odot} = 125.0^{\circ}$ with full width half maximum (FWHM) $-2.8^{\circ}/+5.3^{\circ}$. The maximum activity level was 3.0.

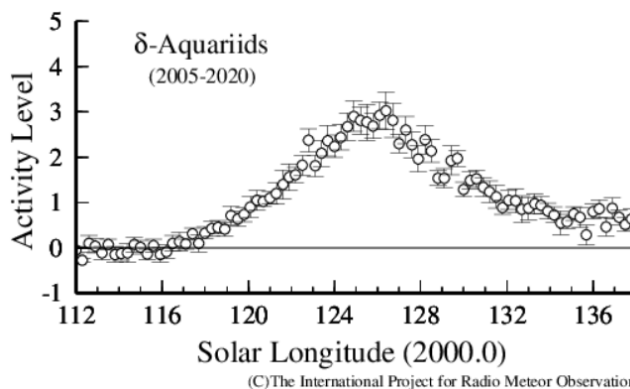


Figure 2 – The long-term activity profile of the delta Aquariids covering the period 2005–2020.

3.2 Perseids

One of the major meteor showers, Perseids displayed annual and unexpected activities based on 39 observations in 11 countries. The annual activity was estimated to have occurred around 17^h on 12th August (Solar Longitude $\lambda_{\odot} = 140.17^{\circ}$) with a maximum activity level = 1.2. The peak time was later than in the long-term activity data.

The unexpected activity was observed around 10^h on 13th August. This activity level was higher than the annual activity. The activity profile shows the estimated peak time around 10^h on 13th August (Solar Longitude $\lambda_{\odot} = 140.85^{\circ}$) and activity level was 1.5. Last year, a sub-peak was also observed around Solar Longitude $\lambda_{\odot} = 140.70^{\circ}$.

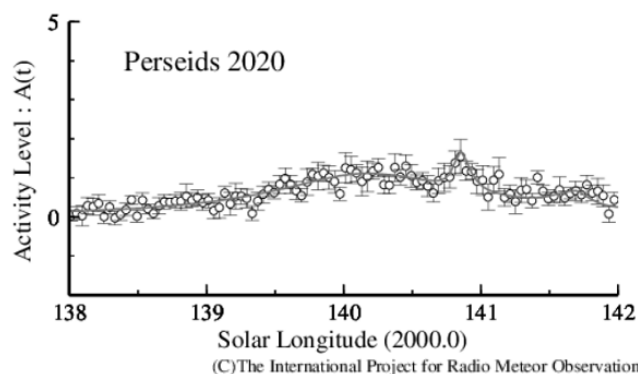


Figure 3 – Perseids 2020 using worldwide radio meteor observations.

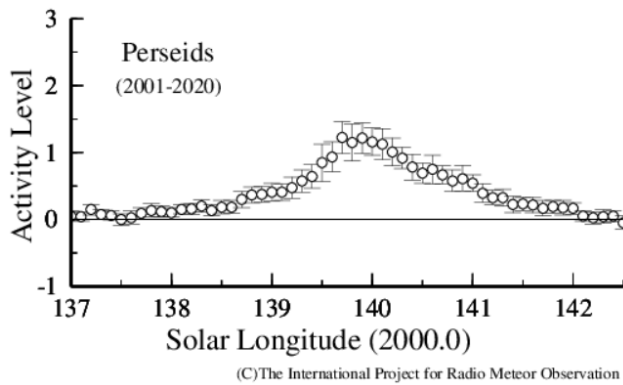


Figure 4 – The long-term activity profile of the Perseids covering the period 2001–2020.

The long-term activity profile for the Perseids for 2001–2020 is shown in Figure 4. The peak is at Solar Longitude $\lambda_{\odot} = 139.95^{\circ}$ with full width half maximum (FWHM) $-0.65^{\circ}/+0.70^{\circ}$. The maximum activity level was 1.2. On the other hand, for the time period of the last ten years (2011–2020), the average activity level is 1.4 (higher than that of the long-term period).

Acknowledgment

The delta Aquariids and Perseids data were provided by the following observers:

Andrew Klekociuk (Australia), Chris Steyaert (Belgium), Johan Coussens (Belgium), test josephco @_Graves (Belgium), Felix Verbelen (Belgium), DanielD SAT01_DD (France), Jacques Molne (France), Pierre Micaletti (France), Jean Marie F5CMQ (France), Fred Espey (Germany), WHS Essen (Germany), Per DL0SHF (Germany), Balogh Laszlo (Hungary), Istvan Tepliczky (Hungary), AAV Planetario_di_Venezia (Italy), GAML Osservatorio_Astronomico_Gorga (Italy), Mario Bombardini (Italy), Oss_Monte_San_Lorenzo DLF (Italy),

Associazione Pontina di Astronomia _APA_ (Italy), Fabio Moschini_IN3GOO (Italy), Hirofumi Sugimoto (Japan), Masaki Tsuboi (Japan), Kenji Fujito (Japan), Hirotaka Otsuka (Japan), Tomohiro Nakamura (Japan), Nobuo Katsura (Japan), Hironobu Shida (Japan), Masaki Kano (Japan), Salvador Aguirre (Mexico), Kees Meteor (Netherlands), Jose Carballada (Spain), Jochen Richert (Switzerland), Ian Evans (UK), Philip Norton (UK), Mike Otte (USA), Stan Nelson (USA), Eric Smestad_KC0RDD (USA), Steve ARS_KF3BH (USA).

Worldwide data were provided by Radio Meteor Observation Bulletin (RMOB)³².

References

- Jenniskens P., Crawford C., Butow S. J., Nugent D., Koop M., Holman D., Houston J., Jobse K., Kronk G., and Beatty K. (2000). “Lorentz shaped comet dust trail cross section from new hybrid visual and video meteor counting technique implications for future Leonid storm encounters”. *Earth, Moon and Planets*, **82–83**, 191–208.
- Ogawa H., Toyomasu S., Ohnishi K., and Maegawa K. (2001). “The Global Monitor of Meteor Streams by Radio Meteor Observation all over the world”. In, Warmbein Barbara, editor, *Proceeding of the Meteoroids 2001 Conference*, 6-10 August 2001, Swedish Institute of Space Physics, Kiruna, Sweden. ESA Publications Division, European Space Agency, Noordwijk, The Netherlands, pages 189–191.
- Ogawa H., Steyaert C. (2017). “Major and Daytime Meteor Showers using Global Radio Meteor Observations covering the period 2001-2016”. *WGN, Journal of the IMO*, **45**, 98–106.

³² <http://www.rmob.org/>

Radio meteors June 2020

Felix Verbelen

Vereniging voor Sterrenkunde & Volkssterrenwacht MIRA, Grimbergen, Belgium

felix.verbelen@skynet.be

An overview of the radio observations during June 2020 is given.

1 Introduction

The graphs show both the daily totals (*Figure 1 and 2*) and the hourly numbers (*Figure 3 and 4*) of “all” reflections counted automatically, and of manually counted “overdense” reflections, overdense reflections longer than 10 seconds and longer than 1 minute, as observed here at Kampenhout (BE) on the frequency of our VVS-beacon (49.99 MHz) during the month of June 2020.

The hourly numbers, for echoes shorter than 1 minute, are weighted averages derived from:

$$N(h) = \frac{n(h-1)}{4} + \frac{n(h)}{2} + \frac{n(h+1)}{4}$$

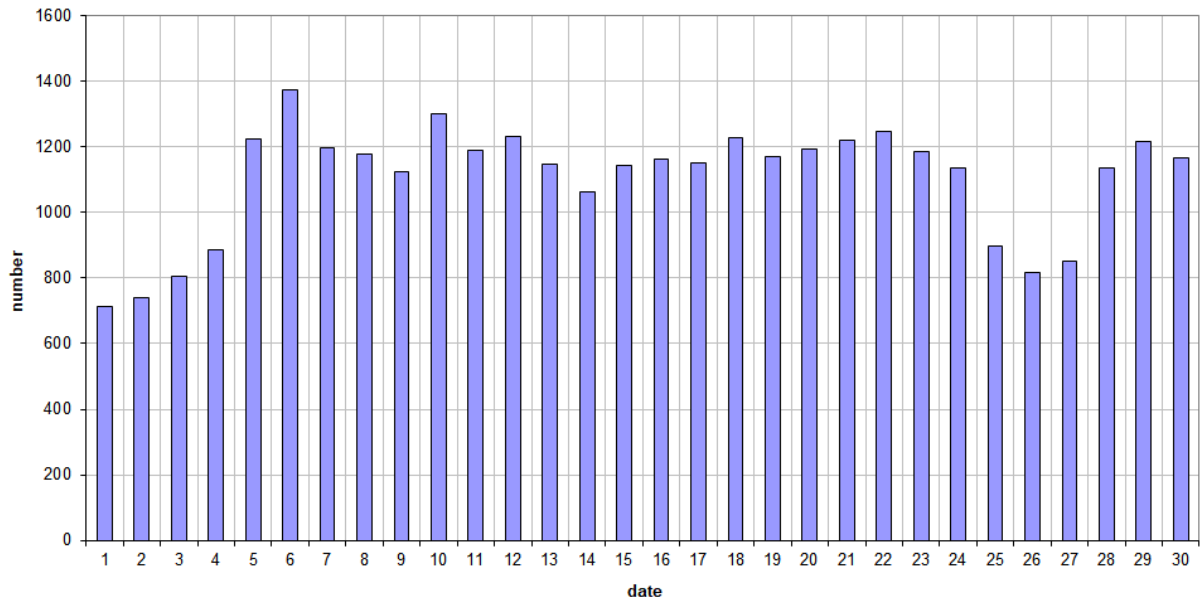
The counts, and in particular the automatic counts, were sometimes complicated by (local) interference, strong unidentified noise and on seven days by often intense lightning activity. On June 17th, 18th and 26th, lightning discharges occurred in the vicinity of our radio beacon. On SpecLab images they usually look very similar to meteor reflections (see *Figures 5 and 6*), but these lightning reflections are distinguishable from meteors because they are broadband and don’t show head echoes.

Most counting errors were corrected manually, sometimes by comparing the registrations on 49.99 MHz with observations on 49.97 MHz (BRAMS beacon at Dourbes).

As expected, the general picture of the activity this month was determined by the known day showers, the Arietids (ARI) being the eye catchers. The greatest activity of this shower was observed here on June 6th. *Figure 9* is a 5-minute SpecLab registration on June 6th. Also, during the rest of the month, there were numerous smaller showers, mostly daylight showers, as the counts of all “overdense” reflections clearly show. During this month, 7 reflections longer than 1 minute were recorded, but some more may have been lost during the period the beacon was out of order. Also included are a few SpecLab recordings of interesting reflections during this month. Attached are also a few examples of the strongest reflections (*Figures 7, 8, 9, 10, 11, 12, 13, 14, 15, 16, 17 and 18*).

If you are interested in the actual figures, please send me an e-mail.

49.99MHz - RadioMeteors June 2020
daily totals of "all" reflections (automatic count_Mettel5_7Hz)
Felix Verbelen (Kamphenhout)



49.99MHz - RadioMeteors June 2020
daily totals of all overdense reflections
Felix Verbelen (Kamphenhout)

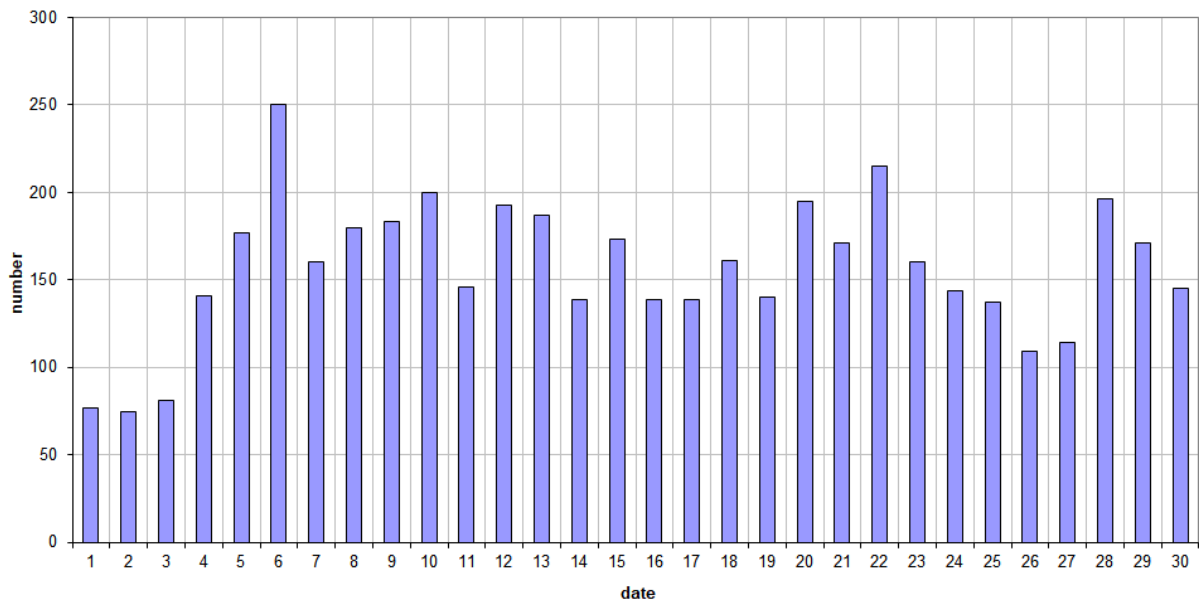
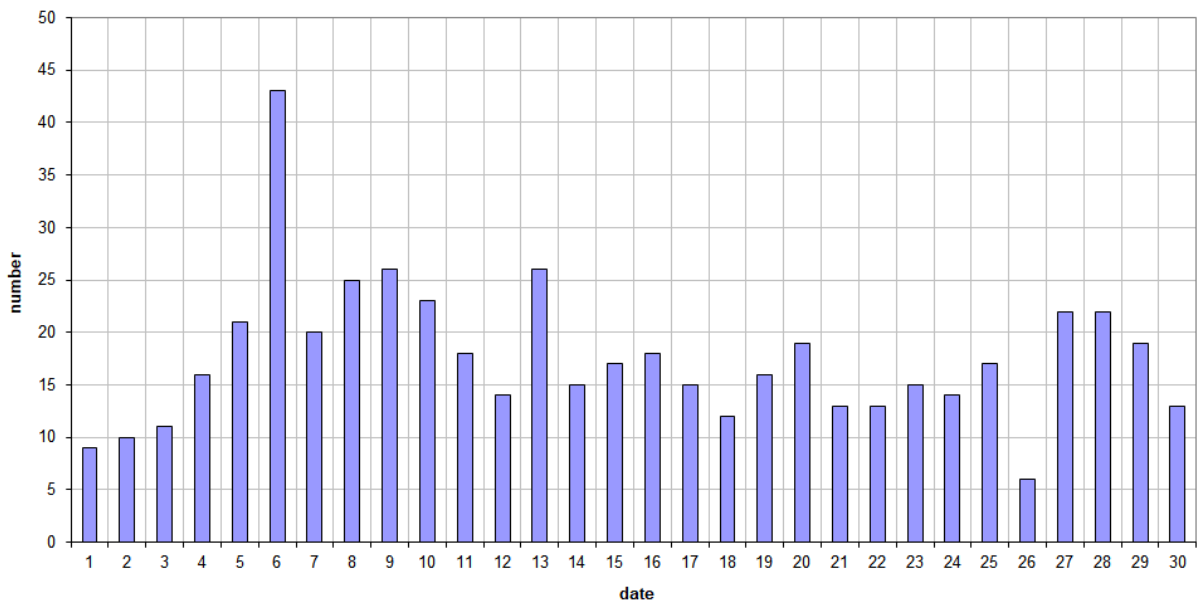


Figure 1 – The daily totals of “all” reflections counted automatically, and of manually counted “overdense” reflections, as observed here at Kamphenhout (BE) on the frequency of our VVS-beacon (49.99 MHz) during June 2020.

49.99MHz - RadioMeteors June 2020
daily totals of reflections longer than 10 seconds
Felix Verbelen (Kamphenhout)



49.99MHz - RadioMeteors June 2020
daily totals of reflections longer than 1 minute
Felix Verbelen (Kamphenhout)

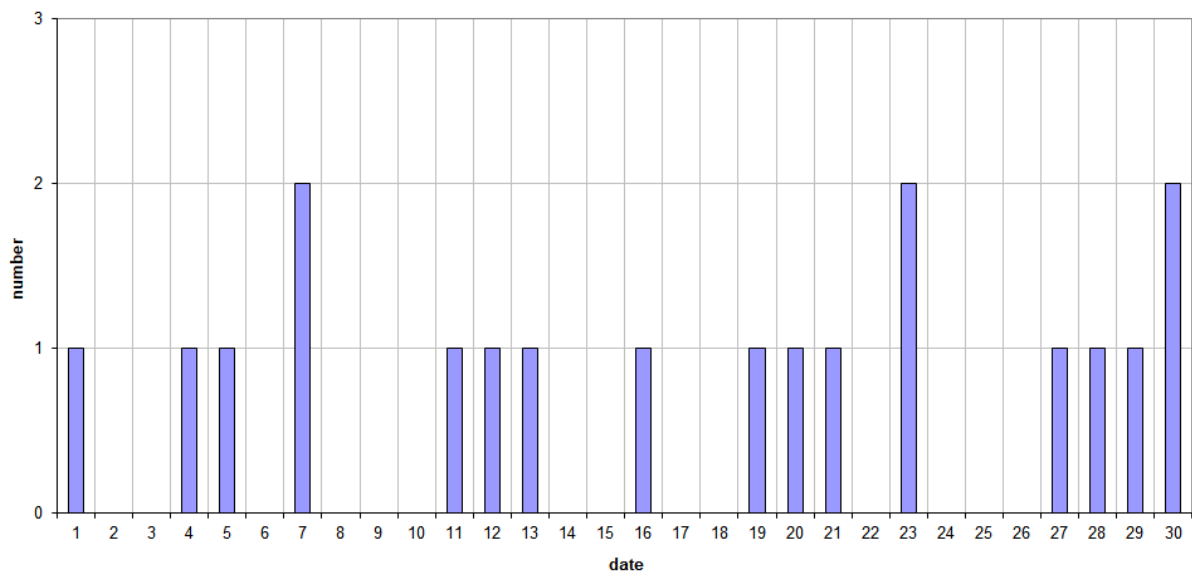
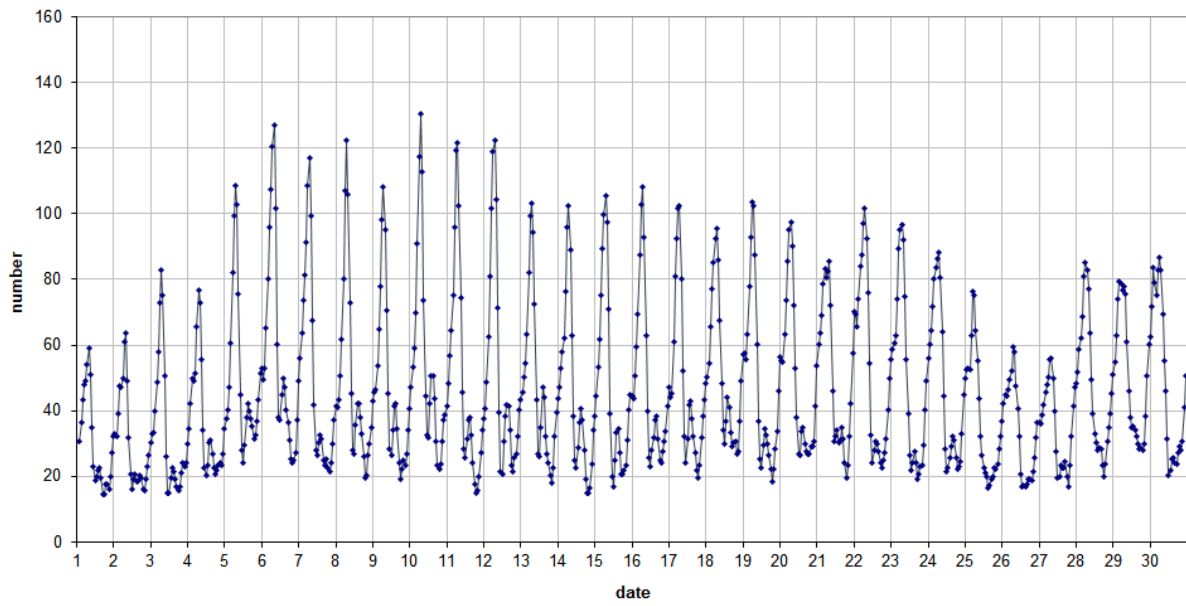


Figure 2 – The daily totals of overdense reflections longer than 10 seconds and longer than 1 minute, as observed here at Kamphenhout (BE) on the frequency of our VVS-beacon (49.99 MHz) during June 2020.

49.99 MHz - RadioMeteors June 2020
number of "all" reflections per hour (weighted average) (automatic count_Mettel5_7Hz)
Felix Verbelen (Kampenhout)



49.99MHz - RadioMeteors June 2020
number of overdense reflections per hour (weighted average)
Felix Verbelen (Kampenhout)

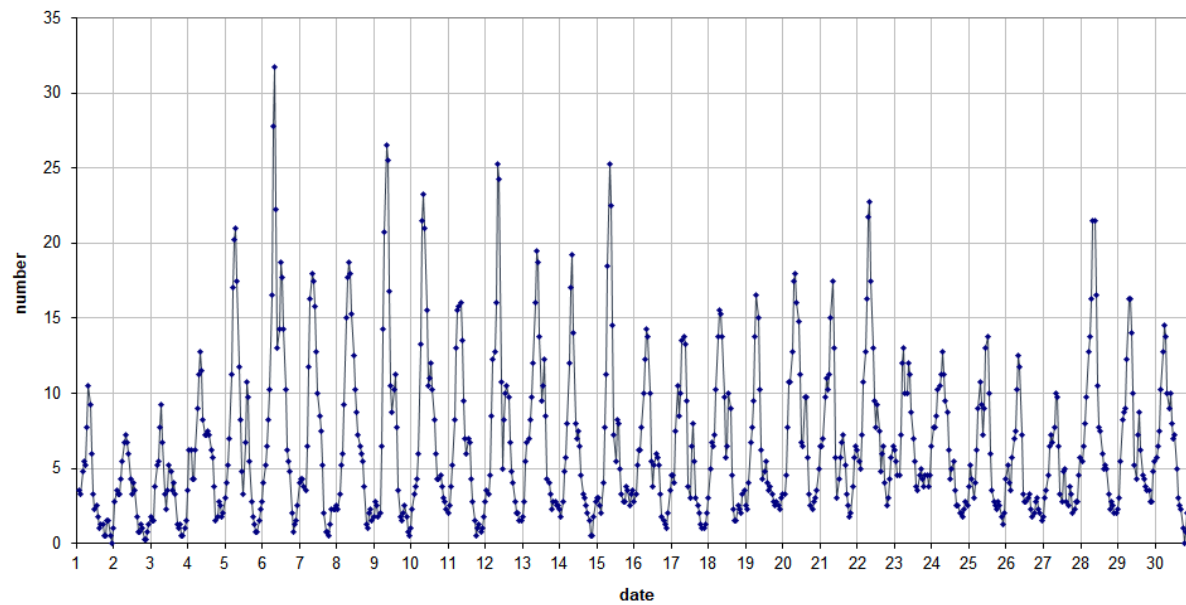
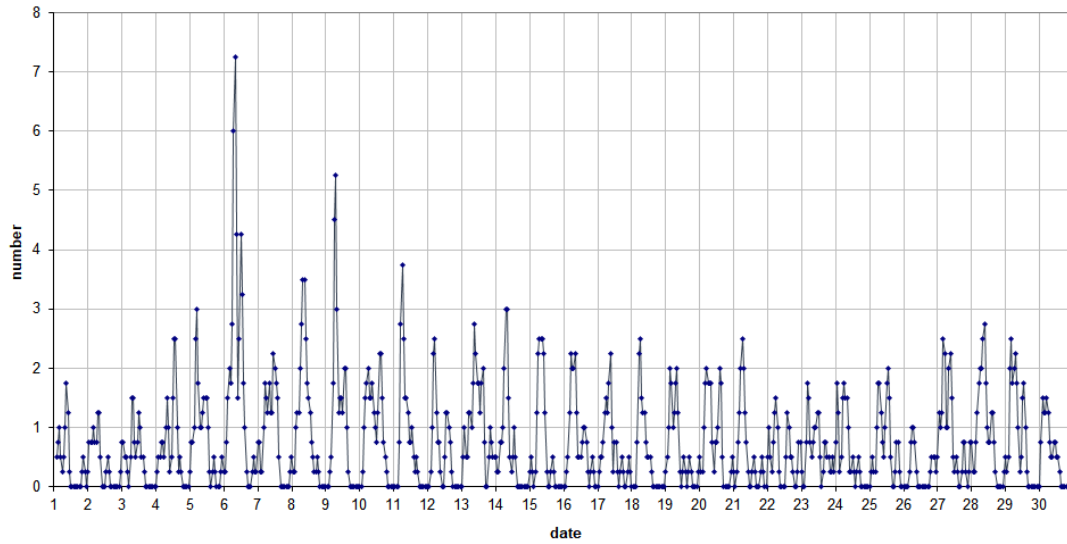


Figure 3 – The hourly numbers of “all” reflections counted automatically, and of manually counted “overdense” reflections, as observed here at Kampenhout (BE) on the frequency of our VVS-beacon (49.99 MHz) during June 2020.

49.99MHz - RadioMeteors June 2020
number of reflections >10 seconds per hour (weighted average)
Felix Verbelen (Kampenhout)



49.99MHz - RadioMeteors June 2020
hourly totals of overdense reflections longer than 1 minute
Felix Verbelen (Kampenhout/BE)

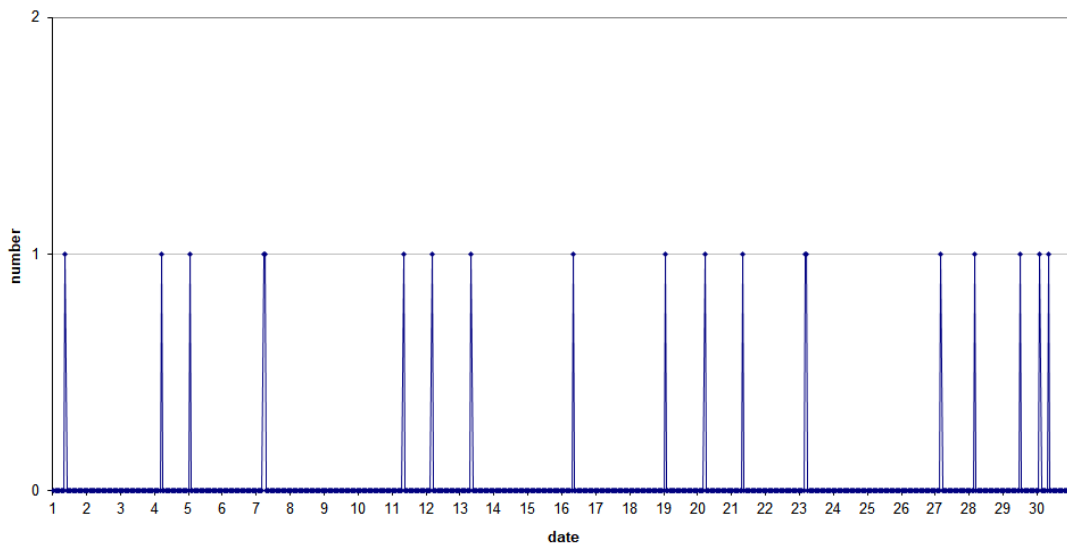


Figure 4 – The hourly numbers of overdense reflections longer than 10 seconds and longer than 1 minute, as observed here at Kampenhout (BE) on the frequency of our VVS-beacon (49.99 MHz) during June 2020.

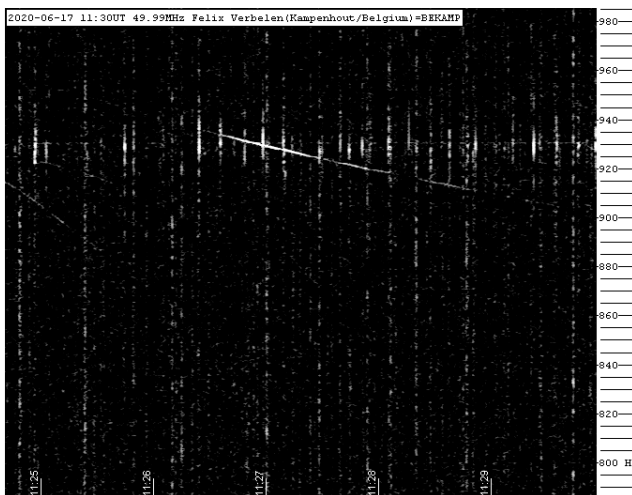


Figure 5 – 2020 June 17 at 11^h30^m UT lightning.

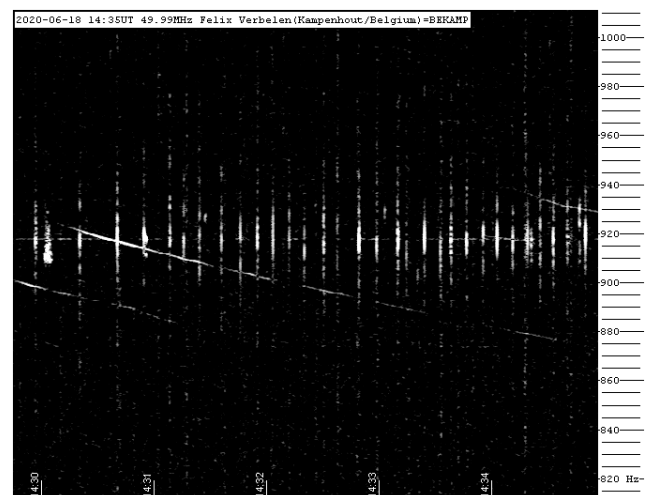


Figure 6 – 2020 June 18 at 14^h40^m UT, lightning.

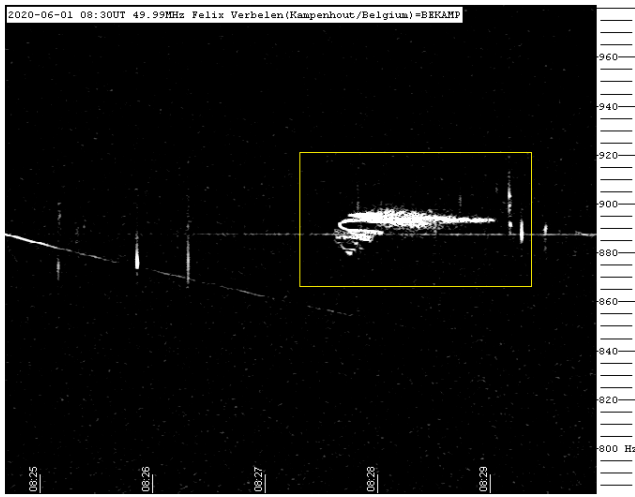


Figure 7 – 2020 June 01 at 08^h30^m UT.

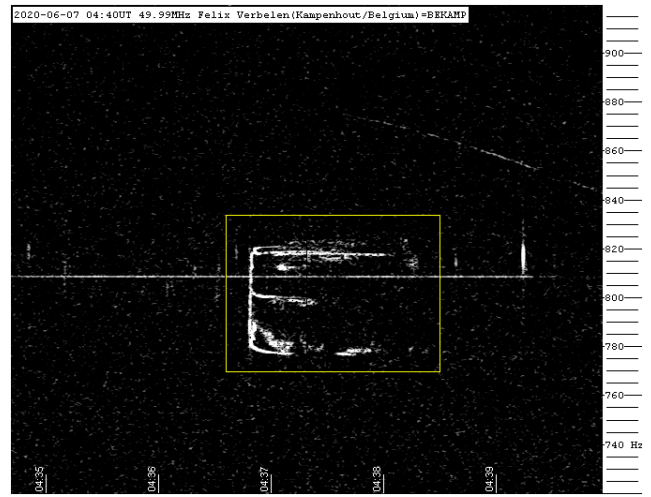


Figure 10 – 2020 June 07 at 04^h40^m UT.

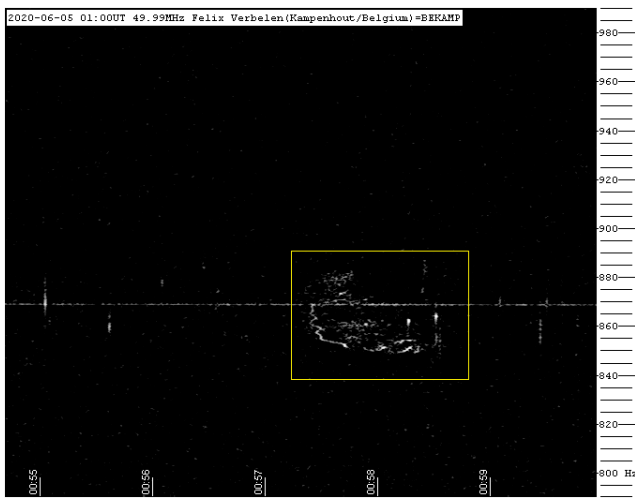


Figure 8 – 2020 June 05 at 01^h00^m UT.

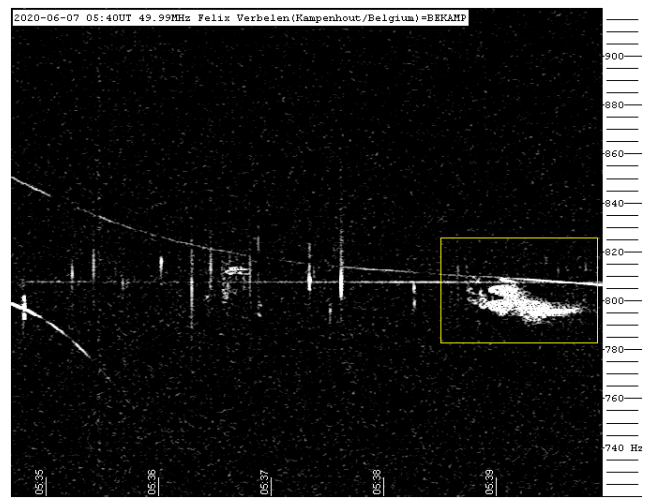


Figure 11 – 2020 June 07 at 05^h40^m UT.

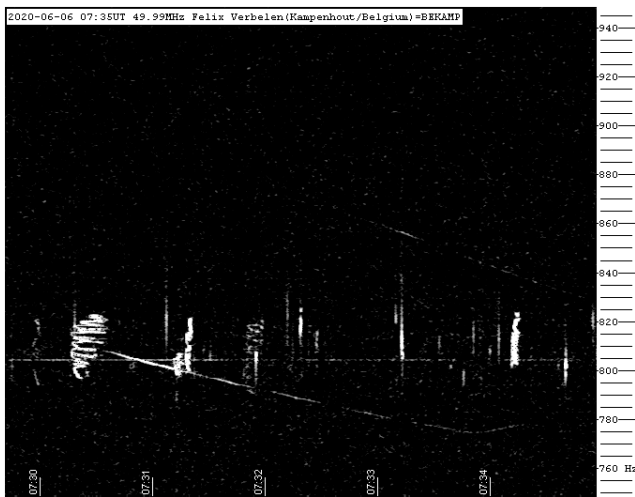


Figure 9 – 2020 June 06 at 07^h35^m UT (Arietids).

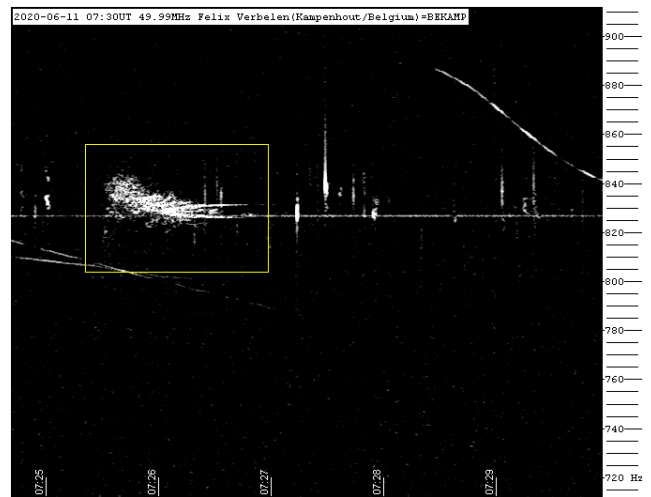


Figure 12 – 2020 June 11 at 07^h30^m UT.

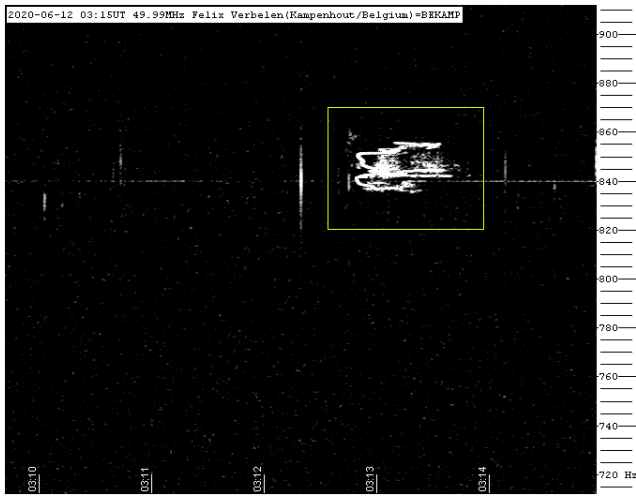


Figure 13 – 2020 June 12 at 03^h15^m UT.

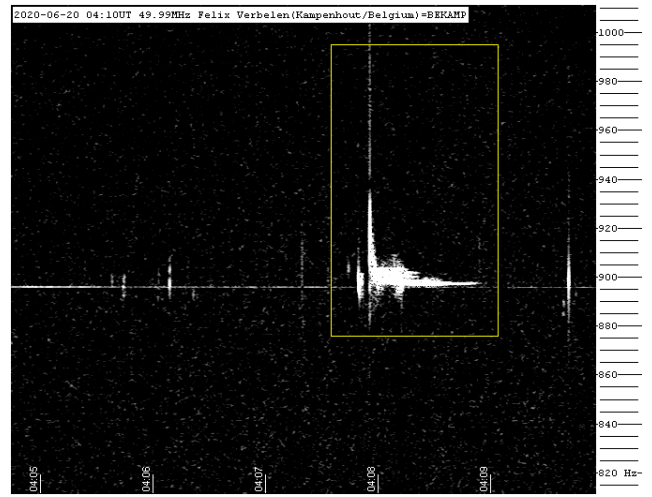


Figure 16 – 2020 June 20 at 04^h10^m UT.

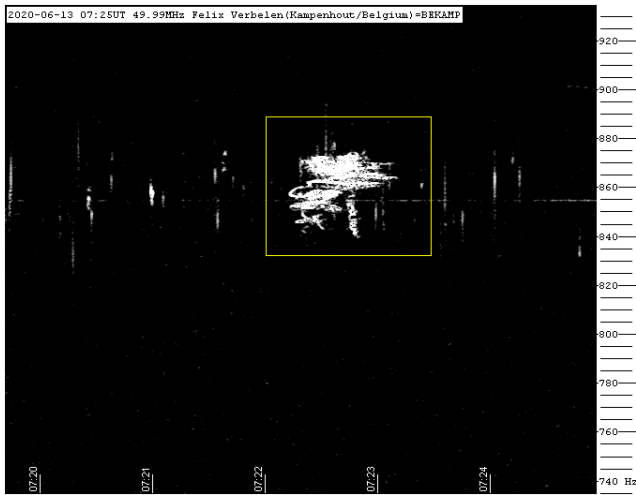


Figure 14 – 2020 June 13 at 07^h25^m UT.

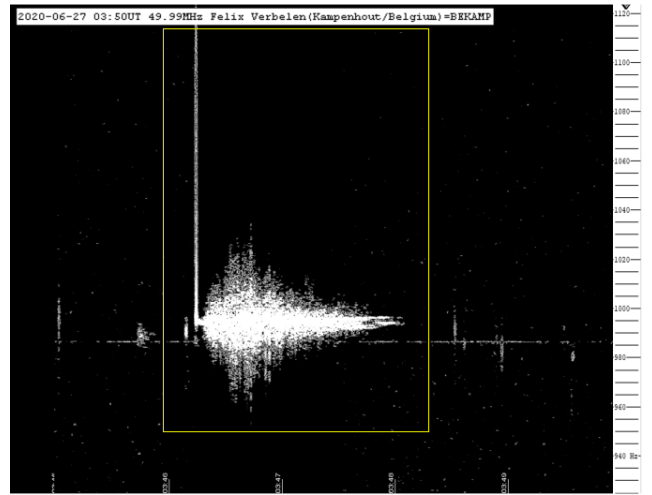


Figure 17 – 2020 June 27 at 03^h50^m UT.

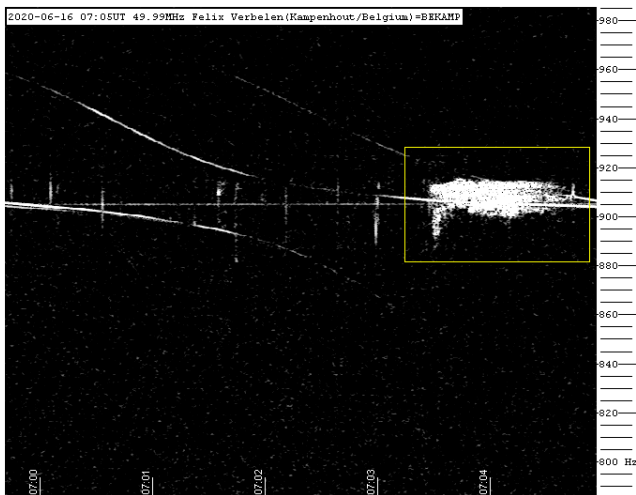


Figure 15 – 2020 June 16 at 07^h05^m UT.

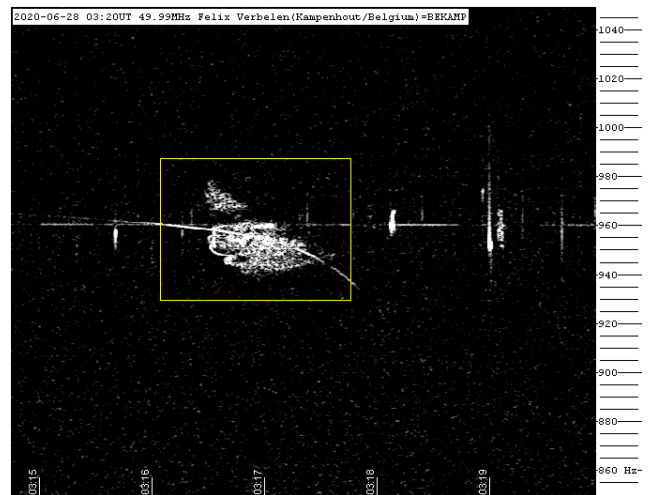


Figure 18 – 2020 June 28 at 03^h20^m UT.

Radio meteors July 2020

Felix Verbelen

Vereniging voor Sterrenkunde & Volkssterrenwacht MIRA, Grimbergen, Belgium

felix.verbelen@skynet.be

An overview of the radio observations during July 2020 is given.

1 Introduction

The graphs show both the daily totals (*Figure 1 and 2*) and the hourly numbers (*Figure 3 and 4*) of “all” reflections counted automatically, and of manually counted “overdense” reflections, overdense reflections longer than 10 seconds and longer than 1 minute, as observed here at Kampenhout (BE) on the frequency of our VVS-beacon (49.99 MHz) during the month of July 2020.

The hourly numbers, for echoes shorter than 1 minute, are weighted averages derived from:

$$N(h) = \frac{n(h-1)}{4} + \frac{n(h)}{2} + \frac{n(h+1)}{4}$$

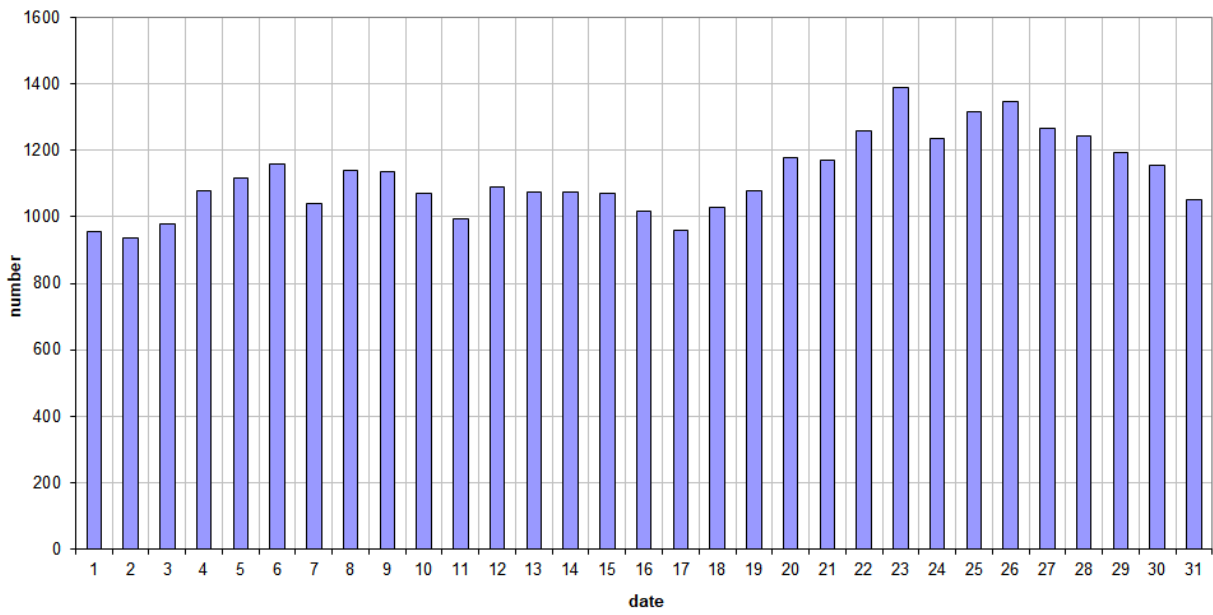
The automatic counts were sometimes complicated by local interference and strong unidentified noise. Lightning activity was only recorded during the last hours of July 31. Most automatic counting errors were corrected manually.

There were no real eye-casting peaks, but the overall activity remained high and increased as expected towards the end of the month, mainly due to the activity of the Southern Delta Aquariids (SDA) and some Perseids, with a number of very strong reflections. There were, however, numerous smaller showers in the course of the month, as shown by the counts of the "overdense" reflections.

A selection of some interesting reflections during this month is also included (*Figures 5, 6, 7, 8, 9, 10, 11, 12, 13, 14, 15, 16 and 17*). It is striking that the long reflections are often accompanied by a number of underdense meteors.

If you are interested in the actual figures, please send me an e-mail.

49.99MHz - RadioMeteors July 2020
daily totals of "all" reflections *(automatic count_Mettel5_7Hz)*
Felix Verbelen (Kampenhout)



49.99MHz - RadioMeteors July 2020
daily totals of all overdense reflections
Felix Verbelen (Kampenhout)

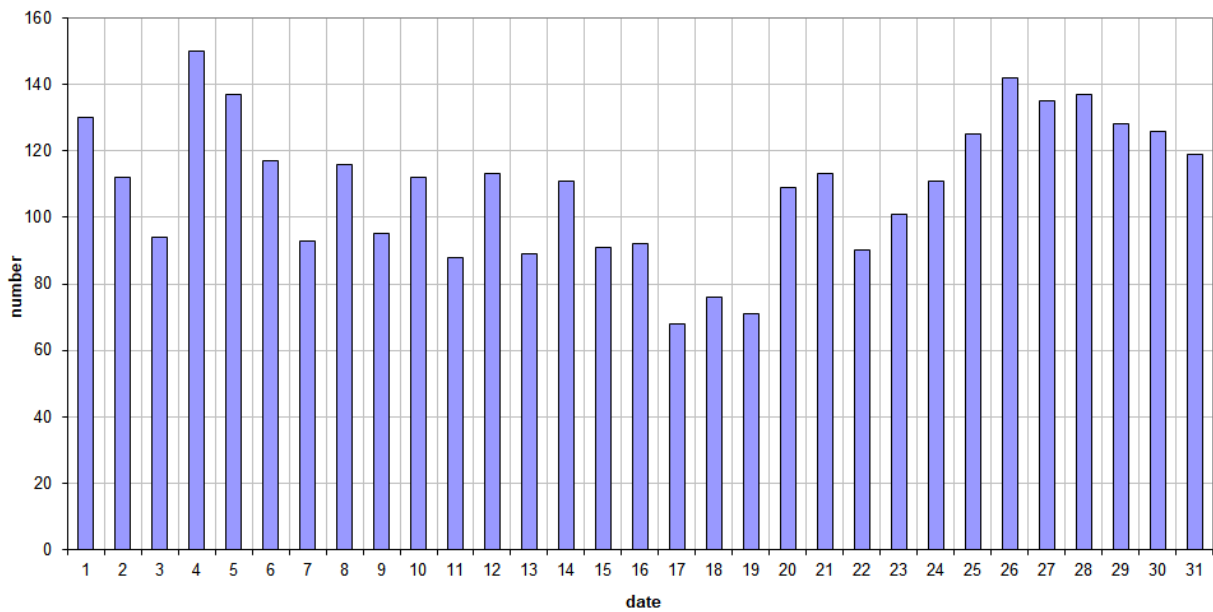
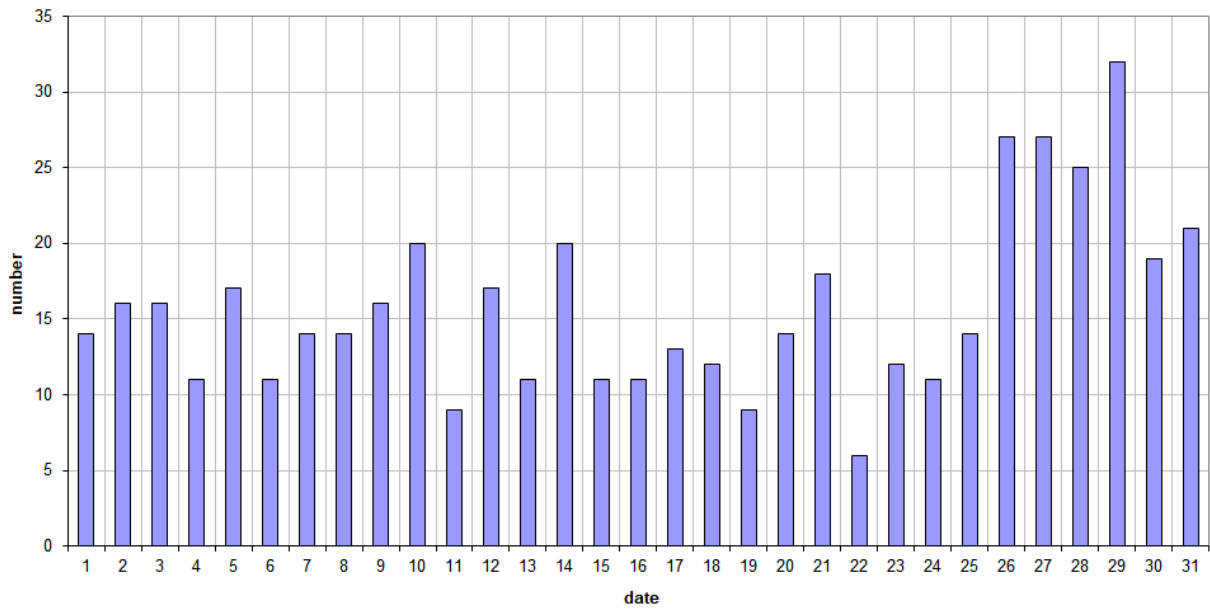


Figure 1 – The daily totals of “all” reflections counted automatically, and of manually counted “overdense” reflections, as observed here at Kampenhout (BE) on the frequency of our VVS-beacon (49.99 MHz) during July 2020.

49.99MHz - RadioMeteors July 2020
daily totals of reflections longer than 10 seconds
Felix Verbelen (Kamphenhout)



49.99MHz - RadioMeteors July 2020
daily totals of reflections longer than 1 minute
Felix Verbelen (Kamphenhout)

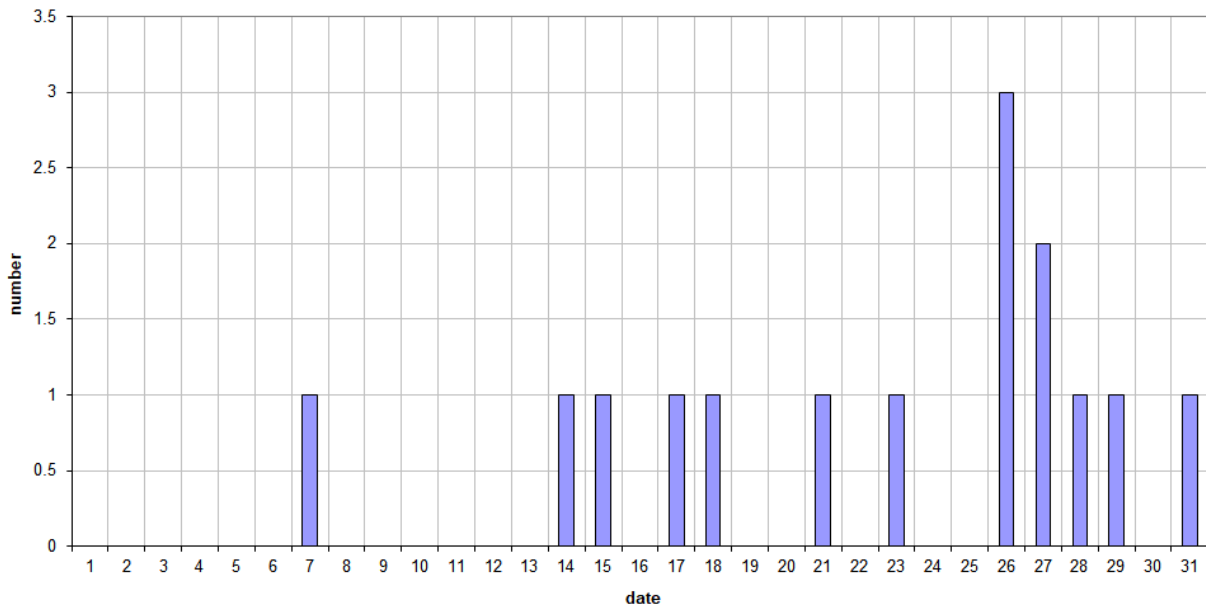


Figure 2 – The daily totals of overdense reflections longer than 10 seconds and longer than 1 minute, as observed here at Kamphenhout (BE) on the frequency of our VVS-beacon (49.99 MHz) during July 2020.

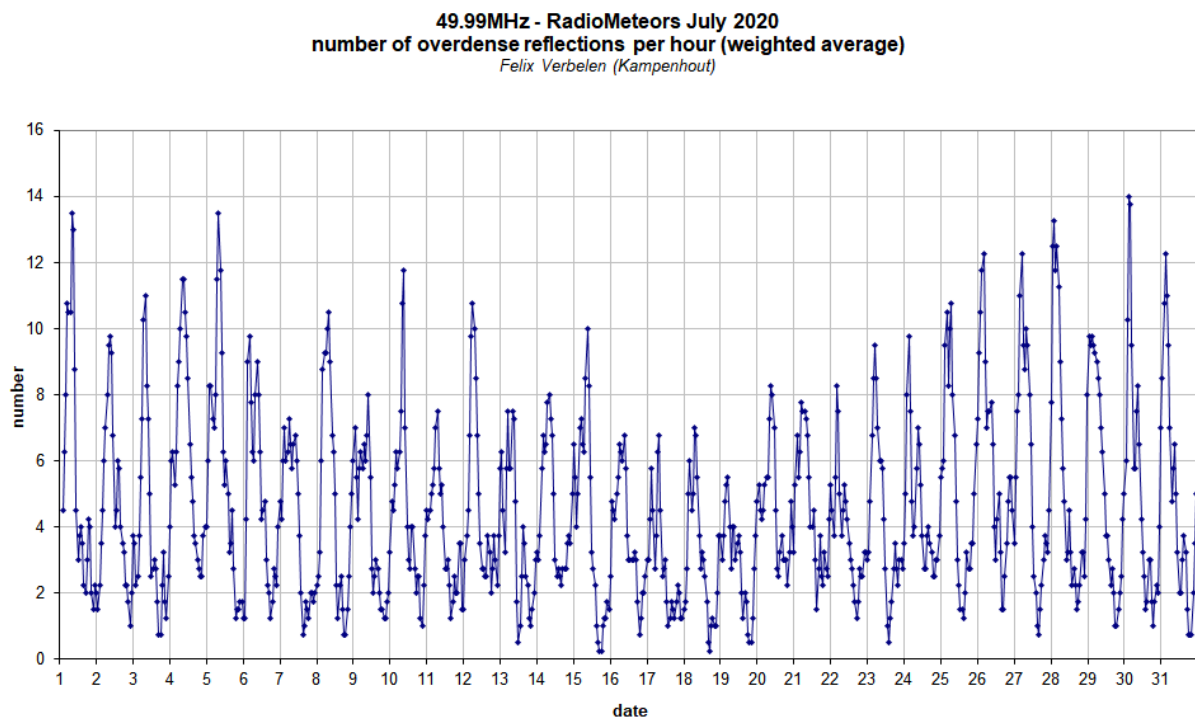
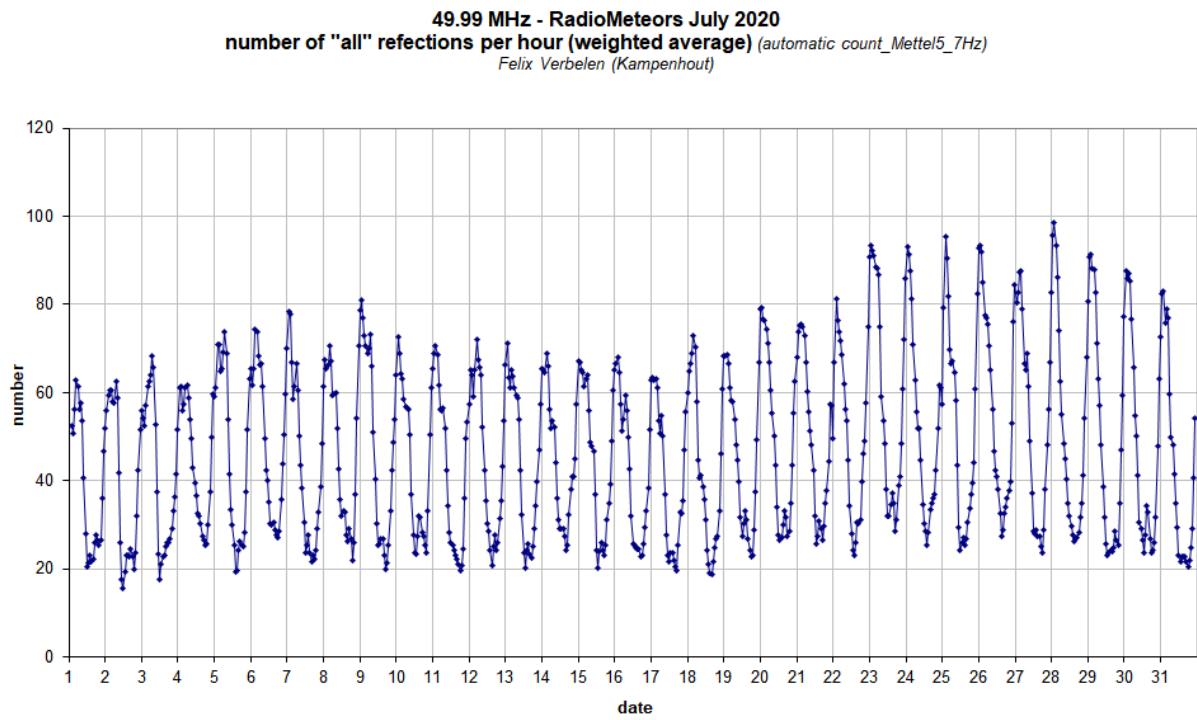


Figure 3 – The hourly numbers of “all” reflections counted automatically, and of manually counted “overdense” reflections, as observed here at Kampenhout (BE) on the frequency of our VVS-beacon (49.99 MHz) during July 2020.

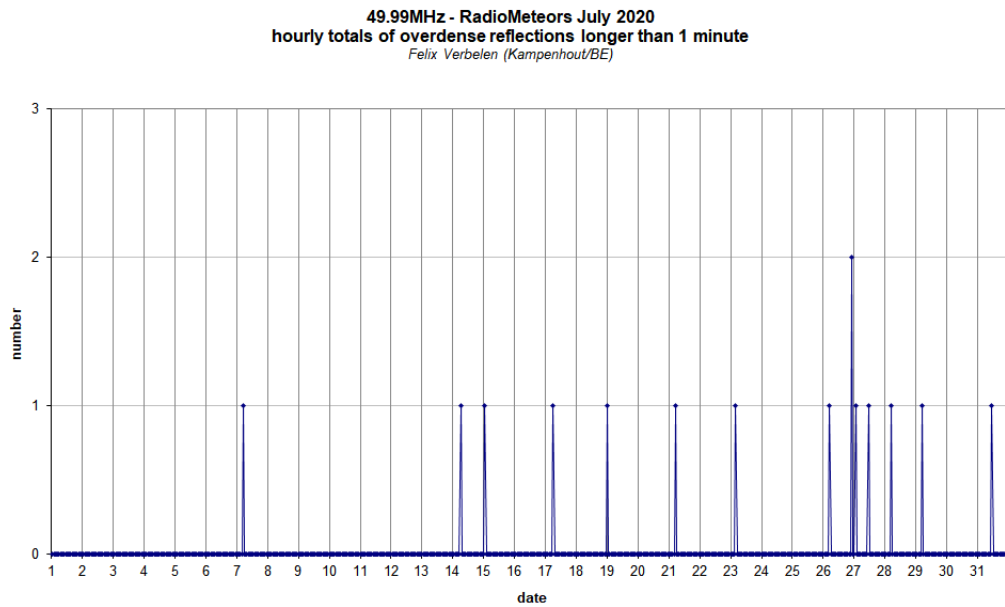
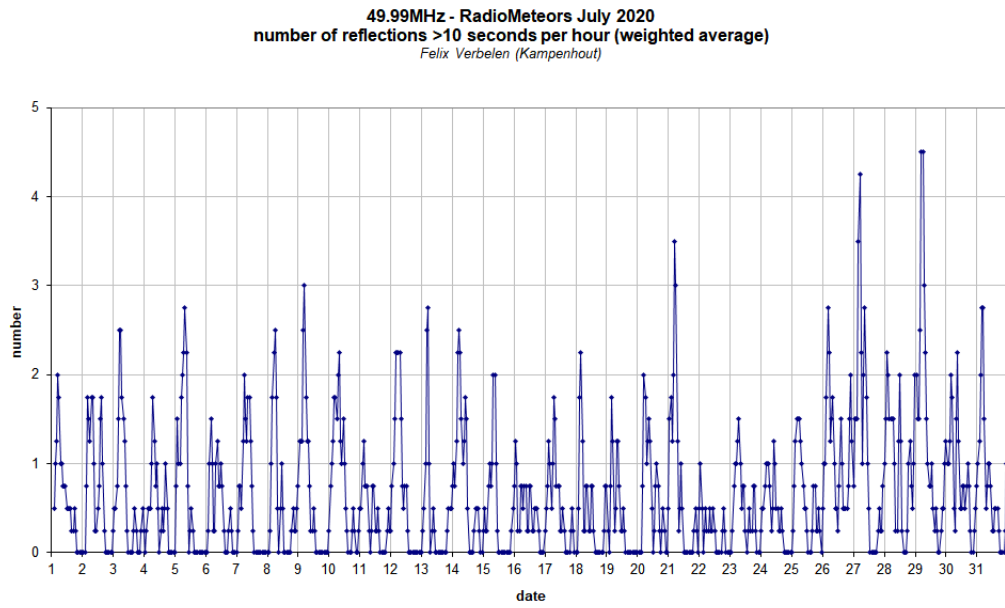


Figure 4 – The hourly numbers of overdense reflections longer than 10 seconds and longer than 1 minute, as observed here at Kamphenhout (BE) on the frequency of our VVS-beacon (49.99 MHz) during July 2020.

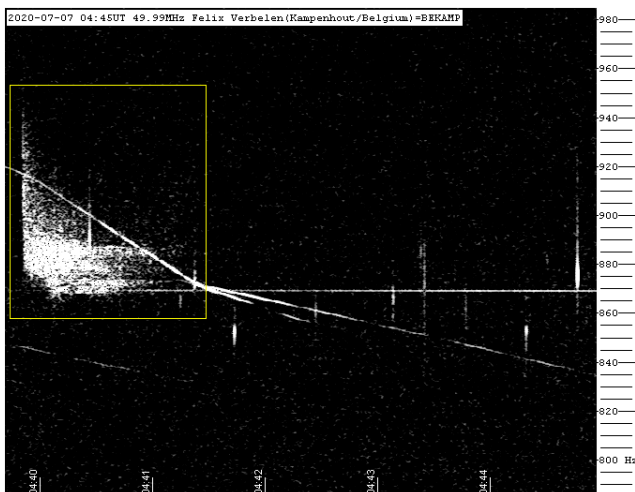


Figure 5 – 2020 July 07 at 04^h45^m UT.

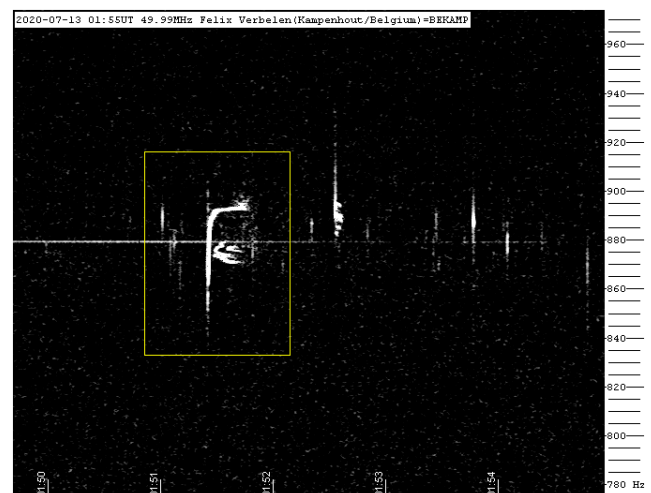


Figure 6 – 2020 July 13 at 01^h55^m UT.

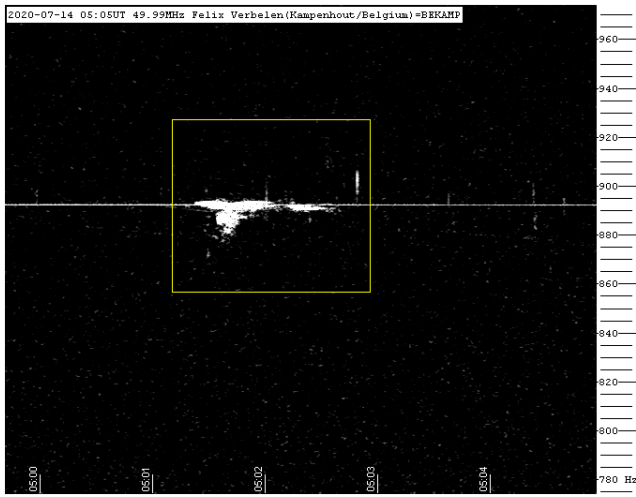


Figure 7 – 2020 July 14 at 05^h05^m UT.

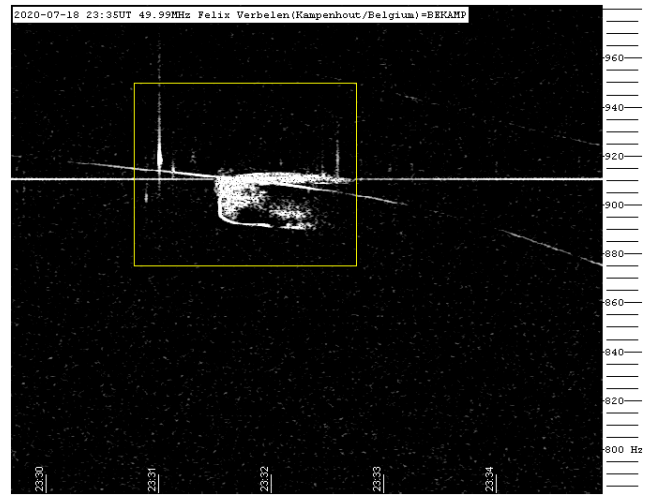


Figure 10 – 2020 July 18 at 23^h35^m UT.

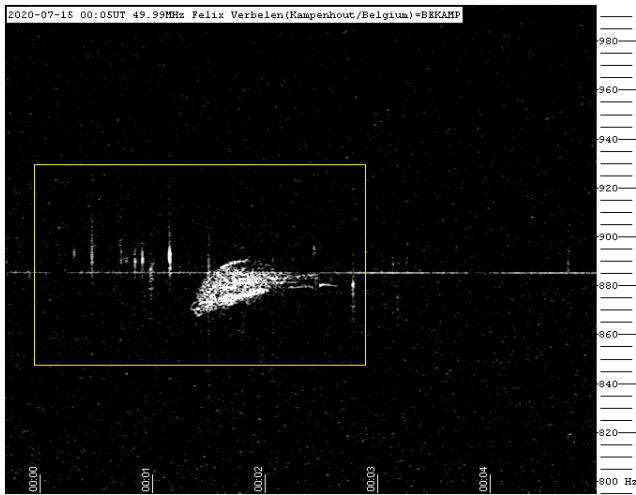


Figure 8 – 2020 July 15 at 00^h05^m UT.

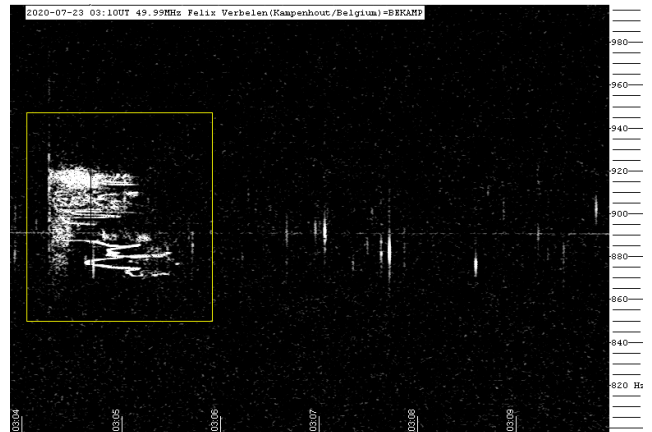


Figure 11 – 2020 July 23 at 03^h10^m UT.

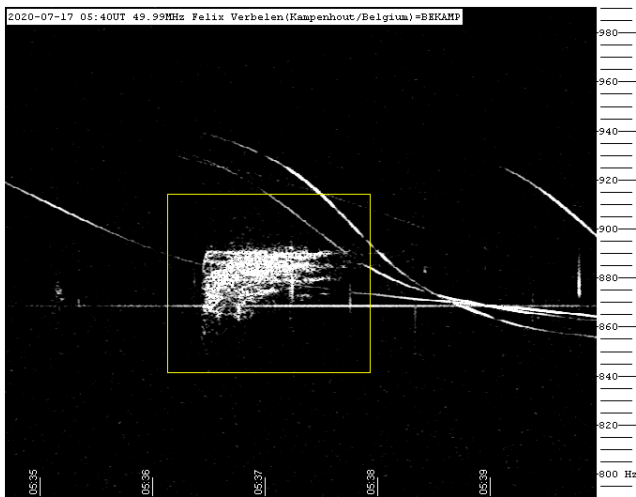


Figure 9 – 2020 July 17 at 05^h40^m UT.

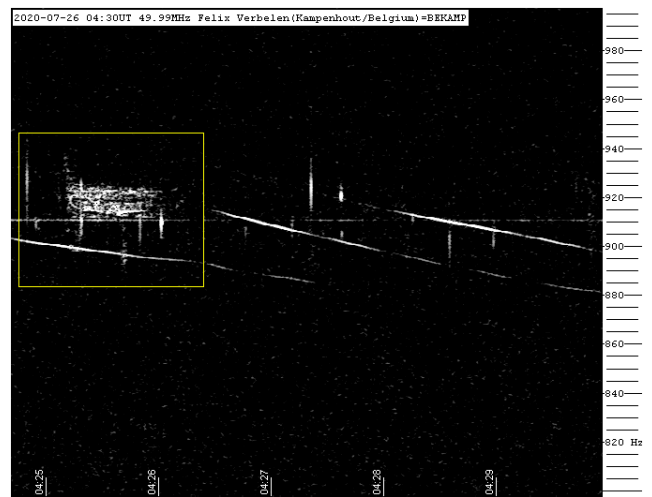


Figure 12 – 2020 July 26 at 04^h30^m UT.

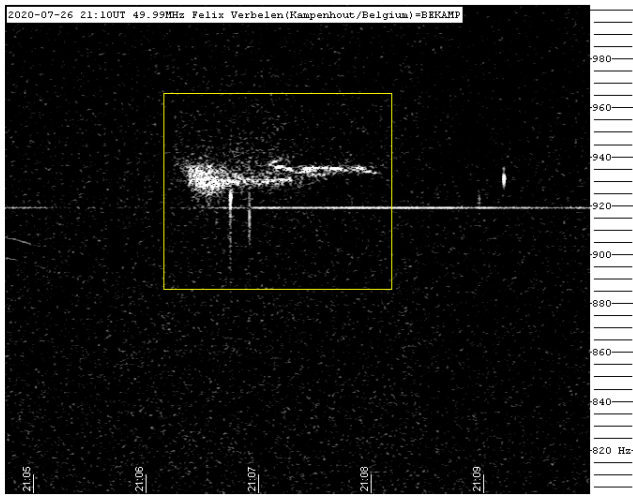


Figure 13 – 2020 July 26 at 21^h10^m UT.

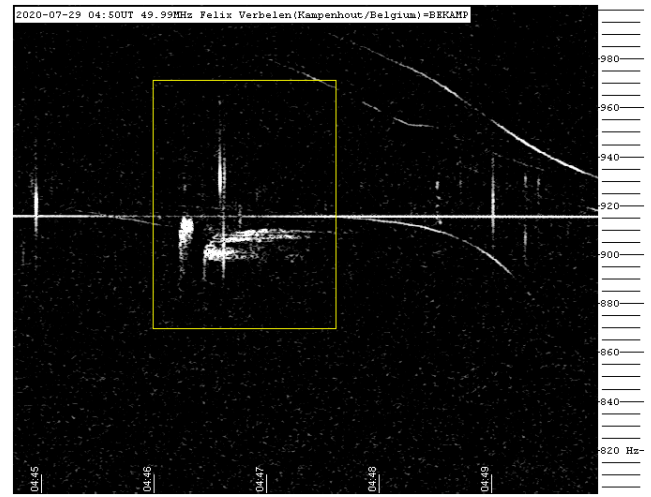


Figure 16 – 2020 July 29 at 04^h50^m UT.

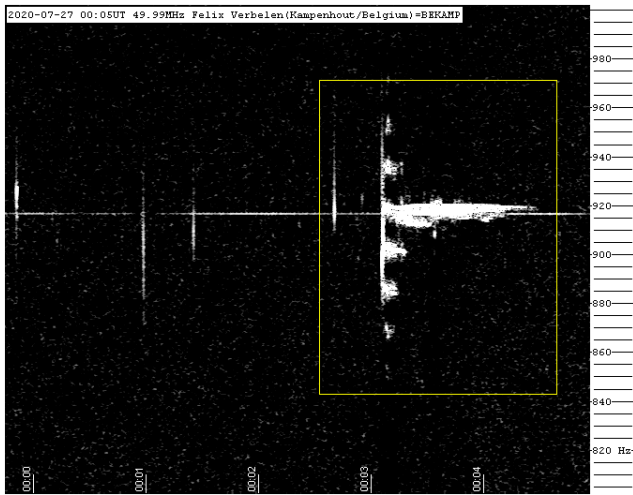


Figure 14 – 2020 July 27 at 00^h05^m UT.

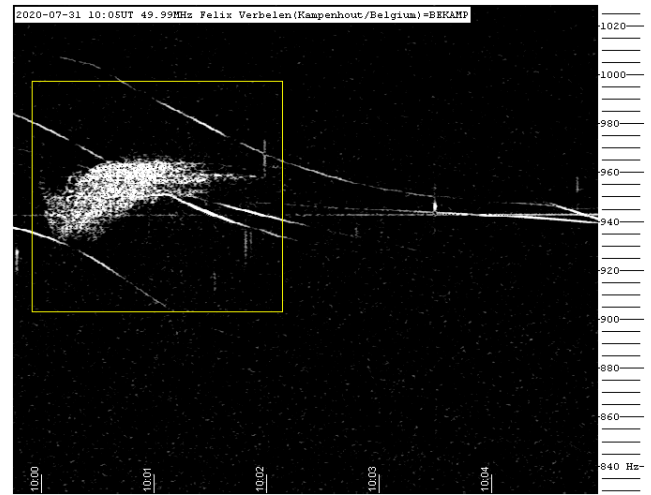


Figure 17 – 2020 July 31 at 10^h05^m UT.

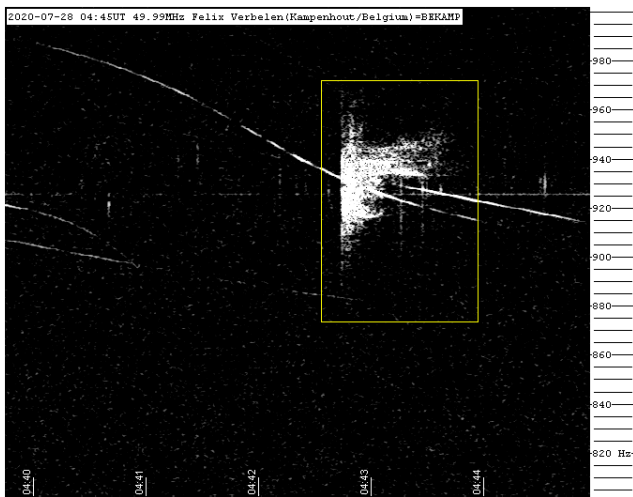


Figure 15 – 2020 July 28 at 04^h45^m UT.

Once upon a time, we had a comet and a fireball

Tioga Gulon

6, rue Rodin, F-54710 Fléville-devant-Nancy, France
france.allsky.camera@free.fr

A great fireball of magnitude -9 appeared above the center of France on July 26th, 2020, at 23h12m UT. It has been seen from all over France and neighboring countries and sonic booms were heard from around Paris.

1 Introduction

The night of 26–27 July 2020, I decided to observe comet C/2020 F3 Neowise. It was the last day to see it without moonlight. I had the chance to be in a holiday place in Cerilly, Auvergne, France, with a nice dark sky.

At 23^h12^m UT, 30 minutes after the moonset, I was making pictures of comet Neowise with Ursa Major when I saw a bright fireball beginning to appear from near my zenith and descending during 10 seconds to the horizon displaying an intense bright green light! It ended disintegrating into small pieces. It was the most beautiful fireball I've seen in real life!

Luckily, the fireball crossed the field of my camera.

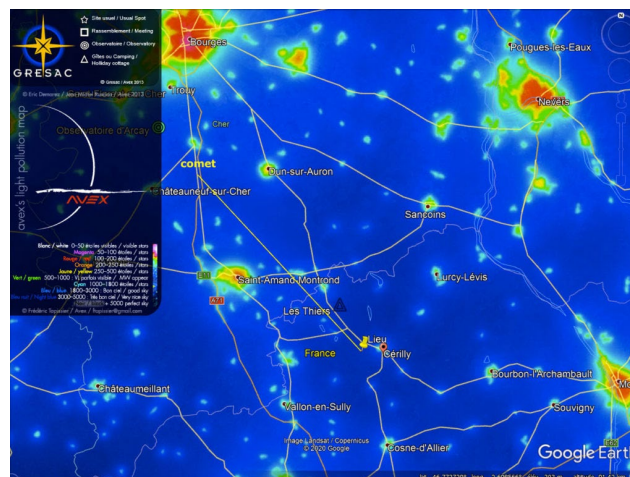


Figure 1 – Light pollution map of the center of France (courtesy www.avex-asso.org).



Figure 2 – Fireball, comet C/2020 F3 Neowise and Ursa Major – Cerilly, France – 26 July 2020 23^h12^m UT canon 700D(aps-c) + sigma 17-70mm @17mm, 60s, F/3.2, ISO800 on star adventurer, fov 66°x47°.

The fireball has also been observed from all over France and even from Belgium, Germany, Switzerland, the Netherlands, as reported by nearly 150 people on the IMO website.

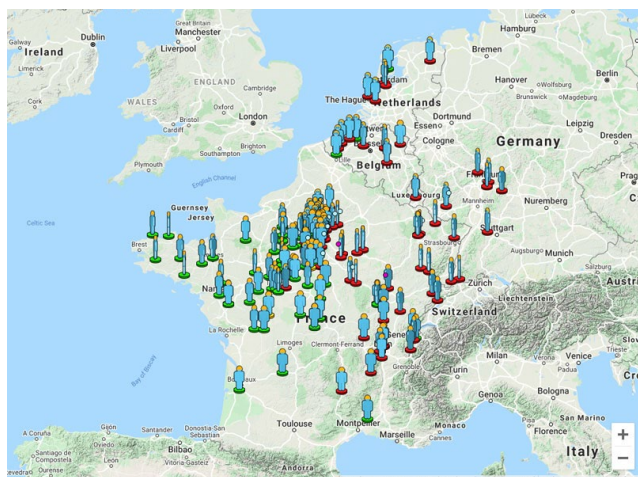


Figure 3 – 149 reports on event 3741-2020 (IMO page).

Sounds like rumble, detonations and booms was reported by about thirty witnesses around Paris.

Julien A. at Athis-Mons (France) reported: “about 1 or two minutes after low pitched attenuated rolling boum during 2 sec.”.

Nicolas B. at Sainville, Centre-Val de Loire (France) said: “double detonation at 1^h16^m00 + -3^s exactly, not necessarily linked?”.

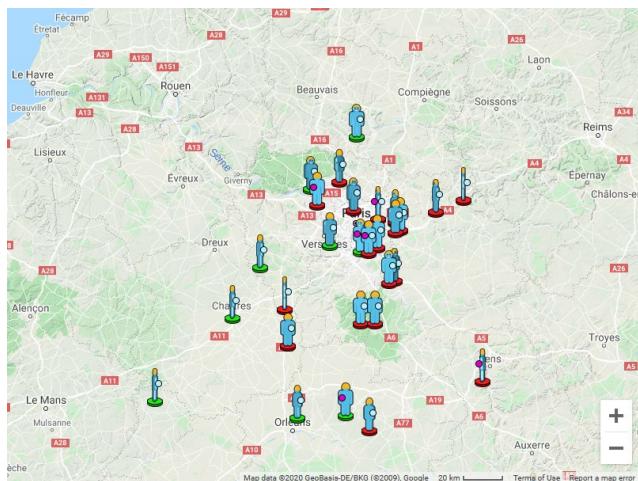


Figure 4 – Map of 28 witnesses who reported sound for 3741-2020 event (IMO page).

2 Observational data

The fireball occurred on 2020 July 26 at 23^h12^m23^s UT and has been caught by many cameras in France: 12 of the FRIPON network, 4 of the BOAM network and furthermore by some individual amateurs.

According to the data from the FRIPON network, the fireball reached its maximum brightness of magnitude -9 at an altitude of 55 km.

The fireball crossed the whole field of view of the Raspberry Meteor System camera, FR000A, located at Cérilly, Auvergne, France. It is the longest trajectory recorded by a camera during 9.30 seconds.



Figure 5 – The 9.30 seconds duration fireball trajectory by the FR000A RMS camera at Cérilly, Auvergne, France.

Three other cameras of BOAM network caught the event: two all sky cameras and a 60° FoV camera.



Figure 6 – Fireball 2020 July 26, 23^h12^m23^s UT at Chaligny, France (courtesy Marc Herrault).



Figure 7 – Fireball 2020 July 26, 23^h12^m23^s UT at Chinon, France (courtesy Astro Chinon).



Figure 8 – Fireball 2020 July 26, 23^h12^m23^s UT at Fléville, France.

An independent amateur station based in Reuil-Malmaison, Paris region, was particularly well placed, on the trajectory of the fireball. A first south-facing camera recorded the meteoroid coming in and starting to split into several pieces and a second facing northwards shows the object breaking up at the end of its light path.



Figure 9 – Fireball 2020 July 26, 23^h12^m23^s UT screenshot of the video from southward oriented camera at Reuil-Malmaison, France (courtesy Dominique André).

Unfortunately, the astrometry has not been calculated and it is not possible to compute a trajectory from these two captures. But a study of the images allows to see the dynamics of the fireball in the atmosphere.

Time synchronization of the cameras is done with Meinberg on a ntp-server and the meteor dynamic as time match to that one on the LITIK1 video.

At 23^h12^m22.28^s, the fireball starts, very faint, on the video of the southward pointed camera. At 23^h12^m24.80^s, a second track (b) appears, following the more important one (a) until 23^h12^m28.88^s.

A series of small explosions take place on the main piece (a) at 27.52s, 27.64s, 27.80s and 27.88s giving rise to a few small bright pieces disintegrating quickly, visible in the capture at 28.00s.

At 23^h12^m28.24^s, the fireball suddenly strongly brightens, certainly corresponding to the shattering of the main object (a) and the creation of a third important piece (c). Piece (c) is clearly visible on the captures at 28.88s and 29.04s and leaving the FoV of the southwards pointed camera at 29.20s.

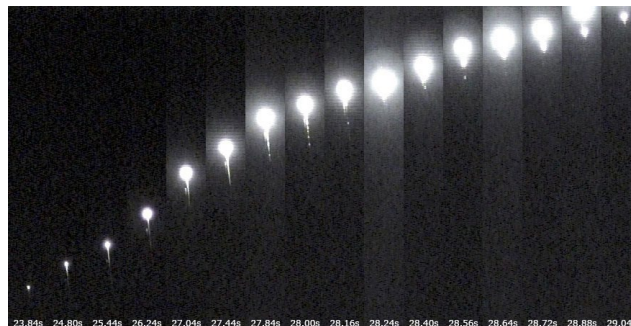


Figure 10 – Fireball dynamic path from southwards pointed camera at Reuil-Malmaison (courtesy Dominique André).

On the northwards pointed camera, the fireball appeared at 23^h12^m31.62^s. According to the synchronization of both cameras, 2.4s of the path is missing and only one of the fragmented objects reappeared. From 32.904s and until the very end of the luminous trajectory at 33.86s, the object seems to break up into three pieces. It started at 23^h12^m22.28^s on southwards pointed camera and ended at 23^h12^m33.86^s on northwards pointed camera, corresponding to a duration of 11.58s.



Figure 11 – The dynamic path from the northwards pointed camera at Reuil-Malmaison (courtesy Dominique André).



Figure 12 – Capture from timelapse of the fireball at Montbellet, France. Dji osmo action camera, fov ~145° (courtesy Romain Buté).

The last very interesting capture comes from an amateur astronomer, Romain Buté, who observed and photographed comet Neowise, near Montbellet, France and reported his observation on the IMO fireball report page. He was lucky to picture the fireball with his DSLR camera with a narrow field of view of $12 \times 18^\circ$ and with a “dji osmo” action camera on time-lapse shooting mode and a 145° field of view.



Figure 13 – Fireball and comet C/2020 F3 Neowise – Montbellet, France. Canon 750D(aps-c) + canon 70-200mm @70mm, 30s, F/2.8, ISO1600 (courtesy Romain Buté).

3 Trajectory

The multiple station data of the BOAM network and DSLR pictures of amateur astronomers allowed to calculate the trajectory and orbit.

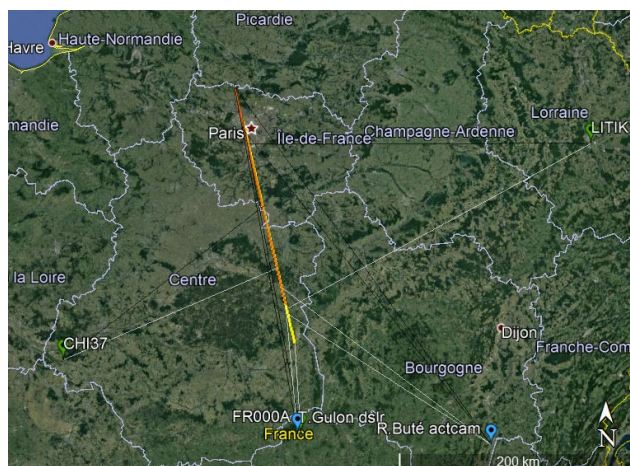


Figure 14 – Groundmap of the trajectory. Yellow: BOAM cameras computation, orange: DSLR camera.

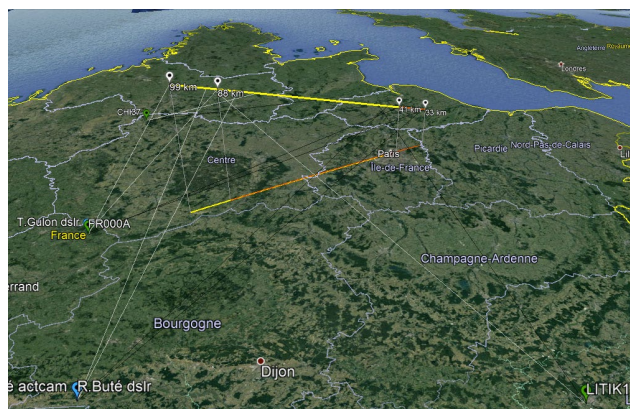


Figure 15 – 3D view of the trajectory. Yellow: BOAM cameras computation, orange : DSLR camera.

Table 1 – Data for T. Gulon and R. Buté extracted with astronomy.net and FR000A, LITIK2 and CHI37 data from UFOsuite.

Observer	Long. (°)	Lat. (°)	Alt. (m)	Dur. (s)	R.A. ₁ (°)	Dec. ₁ (°)	Az. ₁ (°)	Ev. ₁ (°)	R.A. ₂ (°)	Dec. ₂ (°)	Az. ₂ (°)	Ev. ₂ (°)
T.Gulon	2.781	46.6154	304	–	137.75	82.05	356.04	39.12	128.75	47.89	351.14	5.14
R.Buté dslr	4.866	46.4678	212	–	192.25	41.42	390.66	19.9	166	39.67	324.58	6.25
R.Buté act.	4.866	46.4678	212	–	199	41.03	305.6	23.3	161.65	38.74	327.1	3.7
FR000A	2.8161	46.6203	320	9.3	282.87	83.04	177.51	53.01	129.94	50.28	171.1	7.65
LITIK1	6.2072	48.6446	220	6.64	237.8	-3.12	245.67	15.95	211.98	8.37	273.38	8.07
CHI37	0.2755	47.1692	105	2.42	24.99	31.45	66.22	21.45	41.26	37.14	51.94	15.99

Table 2 – Trajectories for the BOAM computation UFOorbit and DSLR cam computation author's table.

Trajectory	dur. (s)	long. _b (°)	lat. _b (°)	H _b (km)	long. _e (°)	lat. _e (°)	H _e (km)	dist (km)	incl. (°)	v _o (m/s)	v _g (m/s)
BOAM	9.3	2.7744	47.2769	99	2.256	48.9308	41	196	17.1	22	19
DSLR cam	–	2.6839	47.562	88	2.169	49.1806	33	192	16.6	-	-

Table 3 – Orbital elements for the BOAM computation UFOorbit - DSLR cam computation author's table.

Orbit	a (A.U.)	q (A.U.)	e	ω (°)	Ω (°)	i (°)	α_g (°)	δ_g (°)
BOAM	1.8	0.634	0.642	304.1	87.726	7	308.2	-30.2

4 Electrophonic, photophonic sound or auditive hallucination?

At the same time of the appearance of the meteor, I heard like a “sound of blowing” or a thin “fff” made with the mouth during 2 to 3 seconds in the first part of path when the object was high in the sky.

A few persons described the same phenomenon as Anthony J. at Dijon who heard the same sound: “Like when you immerse a very hot object in cold water and tamp out”.

Jason C. at Saint-Germain-en-Laye, heard as: “A very light breath like something burning until the fireball crumbles.”

Gregory P., amateur observer at Vitry-aux-Loges, report: “I don’t know at all how to explain it as a kind of sound in the sky at its entry. A sort of hissing.”

Normally, it is impossible to hear the fireball at the same time of appearance, because the object is far away from the observer, some 50 to 100 km or more and the sound takes several minutes to arrive. But this phenomenon had already been reported several times during a fireball event.

From the 1980s years, according to accepted knowledge, hearing sound simultaneously during the appearance of the meteor could be explained by electrophonic noise. Indeed,

the disintegration of a meteor into the atmosphere generate huge energy and creates ionization of the air. This plasma produces low frequency radio emission (ELF/VLF) travelling at the speed of light and that could be transferred into acoustic waves whenever appropriated objects such as fences, hair, vegetation, glasses are in the vicinity of the observer.

In 2017, in the journal “scientific report³³”, Spalding et al. propose a new way to explain this “anomalous” sounds. Intense light from a fireball could rapidly warm common dielectric materials closed nearby the observers and then produce some small oscillation in the air and create sound wave. The process is called photo-acoustic coupling.

And why not an auditory hallucination? It would be interesting that specialists in psychology or neuroscience investigate this possibility. Today, this is not fully explained, studies must continue.

Acknowledgment

The author wishes to thank *Dominique André* and *Romarc Buté* for their cooperation and their permission to include their images and BOAM members and team for providing their camera data and detection.

³³ <https://www.nature.com/articles/srep41251>

Fireball events over Spain in July 2020

José María Madiedo

Instituto de Astrofísica de Andalucía
madiedo@iaa.es

An overview is presented of the exceptional fireball events by the meteor observing stations operated by the SMART Project from Sevilla and Huelva during July 2020.

1 Bright meteor over Spain on July 4

This sporadic fireball³⁴ overflew Spain on 5 July 2020, at about 0^h58^m local time (which is equivalent to 22^h58^m UT on July 4). It was generated by a meteoroid following an asteroid-like orbit that hit the atmosphere at about 72000 km/h. The fireball began at an altitude of about 81 km over the province of Toledo, and ended at a height of around 34 km over Madrid.

The event had an absolute magnitude of about -11. This bright meteor was recorded in the framework of the SMART project, operated by the Southwestern Europe Meteor Network (SWEMN) from the meteor-observing stations located at La Hita (Toledo), Sevilla, La Sagra (Granada), and Calar Alto (Almería). The event has been analyzed by the principal investigator of the SMART project: Dr. Jose M. Madiedo, from the Institute of Astrophysics of Andalusia (IAA-CSIC).



Figure 1 – Fireball 5 July 2020, at 22^h58^m UT.

³⁴ <https://youtu.be/GeRl0woRadg>

2 Bright fireball over the Atlantic Ocean on July 22

This beautiful meteor³⁵ overflowed the south of Spain on 2020 July 22 at about 3^h49^m local time (1^h49^m UT). It was generated by a sporadic meteoroid following a cometary-like orbit that hit the atmosphere at around 220000 km/h.

The event, which reached a peak luminosity equivalent to -12 mag, began at an altitude of about 120 km over the Gulf of Cadiz (Atlantic Ocean), and ended at a height of around 75 km over the sea level. This fireball was recorded in the framework of the SMART project, which is being conducted by the Southwestern Europe Meteor Network (SWEMN). It was spotted from the meteor-observing stations located at Sevilla and Calar Alto.



Figure 2 – Fireball 22 July 2020, at 01^h49^m UT.

³⁵ <https://youtu.be/97BDNvqm8t4>

The mission of MeteorNews is to offer fast meteor news to a global audience, a swift exchange of information in all fields of active amateur meteor work without editorial constraints. MeteorNews is freely available without any fee. To receive a notification: <https://www.meteornews.net/newsletter-signup/>.

You are welcome to contribute to MeteorNews on a regular or casual basis, if you wish to. Anyone can become an author or editor, send an email to us. For more info read: <https://meteornews.net/writing-content-for-emeteornews/>

The running costs for website hosting are covered by a team of sponsors. We want to thank Anonymous (3x), Nigel Cunnington, Kai Frode Gaarder, Pierre Tioga Gulon, J Andreas Howell, Koen Miskotte, Paul Roggemans, Mark Upton, Lorenzo Barbieri and Peter Stewart for their financial contributions.

Gifts are welcome to share the maintenance costs. To join the team of sponsors send your donation by PayPal: <https://www.paypal.com/pools/c/8ks6DnMamJ>

Webmaster & account administrator:

Richard Kacerek (United Kingdom): rickzkm@gmail.com

Contributing to this issue:

- J. Greaves
- T. Gulon
- P. Jenniskens
- R. Kacerek
- J.-M. Madiedo
- P. Martin
- K. Miskotte
- H. Ogawa
- P. Roggemans
- G. Ryabova
- T. Sekiguchi
- F. Verbelen
- T. Weiland

ISSN 2570-4745 Online publication <https://meteornews.net>

Listed and archived with ADS Abstract Service: <https://ui.adsabs.harvard.edu/search/q=eMetN>

MeteorNews Publisher:

Valašské Meziříčí Observatory, Vsetínská 78, 75701 Valašské Meziříčí, Czech Republic
